DISSERTATION

ENABLING PREDICTIVE ENERGY MANAGEMENT IN VEHICLES

Submitted by

Zachary D. Asher

Department of Mechanical Engineering

In partial fulfillment of the requirements

For the Degree of Doctor of Philosophy

Colorado State University

Fort Collins, Colorado

Spring 2018

Doctoral Committee:

Advisor: Thomas H. Bradley

Edwin Chong
Peter Young
Jianguo Zhao

ABSTRACT

ENABLING PREDICTIVE ENERGY MANAGEMENT IN VEHICLES

Widespread automobile usage provides economic and societal benefits but combustion engine powered automobiles have significant economic, environmental, and human health costs. Recent research has shown that these costs can be reduced by increasing fuel economy through optimal energy management. A globally optimal energy management strategy requires perfect prediction of an entire drive cycle but can improve fuel economy by up to 30%. This dissertation focuses on bridging the gap between this important research finding and implementation of predictive energy management in modern vehicles. A primary research focus is to investigate the tradeoffs between information sensing, computation power requirements for prediction, and prediction effort when implementing predictive energy management in vehicles. These tradeoffs are specifically addressed by first exploring the resulting fuel economy from different types of prediction errors, then investigating the level of prediction fidelity, scope, and real-time computation that is required to realize a fuel economy improvement, and lastly investigating a large computational effort scenario using only modern technology to make predictions. All of these studies are implemented in simulation using high fidelity and physically validated vehicle models. Results show that fuel economy improvements using predictive optimal energy management are feasible despite prediction errors, in a low computational cost scenario, and with only modern technology to make predictions. It is anticipated that these research findings can inform new control strategies to improve vehicle fuel economy and alleviate the economic, environmental, and human health costs for the modern vehicle fleet.

ACKNOWLEDGEMENTS

To my mom, Patti. Your love and support has made me into the person I am today.

TABLE OF CONTENTS

LIST OF TABLES

LIST OF FIGURES

Chapter 1

Review of Research Gaps to Optimal Fuel Economy Vehicle Control

This study is a comprehensive literature review of predictive energy management. This research is the result of years of effort reviewing literature in the field. It was originally published as a conference paper [3] but was then expanded into the complete journal paper (in review) reproduced in this chapter [4].

1.1 Introduction

Automobiles first achieved global adoption in the early 20th century, and continue to provide large economic benefits. However, widespread automobile usage poses significant public safety risks, damage associated with energy consumption, and adversely affects the natural environment. Ongoing technological advancements have been continually applied to the light duty transportation sector to reduce these damages, including technologies such as the frontal collision warning, lane departure warning, limited driver-advised driving, and electrification [5].

These evidence the ongoing vehicular evolution, in which human driving responsibilities are increasingly deferred to robust computerized systems of sensor technologies. With each stage of this evolution come advancements in vehicular safety, and opportunities for minimizing fuel consumption.

1.1.1 The Importance of Minimizing Non-Renewable Fuel Consumption

In terms of global energy consumption, the transportation sector is the second largest consumer behind only the industrial sector. Transportation accounts for 30% of the world's energy consumption and the transportation energy demand is projected to increase 30% from current levels by 2040 [6]. Associated utilization of energy conversion devices such as the internal combustion en-

gine, result in issues spanning climate stability, domestic energy security, local air quality impacts, and human health risks.

The global transportation sector accounted for 64.5% of worldwide petroleum consumption in 2014 [6]. On a per-country basis, petroleum consumption is often unbalanced from domestic production, where disparity between the two creates the issue of energy security and vulnerability to geopolitical stability [7]. For example, a 2016 estimation shows that the United States alone paid $150 billion to Organization of Petroleum Exporting Countries (OPEC) [8, 9] and estimated annual costs to ensure continued petroleum importation are around $200 billion [10].

The transportation sector is also responsible for 23% of global greenhouse gas emissions in 2014 [11] which has been linked to climate change [12]. To combat climate impacts, the Paris climate agreement has been adopted by most countries to limit greenhouse gas emissions and thus global warming to 2°C [13]. Limiting greenhouse gas emissions from transportation is proposed to be accomplished primarily through the increasing of **fuel economy (FE)** with technologies such as improved vehicle control and electrification [14]. It is widely accepted that without successfully stabilizing global climate, major human health, ecosystem service, and environmental impacts will be imminent [12].

The transportation sector is also a major contributor to air pollution. Of the six primary air pollutants, transportation significantly contributes to worldwide nitrogen oxide/nitrogen dioxide (NOx), carbon monoxide (CO), volatile organic compounds (Voc), particulate matter (PM), and sulfur dioxide (SO_2) [15]. As a result, 6.5 million premature deaths were attributed to air pollution in 2012, making it the worldâĂŹs fourth-largest threat to human health [16]. Premature deaths from air pollution is expected to rise to 7.4 million by 2040 but is strongly region dependent [15].

Increases in vehicle FE will reduce petroleum consumption, thus lowering global energy consumption, while decreasing greenhouse gas emissions and air pollution emissions. Automotive FE standards, such as those adopted by the United States, Japan, Canada, Australia, China, Taiwan, South Korea, and others, have proven to be one of the most effective tools in controlling petroleum demand and greenhouse gas emissions in many regions and countries around the world [17].

1.1.2 The Evolution of Modern Vehicles

Modern vehicles are gradually incorporating some form of electrification to evolve from conventional vehicles (CVs) to hybrid electric vehicles (HEVs), plug-in hybrid electric vehicles (PHEVs), or fully electric vehicles (EVs) with increasing prevalence projected to continue to beyond 2040 [3, 18]. But, HEVs and PHEVs are unique in that there are multiple sources of vehicle propulsion from either battery power, engine power, or a combination of both. This extra source of energy adds an additional degree of freedom to powertrain propulsion and numerous degrees of freedom to on-the-fly powertrain configurations. Examples of how this increased vehicle powertrain operational freedom can be used to reduce fuel consumption include regenerating energy during braking, storing excess energy from the engine during coasting [19], and modifying the power-split powertrain component usage for maximum efficiency [20].

Another trend, which is in stark contrast to the first 100 years of automobile development, is that the past 10 years have brought forth the most safety and convenience upgrades due to rapid advancements in computational technology [5]. The modern vehicle is one distinguished by an ability to perceive its environment by use of sensor technologies and computer systems. This vehicle intelligence can manifest as driver help, as is provided by advanced driver assistance systems (ADAS) [21], or can manifest as a vehicle which is afforded responsibility to make driving decisions independent of a human driver through autonomous technologies [22].

An intelligent vehicle is defined as a system that can sense the driving environment and provide information or vehicle control to assist the driver in improved vehicle operation [23]. Intelligent vehicle aspects include the ability to:

- Sense the vehicle's own status and its environment [24]

- Communicate with the environment [24]

- Plan and execute appropriate maneuvers [23]

3

Note that the "environment" is defined as the vehicle surroundings which can include other vehicles, traffic lights, pedestrians, and so on. This increased environmental knowledge enables improved vehicle control strategies that can operate in tandem with inputs from a human driver.

Current examples of intelligent electrified vehicles include the 2017 Toyota Prius, 2017 Ford Fusion, 2017 Chevrolet Malibu, and others which offer HEV architecture, radar based adaptive cruise control to assist drivers [25], and vehicle tracking through the global positioning system (GPS) which has been in high demand since 1998 [26]. Other vehicles are now offering 360 degree cameras to further assist drivers and increase vehicle intelligence [27].

The thesis of many researchers in this field is that the combination of intelligent vehicle control and electrification is a synergistic means to realize large fuel consumption improvements. This review summarizes research that incorporates both intelligent vehicle control and electrification to then identify research gaps preventing large fuel consumption improvements in the next generation vehicle.

1.1.3 Using Modern Vehicles to Minimize Fuel Consumption

There are three types of vehicle control that reduce fuel consumption for a drive cycle with a fixed starting point and a fixed ending point: (1) eco-routing, (2) eco-driving, and (3) an improved energy management strategy. Eco-routing and eco-driving decrease fuel consumption by decreasing the energy output of the vehicle through modification of the drive cycle. An improved energy management strategy decreases fuel consumption by increasing the efficiency of the vehicle powertrain without modification of the drive cycle.

Eco-routing reduces fuel consumption for all types of vehicles by exploring alternate vehicle routes between a fixed starting and ending location. Routes that minimize travel time enable social efficiency while routes that minimize fuel consumption enable vehicle powertrain efficiency. Modern commercially available routing techniques are currently designed for minimum travel time/social efficiency only. Eco-routing is an active research subject which seeks to balance travel time and fuel consumption to maintain social efficiency and improve powertrain efficiency.

Research on a large geographic scale indicates that a 3.9% FE improvement for a 4.5% travel time increase is possible in Cleveland, Ohio and a 6.6% FE improvement for a 1.0% travel time increase is possible in Columbus, Ohio [28]. As vehicles become more intelligent, eco-routing can affect vehicles in real time but several research gaps have been identified [29].

Eco-driving reduces fuel consumption for all types of vehicles by implementing fuel efficient driving behaviors along a fixed route which may alter the travel time. Eco-driving can be formulated as an optimal control problem if the driving conditions along the route can be predicted. Current practical use of eco-driving is realized through a heuristic set of goals such as removing stops, traveling at a fuel efficient speed (in general this could be a higher or lower overall speed), and limiting acceleration and deceleration magnitudes, which together can achieve FE improvements of 10% for modern vehicles and 30% for autonomous vehicles [30]. Research has typically focused on the FE impact of one particular intelligent vehicle technology, such as camera systems, radar systems, LiDAR, vehicle-to-vehicle (V2V) communication or vehicle-to-infrastructure (V2I) communication. An example of a typical study on eco-driving used predictions of traffic light signal phase and timing, a V2I technology, to change driving behavior and demonstrated a FE improvement of 12%-14% [31].

Improved energy management strategies seek to reduce the energy consumption over a fixed drive cycle. Typically, an optimal control problem is formulated and an **Optimal Energy Management Strategy (Optimal EMS)** is computed. An Optimal EMS realizes FE improvements by explicitly or implicitly modeling future vehicle operation and controlling the vehicle powertrain to minimize fuel consumption. An Optimal EMS does not require a change in driver behavior, thus this FE improvement technique has a consumer acceptance advantage over eco-driving and eco-routing. An Optimal EMS can realize FE improvements for conventional vehicles and electric vehicles, but the greatest FE improvements are realized from vehicles with more powertrain operation degrees of freedom such as HEVs and PHEVs. The effectiveness of the Optimal EMS FE improvement is strongly dependent on the chosen drive cycle and vehicle architecture. As an

example, one of earliest relevant studies demonstrated a 28% FE improvement in a hybrid electric truck through optimal control of the gear shifting and battery charging/discharging [32].

Optimal EMS Background

Developing and implementing an Optimal EMS has most commonly been posed as an application of optimal control. A mathematical optimization problem is formulated by defining the mass of fuel used as a cost to be minimized over a fixed drive cycle. This mathematical optimization problem can be formulated as either a second by second instantaneous optimization, or as a global optimization which includes future vehicle operation prediction. The result from either of these schemes is the minimum fuel consumption strategy (Optimal EMS) which can be applied to the fixed drive cycle.

Instantaneous Optimal EMS

An instantaneous Optimal EMS involves finding the optimal control strategy that minimizes fuel consumption for the instant in time for which sampled data is available. In practical implementation, the instantaneous Optimal EMS depends on the vehicle type.

Many aspects of modern CV engine and transmission control techniques are classifiable as an Instantaneous Optimal EMS including deceleration fuel cutoff (DFCO) [33], fuel enrichment [34], variable valve timing (VVT) [35], cylinder deactivation [36], and more. A basic example of the use of an instantaneous Optimal EMS in a CV is choosing the gear in which the vehicle will operate. When the vehicle is operating at fixed speed and fixed driver torque request, the vehicle requires a fixed power demand and the vehicle must choose one transmission gear in which to operate. A control strategy that selects the gear to minimize fuel consumption is an example of basic instantaneous Optimal EMS.

For HEVs, large FE improvements can be achieved by restricting engine power operation to the minimum fuel consumption solution (also known as the ideal operating line [37]) which is a primary fuel saving technique employed by HEVs [38].

In PHEVs such as the Toyota Prius Prime and the Chevrolet Volt, studies using an instantaneous Optimal EMS have led to the "charge-depleting, charge-sustaining" EMS, where all excess battery power is used first, then the battery charge is sustained afterwards [39]. This EMS is the standard operating mode for PHEVs where usage of charge sustaining mode is intended to be minimized. A standard measurement of charge sustaining mode minimization is the utility factor [40]. In other words, for PHEVs, the objective is to minimize non-renewable liquid fuel consumption through maximization of renewably generated electrical energy consumption.

Electric vehicles (EVs) also make use of instantaneous Optimal EMS improvements to minimize energy consumption and improve range through powertrain configuration optimization. Tesla Motors, an electric vehicle company, has multiple patents related to the use of an instantaneous Optimal EMS [41, 42].

Instantaneous Optimal EMS remains an active research topic. Such efforts are focused on an implementation and quantification of the effects of an instantaneous equivalence calculation between electrical energy and fuel energy [43, 44].

Predictive Optimal EMS

A predictive Optimal EMS involves finding the optimal control strategy that minimizes fuel consumption for the window of time in which prediction data is available. Hundreds of papers have been written on the development and application of a predictive Optimal EMS in the past decade alone [45]. Most of these papers describe the development of an Optimal EMS fitting one of three categories: (1) a globally Optimal EMS with deterministic prediction, (2) an Optimal EMS with stochastic prediction, and (3) a computationally limited Optimal EMS to enable practical implementation.

A globally Optimal EMS with deterministic prediction is derived using either dynamic programming (DP) [32] or Pontryagin's minimization principle (PMP), which is based on calculus of variations [46]. When deriving a globally Optimal EMS using deterministic prediction, DP has been the overwhelming favorite of researchers due to its ease of use, robustness, and that no derivatives or analytic expressions are required [45]. A globally Optimal EMS with deterministic

prediction is difficult to implement in practice because of the relatively high computational cost, but this strategy has the benefit of being able to define the upper practical limit on FE benefits for a given vehicle and cycle.

An Optimal EMS with stochastic prediction is used in applications where researchers are willing to forgo a guarantee of global optimal FE in favor of a robustness to stochastic prediction errors. In other words, stochastic derivation strategies are appropriate for applications where a small increase in FE over a wide range of drive cycles is desired. Stochastic derivation strategies include stochastic dynamic programming [47] and adaptive equivalent consumptions minimization strategy [48].

Lastly, a computationally limited practical implementation Optimal EMS also forgoes the guarantee of global optimal FE in favor of computationally efficient algorithms that can be used in current and near future vehicles. Practical implementation derivation strategies in current vehicles include optimized rules-based control [49], equivalent consumption minimization strategy (ECMS) [50], and model predictive control (MPC) [51].

1.1.4 Contributions of this Literature Review

Based on this precedent understanding of the literature, this review will seek to determine and develop three contributions:

1. A more holistic and systems-level understanding of the subsystems and integrations needed to implement an Optimal EMS in vehicles

2. A definition of the research gaps existing between the current state-of-the-art and the end state of predictive Optimal EMS usage in vehicles

3. A proposal for a set of research directives that will enable progress towards predictive Optimal EMS implementation in vehicles

1.2   Systems Level Viewpoint

Many studies of Optimal EMS conclude that vehicle perception, operation prediction, and vehicle actuation must all be achieved for successful implementation. However, a systems level understanding of how each of these pieces fit together is not as well defined.

To improve communication between academic researchers, the automotive industry, and other entities, the systems level model of an Optimal EMS implementation shown in figure 1.1 is proposed. To define a systems level viewpoint of an Optimal EMS implementation, currently available systems models from autonomous vehicle literature can be used as inspiration [22, 52]. The systems model is composed of four pieces: vehicle perception, vehicle planning, a vehicle running controller, and a vehicle plant. The Optimal EMS takes input from a suite of sensors which detect environmental information, thus defining vehicular surroundings (worldview) and ultimately generating a vehicle operation prediction. From this vehicle operation prediction, the FE can be maximized through vehicle optimal control. The maximum FE vehicle control is then issued as a request to the vehicle running controller, which enforces component constraints and may be subject to various control disturbances such as vehicle operation disturbance or operation environment disturbances. The running controller output is then actuated in the vehicle plant and the FE or energy consumption can be measured.
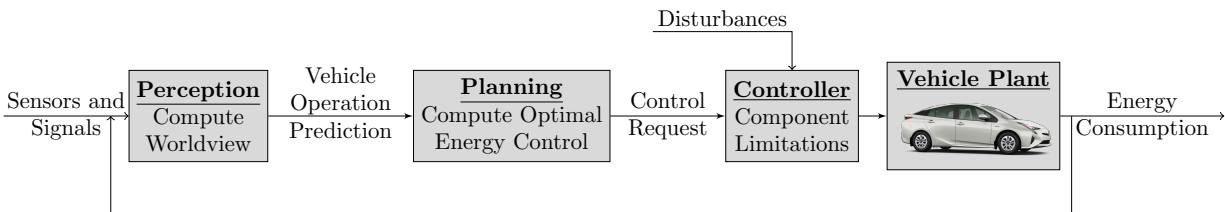
Figure 1.1: Systems level viewpoint of predictive Optimal EMS implementation.

1.3   Research Gap Derivation

In order to assess the research gaps for an Optimal EMS implementation, a technology maturity framework is adopted. The Technology Readiness Level (TRL), originally proposed by the U.S.

National Aeronautics and Space Administration (NASA), is one of the most prominent methods to assess technological maturity and help improve research and development outcomes [53]. The TRL scale has since been formally adopted worldwide despite known difficulties in application to large systems [54]. In response to these challenges, a popular and more comprehensive analysis is available which requires defining not only individual subsystem TRLs, but Integration Readiness Levels (IRLs), and an overall System Readiness Level (SRL) [55]. For the purpose of identifying the technological maturity of an Optimal EMS implementation, we adopt the framework of an SRL in which the TRL of each subsystem and the IRL of various integrations must be defined.

1.3.1 Technology Readiness Levels

Table 1.1 describes the authors' assessment of the TRL for each of the subsystems defined in figure 1.1. The technologies are: vehicle *perception* for worldview building and prediction, vehicle *planning* for fuel consumption reductions through optimal control, and usage of a *running controller in a vehicle plant* to achieve a fuel consumption reduction. The perception subsystem receives sensor and signal inputs, defines vehicle surroundings, and thus derives a vehicle operation prediction as an output. The planning subsystem receives the vehicle operation prediction as an input, and computes the optimal control as an output. Note that the planning subsystem is only required to compute the optimal control and issue a control request, this subsystem is not tasked with achieving the optimal control in the vehicle; achieving the optimal control is accomplished with the vehicle running controller. The final subsystem is comprised of the vehicle running controller and the vehicle plant. This system receives the optimal control request and instantaneous vehicle state as inputs, determines physically feasible vehicle operation that does not violate torque, battery state of charge, speed, acceleration, etc. limits and actuates the vehicle plant thus producing a measurable FE or energy consumption as an output.

Table 1.1: The Technology Readiness Level (TRL) analysis demonstrates that the individual technologies involved in predictive Optimal EMS implementation are very mature.

Technology and TRL	Technology Description	TRL Definition	TRL Justification
Perception TRL: 7	Receives sensor/signal data and derives a vehicle operation prediction	"System prototype demonstration in an operational environment"	The success of autonomous vehicle grand challenges [22] and adoption of ADAS technology in modern vehicles [21]
Planning TRL: 8	Receives vehicle operation prediction and computes the maximum FE control	"Actual system completed and qualified through test and demonstration"	Hundreds of research paper demonstrations for various EMS types, vehicles, and drive cycles [45]
Controller and Vehicle Plant TRL: 9	Receives driver requests and component statuses and actuates vehicle operation	"Actual system proven through successful mission operations"	Modern vehicles currently use running controllers to enforce component constraints and meet power demands

1.3.2 Integration Readiness Levels

Table 1.2 describes the authors' assessment of the IRL for the three integration points possible in figure 1.1. While the TRL is used to evaluate individual subsystems, the IRL is used to evaluate the readiness for each subsystem to integrate with one another [54]. An accurate evaluation of each subsystem integration requires a larger scope than that of the individual subsystem, which typically consists of a simple input/output framework. Three conceptually unique integration points exist if the vehicle running controller and the vehicle plant are treated as one subsystem of high IRL:

perception and planning integration, planning and control disturbances integration, and lastly planning and running controller/vehicle plant integration. Each of these integration points was found to have a low technological maturity, due to the limited amount of research that has sought to define and evaluate the integration.

Table 1.2: The Integration Readiness Level (IRL) analysis demonstrates that the technology integrations involved in predictive Optimal EMS implementation require significant research.

Integration and IRL	Integration Description	IRL Definition	IRL Justification
Perception and Planning IRL: 1	Receives sensor/signal data and computes the maximum FE control	"An interface between technologies has been identified with sufficient detail to allow characterization of the relationship"	Data transfer types are not standardized and world-views are not standardized
Planning and Control Disturbances IRL: 2	Receives incorrect vehicle operation prediction but still requests FE improved control	"There is some level of specificity to characterize the interaction between technologies through their interface"	There is limited research demonstrating improved FE with incorrect predictions
Planning and Use of a Vehicle Plant IRL: 3	Receives vehicle operation prediction and achieves maximum FE control in the vehicle	"There is compatibility between technologies to orderly and efficiently integrate and interact"	There are a few demonstrations of this integration in the literature

1.3.3 System Readiness Level

Where the TRL analysis has been applied to individual subsystems, and the IRL has been applied to the integration between subsystems, an SRL method is the appropriate means of evaluation for the entire system of predictive Optimal EMS implementation. SRL provides clear insight to specific research tasks which can be undertaken to improve technology maturity. Additionally, ensuring safe and reliable operation, also known as verification and validation, for autonomous vehicles (conceptually similar to predictive Optimal EMS implementation) is an active subject of research due to challenges of working with an entire system of perception, planning, and control [52]. Accurate assessment of verification and validation requires understanding and usage of a scope higher than IRLs.

From assessing the SRL by applying various integration scopes, *three research gaps have been identified* based on their low IRL, each of which will be discussed in the following sections. Once research efforts can improve predictive Optimal EMS IRLs, the overall SRL can be improved to suffice incorporation into demonstration and production vehicles. Table 1.3 describes the authors' assessment of the SRL of an Optimal EMS implementation.

Table 1.3: The System Readiness Level (SRL) argues that significant research is required before predictive Optimal EMS implementation can be achieved in practice.

System and SRL	System Description	SRL Definition	SRL Justification
Optimal EMS Implementation SRL: 2	Perception and planning subjected to disturbances and implemented in a vehicle plant	"Reduce technology risks and determine appropriate set of technologies to integrate into a full system"	IRLs are too low and there is almost no research that includes a fully realized system

1.4 Research Gap 1: What Worldviews Can Enable an Optimal EMS?

Although numerous vehicle sensor and signal information could be used, an Optimal EMS may only require a perception limited worldview to achieve optimal FE control. This first research gap was identified by applying an integration scope to include the perception and planning technologies shown in figure 1.2. To understand this integration, studies should consider (1) a perception model with sensor/signal inputs and future vehicle operation prediction as an output, (2) a planning model that uses future vehicle operation prediction to derive an Optimal EMS, and (3) FE results. Studies that include perception, Optimal EMS planning, and FE results would contribute to the overall goal of identifying the worldviews that can enable a prediction based Optimal EMS.
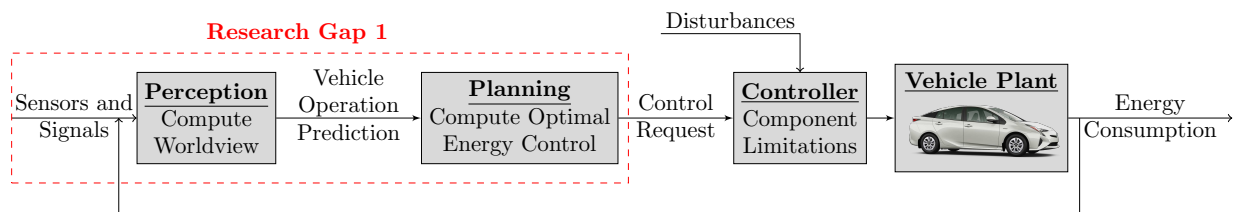
Figure 1.2: The integration scope defined in research gap 1: perception, Optimal EMS planning, and FE results.

A small number of existing studies include vehicle perception, Optimal EMS planning, and FE results. Perception technology is mature due to the recent success and proliferation of the autonomous vehicle, and as a result, there are numerous sensors and signals that can be used. Existing sensors/signals on modern vehicles include cameras, radar, and GPS. Commercially available sensors/signals include weather information, previous trip data, and traffic information. Near future sensors/signals include V2V and V2I communication, and vehicle-to-everything communication (V2X). A perception model used in research could include any or all of these sensors/signals.

The earliest and presently most cited research pertaining to perception, Optimal EMS planning, and FE results comes from researchers at the University of Florida and the University of Wisconsin-

Milwaukee. These researchers used V2I and GPS signals as inputs into a perception model. The perception model was able to output vehicle operation predictions using an analytical traffic model [56], and the approach was later revised to employ a neural network defined vehicle operation prediction [57]. The use of a neural network to characterize a driving pattern was found to be effective, and FE improvements using an Optimal EMS in a PHEV were realized.

Researchers at the University of Stuttgart have begun integrating a perception model and a planning model. Their perception model is based on repeated driving cycles of a hydraulic hybrid garbage truck. They use GPS and current vehicle state to characterize and store a drive cycle. The perception model creates predictions by using the stored drive cycle data for current vehicle operation. The planning Optimal EMS only determines the optimal time to implement the hydraulic power. This team demonstrated significant FE improvements when driving behavior was predicted, but noted that inclusion of traffic information is required for real-world implementation [58].

Researchers at the University of Minnesota applied a traffic model to predict future vehicle velocity with V2V and V2I as inputs. They employed Pontryagin's Minimization Principle as their Optimal EMS planning, but realized a modest FE improvement. FE gains were limited by the difficulty of incorporating constraints [59].

Researchers from the University of California at Berkeley have also recognized the important relationship between perception and planning. In their research, they investigate three perception models and use model predictive control as their Optimal EMS planning. They use previous driving data and the current vehicle state as inputs to test an exponentially varying perception model, a stochastic Markov chain perception model, and an artificial neural network (NN) perception model [60]. Their results show that the artificial neural network perception model with model predictive control as the Optimal EMS produced the best FE results, though this result was not a full realization of globally optimal FE. Additional studies by this group have shown FE results closer to optimal with the inclusion of traffic information [61].

Researchers at Colorado State University have also investigated perception, Optimal EMS planning, and FE results. One recent study uses a perception model with sensor/signal inputs of current

vehicle status, previous drive data, and GPS data. Vehicle velocity predictions are formulated using a NN, and an Optimal EMS is computed using dynamic programming. The FE results are measured using a validated model of a 2010 Toyota Prius. A trade-off between vehicle prediction accuracy and vehicle prediction time length was discovered, and the maximum FE improvement was achieved using 30 seconds of prediction [62].

Lastly, a variety of studies analyze ECMS in the perception, planning, and FE integration scope. ECMS only requires computation of an equivalence factor to determine engine/battery operation. Though for real-world driving, the optimal equivalence factor must be continually updated, thus requiring prediction [48]. Although several prediction-limited formulations have been proposed, it has been shown that ECMS benefits from a velocity prediction perception model. For example, researchers at the Bejing Institute of Technology demonstrated greater and more consistent FE improvements with the aide of perception [63].

Each of these studies has been summarized in table 1.4. Initial successes in addressing this research gap was achieved using a NN to derive a vehicle velocity prediction. However, many new research opportunities exist pertaining to the FE impacts of existing, state-of-the-art, and novel prediction techniques implemented with novel groups of sensors/signals. Additionally, existing research has focused on vehicle velocity prediction in the time domain which is only one of many potential worldviews that are possible. Examples of an alternate worldview that could be used to assist the development of a predictive Optimal EMS is prediction of stop locations and wind speed in the distance domain or inclusion of electric grid status when charging [64].

Table 1.4: Summary of existing research that includes the integration scope of perception, Optimal EMS planning, and FE results.

Research Group	Sensors/ Signals	Perception Model	Planning Technique	Vehicle Model
University of Wisconsin -Milwaukee 2009 [56, 57]	GPS, V2I	Traffic Model, Neural Network	Dynamic Program- ming	Generic Hybrid SUV
University of Stuttgart 2013 [58]	Vehicle State, Drive Data, GPS	Database Look-up	Custom Hydraulic Power Opt.	Parallel Hydraulic Hybrid Truck
University of Minnesota 2014 [59]	V2V, V2I	Traffic Model	Pontryagin Minimum Principle	Generic Power-Split HEV
University of California at Berkeley 2015 [60, 61]	Vehicle State, Drive Data, V2I	Exp. Varying, Markov Chain, Neural Network	Model Predictive Control	Generic Power-Split HEV
Colorado State University 2017 [62]	Vehicle State, Drive Data, GPS	Neural Network	Dynamic Program- ming	Validated 2010 Toyota Prius
Beijing Institute of Technology 2017 [63]	Vehicle State, Drive Data	Neural Network	Adaptive ECMS	Generic Power-Split HEV

1.5 Research Gap 2: How Sensitive Are Optimal Fuel Economy Strategies To Worldview/Prediction Scope, Fidelity, And Uncertainty?

Optimal FE vehicle control is derived based on predictions of vehicle velocity, configuration, weight, and environmental conditions, none of which can be perfectly and exactly accurate thus potentially affecting the achieved FE. This second research gap was identified by applying an integration scope to include Optimal EMS planning technology subjected to disturbances as shown in figure 1.3. To understand this integration, studies were sought to consider (1) a planning model that uses future vehicle operation prediction to derive an Optimal EMS, (2) disturbances, and (3) FE results. Studies that include Optimal EMS planning, disturbances, and FE results would contribute to the overall goal of understanding the sensitivity of worldview prediction scope on FE.
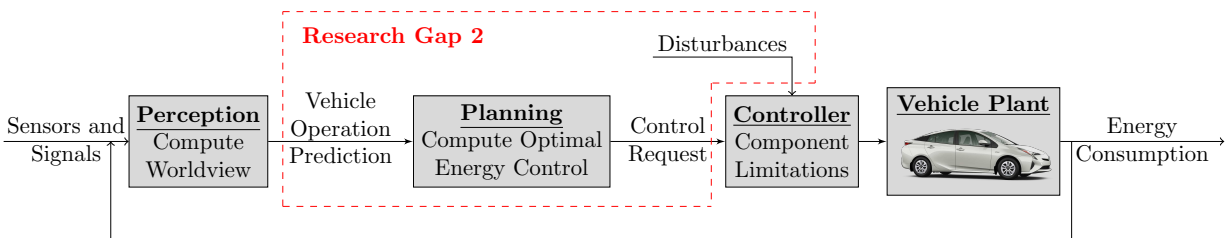
Figure 1.3: The integration scope defined in research gap 2: Optimal EMS planning subject to disturbances.

Though academic literature has investigated Optimal EMS planning, disturbances, and associated FE results, there exists a relatively vast array of vehicle architectures, drive cycles, Optimal EMS types, and disturbance types. In the author's assessment, the imbalance between the scope and scale of the challenge and level of research performed to date makes this research gap worthy of further investigation. For example, a globally Optimal EMS, Real-Time EMS, and Stochastic EMS may all have different sensitivities to stochastic disturbances, driving-derived disturbances, and vehicle power disturbances. In addition, series, parallel, and power-split HEVs or PHEVs may produce different results over city, highway, aggressive, or elevation varying drive cycles.

An early study from researchers at the National Renewable Energy Lab performed dynamic programming to half battery size and full battery size PHEVs to compare optimal solutions for drive cycles of various lengths. They found that for drive cycle distances exceeding PHEV all electric range (charge depleting strategy), the optimal solution seeks a "blended" strategy (a mix of charge depleting and charge sustaining strategies) such that the minimum battery state of charge is achieved at the end of the drive cycle [65]. But, in considering the "cost of being wrong", they demonstrated that if the vehicle distance is less than predicted for optimal control, there is a significant FE loss. In other words, if the Optimal EMS assumes the trip will be longer than it actually is, the vehicle will not use all the stored electrical energy thus requiring more liquid fuel consumption.

Researchers at The Ohio State University conducted a study using alternate drive cycles as a prediction input error for two real time implementable Optimal EMS: a modified model predictive control strategy, and an adaptive ECMS [66]. They found that the FE cost of prediction of the wrong drive cycle was small for both Optimal EMS, but no baseline FE results were shown.

Another study including Optimal EMS planning, disturbances, and FE results came from researchers at Clemson University who investigated the effects of stochastic misprediction errors on a stochastic Optimal EMS known as adaptive-ECMS [67]. This group used the U.S. EPA drive cycles of UDDS, US06, and HWFET for 25, 50, 75, 100, and 150 miles. Their results show a degradation in FE at all values of mean absolute percent error greater than zero. But, no correlation between error magnitudes and FE was found.

Researchers at the University of Michigan have taken their initial Stochastic Dynamic Programming derived Optimal EMS [47] and have studied the impact of driving alternate drive cycles [68]. These researchers used a large real-world drive cycle data set to derive a stochastic Optimal EMS. The stochastic Optimal EMS was demonstrated to improve FE over a baseline strategy when tested on alternate drive cycles.

Researchers at the University of Minnesota investigated an Optimal EMS which was focused on fast computation through separable programming while also being subjected to disturbances [69].

Using a traffic simulator to develop drive cycles and 30 different vehicle platforms, they compared their Optimal EMS to dynamic programming and showed favorable results. When the drive cycle predictions were subjected to a normally distributed random prediction error, FE improvements were maintained at a 3% mean absolute deviation percentage, but FE improvements were lost at a 6% mean absolute deviation percentage.

Our research group at Colorado State University has also investigated Optimal EMS planning, disturbances, and FE results. Initial research [70, 71] was expanded to rigorously investigate driving-derived and vehicle parameter disturbances on optimal FE. A set of driving-derived disturbances such as mispredicted stops, traffic, and route changes were compared to a validated model of a 2010 Toyota Prius. It was found that with an Optimal EMS based on dynamic programming, FE improvements between 1.7% and 10.8% out of 10.9% possible could still be achieved when compared to the standard 2010 Toyota Prius [72].

Each study addressing this research gap has been summarized in table 1.5. To date, research has concentrated on using stochastic disturbances, but the use of driving-derived disturbances should be used to quantify the robustness or uniqueness of Optimal EMS control requests.

Table 1.5: Summary of existing research that includes the integration scope of Optimal EMS planning, disturbances, and FE results.

Research Group	Drive Cycle	Planning Technique	Error Type	Vehicle Model
National Renewable Energy Lab 2006 [65]	LA92, approx-imated UDDS	Dynamic Program-ming	Drive Cycle Distance	Half-size, Full-size PHEVs
Ohio State University 2011 [66]	Real World	MPC, Adaptive ECMS	Alternate Drive Cycle	Generic Parallel HEV
Clemson University 2012 [67]	UDDS, US06, HWFET	Adaptive ECMS	Stochastic	Generic Power-Split PHEV
University of Michigan 2014 [68]	Real World	Stochastic Dynamic Program.	Alternate Real World	Prototype Volvo S-80
University of Minnesota 2016 [69],	Traffic Simulation	Separable Program-ming	Stochastic	Generic Power-Split HEV
Colorado State University 2017 [72]	Real World	Dynamic Program-ming	Driving Derived, Vehicle Power	Validated 2010 Toyota Prius

1.6 Research Gap 3: What Operational Challenges Have Not Been Validated And Qualified In The Conceptual Work?

Incorporation of optimal FE vehicle control with physical vehicle components or full vehicles has been limited. This third research gap was identified by applying an integration scope to include Optimal EMS planning technology with the use of a physical vehicle plant as shown in figure 1.4. To understand the challenges associated with this integration, studies should consider (1) a planning model that uses future vehicle operation prediction to derive an Optimal EMS, (2) real-world vehicle plant considerations such as software, hardware, or an actual vehicle, and (3) FE results. Studies that include Optimal EMS planning, vehicle plant considerations, and FE results would contribute to the overall goal of understanding the operational challenges that have not been addressed in the literature.
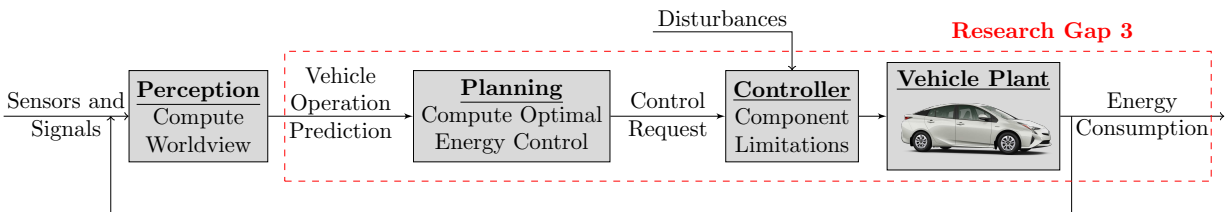
Figure 1.4: The integration scope defined in research gap 3: Optimal EMS planning with actual vehicle plant considerations.

There is limited research that includes Optimal EMS planning, vehicle plant considerations, and FE results because software-in-the-loop, hardware-in-the-loop, and vehicle-in-the-loop research is expensive and the technologies for specific vehicles are proprietary. The initial research in this area has been focused on rules-based implementation an Optimal EMS because of the ease of implementation [73–76]. But, research programs designed to overcome cost and proprietary information challenges such as FutureCar and EcoCAR have had significant success.

An initial, computationally limited, Optimal EMS implementation was achieved by researchers at The Ohio State University who implemented ECMS in an SUV as part of the FutureTruck

program [77]. This initial demonstration produced promising FE results and inspired more rigorous research of ECMS at The Ohio State University [78].

Researchers at the Eindhoven University of Technology have successfully implemented an Optimal EMS using Pontryagin's minimization principle to achieve a moderate FE improvement over a baseline, rules-based, control strategy on a hybrid electric truck. The FE improvement was demonstrated on a variety of drive cycles, including road grade variations. With the assistance of stored solutions from offline computations, they achieved success in implementing the Optimal EMS on the vehicle's engine control unit (ECU) [79].

Researchers at Shanghai Jiao Tong University have demonstrated FE improvements over a baseline rules-based control strategy using a hard-ware-in-the-loop real time simulation based on dynamic programming. These researchers derived an Optimal EMS using a form of dynamic programming, and then used the solution to train an artificial neural network. The trained neural network then accepted drive cycle inputs and output an improved control strategy [80].

Researchers at IFP Energies Nouvelles, French Institute of Petroleum have successfully implemented an Optimal EMS in a hardware-in-the-loop simulation for a diesel hybrid vehicle. Diesel-powered vehicles add the extra challenge of incorporating emissions minimization into the optimization scheme. Using ECMS, they were able to significantly improve FE, while reducing and oxides of Nitrogren (NOx, an emissions constituent) by parallel HEV architecture. [81, 82] [83].

Researchers at the University of Michigan have taken their initial stochastic dynamic programming derived Optimal EMS [47] and first included engine-in-the-loop simulations to closer approximate a real vehicle [84] and have since applied it in a prototype vehicle [85]. Although a hardware problem prevented them from attaining a full FE assessment from their stochastic dynamic programming controller, they conclude that an Optimal EMS can be implemented in a real vehicle and requires minimal tuning.

Researchers at the University of Stuttgart have incorporated a perception model and a planning model into an actual vehicle. Perception and planning were discussed in section 1.1.2, and they were also able to incorporate planning and the use of a vehicle plant. They were able to test

23

their Optimal EMS using a rapid prototyping unit on their hybrid hydraulic truck. When testing on a closed track, this team found FE improvements as well as instances of reduced FE when compared to the baseline control strategy, though these results were briefly mentioned and no detailed analysis was shown [58].

Lastly, researchers at the University of Salento have investigated the implementation of a Pontryagin's minimization principle Optimal EMS in a hardware-in-the-loop simulation of a custom built series PHEV. These researchers investigated both full and multiple local drive cycle section prediction cases. The researchers were able to demonstrate an overall FE improvement despite needing to reduce complexity on their Optimal EMS planning formulation, as required due to high computational cost [86].

Each of the initial studies addressing this research gap have been summarized in table 1.6. To date, research addressing this research gap has achieved success using a gradual incorporation of vehicle plant components through software-in-the-Loop, hardware-in-the-Loop, and vehicle-in-the-Loop experiments. Numerous research opportunities still exist that could fill this research gap by focusing on the demonstration of an Optimal EMS in a variety of vehicle operational environments with a variety of vehicle types, platforms, and powertrains.

Table 1.6: Summary of existing research that includes the integration scope of Optimal EMS planning, a vehicle plant, and FE results.

Research Group	Drive Cycle	Planning Technique	Vehicle Plant Model	Vehicle Realization
Ohio State University 2001 [77]	Real World	ECMS	2000 Chevrolet Suburban	Actual Vehicle
French Institute of Petroleum 2011 [83]	NEDC, FTP	ECMS	Micro-Hybrid, Parallel Hybrid	Hardware-in-the-Loop
Eindhoven University of Technology 2012 [79]	Real World	Pontryagin Minimum Principle	Parallel Hybrid Electric Truck	Hardware-in-the-Loop
Shanghai Jiao Tong University 2012 [80]	CTBDC	Iterative Dynamic Program-ming	Power-Split Hybrid Electric Bus	Hardware-in-the-Loop
University of Michigan 2013 [85]	Real World	Stochastic Dynamic Program.	Prototype Volvo S-80	Actual Vehicle
University of Stuttgart 2013 [58]	OC Bus Cycle, Real World	Custom Hydraulic Power Opt.	Parallel Hydraulic Hybrid Truck	Actual Vehicle
University of Salento 2013 [86]	Real World	Pontryagin Minimum Principle	Prototype Series PHEV	Hardware-in-the-Loop

1.7 Conclusions

In this literature review, vehicle control for optimal FE was introduced and discussed through methods that decrease vehicle energy output (eco-routing, eco-driving) and methods that fix vehicle energy output while increasing powertrain efficiency (Optimal EMS). Focusing on efficiency improvements towards the optimal FE through implementation of an Optimal EMS, it was demonstrated that there are hundreds of relevant research papers, although integration and system-level research gaps still exist. In applying systems level analysis, three research gaps were identified which are derived from consideration of various integration scopes: Optimal EMS planning with perception, Optimal EMS planning including disturbances, and Optimal EMS execution with a vehicle plant. In other words, gaps in optimal FE vehicle control academic knowledge exist regarding (1) an understanding of essential sensors and signals for perception and prediction enabling optimal FE vehicle control, (2) a deep understanding of disturbance types that can affect optimal FE vehicle control, and (3) the operational and real-world vehicle implementation challenges of optimal FE vehicle control. A review of insightful research efforts in each of these areas was presented and recommendations for future efforts that can advance the body of knowledge of Optimal EMS was discussed.

Engineering research is responsible for providing actionable ideas for industry incorporation. Because there are hundreds of combinations of vehicle architectures, drive cycles, and optimization routines, there have been hundreds of research papers [45] showing the same result: an Optimal EMS can increase FE. We present this comprehensive literature review on the Optimal EMS concept with the objective of focusing the efforts of the research community on increasing the readiness level associated with the key interfaces in the vehicle. Once the integration readiness level of the various subsystems is increased, Optimal EMS can be incorporated in the automotive industry. Once an Optimal EMS has achieved widespread usage in vehicles, the burdens of low FE such as oil importation, climate change, and air pollution can be reduced.

Chapter 2

Research Questions and Definition of Research Scope

2.1 Primary Research Question

Based on the research gaps outlined in the previous chapter, a primary research question can be posed:

Primary Research Question: What are the tradeoffs between information sensing, computation power requirements for prediction, and prediction effort when implementing predictive energy management in vehicles?

To answer this question, the research effort will establish the methods and framework for predictive energy management implementation. First a small systems-level scope will be used to investigate types of prediction errors. Then the systems-level scope will be expanded to include a limited prediction case. Finally, the systems-level scope will be expanded one more time to include current sensing technologies will be used to generate predictions.

These individual steps can be broken down into research questions of smaller scope. These smaller scope research questions then have associated tasks.

2.2 Research Question 1 - Prediction Errors

As stated in Chapter 1, section 1.5, a major research gap is understanding how sensitive optimal fuel economy (FE) strategies are to worldview/prediction scope, fidelity, and uncertainty. The first research question addresses this research gap.

Research Question 1: What are the effects of different types of prediction errors on the FE results enabled by predictive energy management?

This research question has not been directly approached in the literature to date. Researchers have instead opted to derive stochastically robust but suboptimal control strategies. If it can be

27

established that prediction errors with a globally optimal control strategy maintain a FE improvement, this may impact future research directions of the field.

Hypothesis 1: *Certain misprediction types will result in FE improvements being maintained while other misprediction types will result in a FE loss.*

There are two tasks associated with testing this hypothesis.

Task 1.1: Develop drive cycles that represent various types of mispredictions such as mispredicted stops, route changes, traffic, and compounded mispredictions for FE improvement evaluation.

Task 1.2: Develop vehicle parameter mispredictions such as vehicle mass changes, drag changes, and rolling resistance changes for FE improvement evaluation.

Upon completion of these tasks the hypothesized misprediction impacts can be understood. If it can be shown that FE improvements are maintained despite misprediction when using a globally optimal control strategy, near-term implementation feasibility of predictive energy management is improved. This also provides a metric to compare against stochastically robust but suboptimal control strategies.

2.3   Research Question 2 - Prediction Fidelity and Scope

To expand upon the results from Research Question 1, the systems-level scope can be expanded to include limited perception.

As stated in Chapter 1, section 1.4, another major research gap is understanding what world-views can enable an Optimal EMS. This second research question begins addressing this research gap by building upon Research Question 1 and incorporating a prediction scheme.

Research Question 2: *What level of prediction fidelity and scope is required to realize a FE improvement through predictive energy management and potentially eliminate the need for real-time computation?*

Since this research question builds on the results from Research Question 1, it can continue to progress new understanding about predictive energy management implementability.

Hypothesis 2: *Implementing a general prediction solution for the acceleration portions of a drive cycle will result in FE improvements without the need for perfect prediction.*

There are two tasks associated with testing this hypothesis.

Task 2.1: Build, organize, and demonstrate a statistical understanding of general AE control for improved FE.

Task 2.2: Investigate the FE improvements from limited AE prediction in full drive cycles.

Upon completion these tasks, an improved understanding of prediction and computational requirements can be realized. If it can be shown that FE improvements are possible using an Optimal EMS on short sections of driving such as AEs, implementability of predictive energy management improves. Additionally, if it can be shown that the exact AE doesn't need to be predicted, then a previously computed Optimal EMS can be used thus further improving the implementability of predictive energy management.

2.4   Research Question 3 - Prediction and Computational Effort

The research gap in Chapter 1 section 1.4, understanding what worldviews can enable an Optimal EMS, can further be explored using actual sensor and signal data from current vehicle technologies. This third research question investigates this research gap by integrating a perception model.

Research Question 3: *What prediction and computational effort is required to realize a FE improvement when using current technology integrated with predictive energy management?*

This research question has not received significant emphasis from researchers and the studies that do exist only consider future technologies that could enable full drive cycle prediction.

Hypothesis 3: *FE improvements can be realized using only current vehicle technology.*

There is one task associated with testing this hypothesis.

Task 3.1: Use currently available vehicle technology outputs to train an artificial neural network to make predictions for repeated city and highway drive cycles.

Upon completion of this task, an improved understanding of the prediction capabilities of current vehicle technologies can be realized. If it can be shown that FE improvements are possible using current vehicle technologies to make predictions combined with an Optimal EMS, feasibility of predictive energy management can be improved. Additionally, since this framework has a larger computational cost, this result can be compared to the results from Research Question 2 to elucidate computation tradeoffs.

2.5 Definition of Research Scope

The research effort will focus on improving feasibility for predictive energy management using HEVs. HEVs have a significant potential for FE improvements due to their two modes of vehicle propulsion, electric power and engine power (more degrees of freedom). As stated in Chapter 1, predictive energy management can improve performance of all vehicle architectures but HEVs provide a convenient architecture for feasibility studies. The research effort is focused on simulations using high fidelity and physically validated vehicle models. The methods developed for this research effort are general and have wide applicability.

Chapter 3

Prediction Error Applied to Hybrid Electric Vehicle Optimal Fuel Economy

This study investigates the FE impacts of various types of mispredictions and involves development of numerous drive cycles, a dynamic programming algorithm, a high fidelity model of a 2010 Toyota Prius, and a technique to evaluate mispredictions with the optimal control matrix result from the dynamic programming algorithm. This research was originally funded by Toyota where I assisted with translation into two conference publications [70, 71]. I was able to expand the scope into the complete journal paper reproduced in this chapter [72].

3.1 Introduction

Modern plug-in hybrid electric vehicle (PHEV) and hybrid electric vehicle (HEV) fuel economy (FE) can be optimized for a fixed drive cycle using a vehicle predictive optimal energy management strategy (EMS).

3.1.1 What Enables an Optimal EMS: Modern Vehicles

Modern vehicles are incrementally incorporating autonomous technologies and transitioning to intelligent vehicles. An intelligent vehicle is defined as a system that can sense the driving environment and provide information or vehicle control to assist the driver in improved vehicle operation [23]. Intelligent vehicle aspects include the ability to:

- Sense the vehicle's own status and its environment [24]

- Communicate with the environment [24]

- Plan and execute the most appropriate maneuvers [23]

31

As modern vehicles continue to evolve into intelligent vehicles, controls can utilize this new environmental information in addition to inputs from the human driver.

Along with the evolution of modern vehicles into intelligent vehicles, conventional vehicles are being subverted by PHEVs and HEVs [3] which provide more degrees of freedom for powertrain operation. As an example, HEVs can be powered by either stored electric energy from the battery, or mechanical energy from the engine. This increase in powertrain degrees of freedom provides energy management capabilities such as regenerating energy during braking and storing excess energy from the engine during coasting [19].

3.1.2   Why an Optimal EMS is Important: Fuel Economy

Worldwide, transportation is the second largest consumer of energy behind only the industrial sector. Transportation accounts for 30% of the world's energy consumption and the transportation energy demand is projected to increase 30% by 2040 [6]. Additionally, energy consumption by combustion engine powered vehicles has the following negative impacts:

- Requires policy costs for oil importation [10] and to prevent supply disruptions [7]

- Results in the release of greenhouse gas emissions which are responsible for climate change [11]

- Results in the release of air pollution [87] which is the fourth leading cause of premature death worldwide [16]

Increases in vehicle FE reduces energy consumption, oil importation, greenhouse gas emission, and air pollution. It has been shown that implementing FE standards, labels, and policies has improved the development of fuel saving technologies which have helped combat these issues [17]. But, although FE has been steadily increasing, there is still a lot of fuel economy that can be gained.

3.1.3 Optimal EMS Background

An HEV Optimal EMS is an application of optimal control. A mathematical optimization problem is formulated by defining the mass of fuel used as a cost to be minimized over a fixed drive cycle. The result from the mathematical optimization scheme is the minimum fuel control strategy that can be used for the fixed drive cycle. The mathematical optimization problem can be implemented using either instantaneous information or with prediction information from a drive cycle. But, a consistent globally optimal control is achieved with drive cycle prediction.

Instantaneous Optimal EMS

An instantaneous Optimal EMS is derived by finding the optimal control strategy that minimizes fuel consumption for the instant in time for which sampled data is available. For HEVs, large FE improvements can be achieved by restricting engine operation to minimum fuel consumption solution (also known as the ideal operating line [37]) which is the primary fuel saving technique employed by current HEVs [38]. In PHEVs, studies using an instantaneous Optimal EMS have led to the "charge-depleting, charge-sustaining" EMS, where all excess battery power is used first, afterwhich the battery charge is sustained [39]. Research in instantaneous optimal energy management is an active topic of research with efforts focusing on a realization of the minimal fuel consumption through instantaneous equivalence calculations between electrical energy and fuel energy [44].

Predictive Optimal EMS

A predictive Optimal EMS seeks to find and achieve the absolute minimum fuel consumption in the full drive cycle by enforcing global optimal control at every point. The solutions require prediction of the full drive cycle because energy trade-offs occur between all points in the drive cycle.

There have been hundreds of papers written on predictive optimal energy management over the last ten years [45], most of which describe predictive Optimal EMS that are either: derived to be the

global optimal FE, derived for practical/real-time implementation, or derived based on stochastic or random drive cycle predictions. Global optimal FE derivation strategies are developed through either dynamic programming (DP) [32] or through Pontryagin's minimization principle which is based on calculus of variations [46]. For global minimum derivation strategies, DP has been the overwhelming favorite of researchers due to its ease of use, robustness, and that no derivatives or analytic expressions are required [45]. Globally optimal control strategies are difficult to implement in practice because of the large number of computations that are required. Practical implementation derivation strategies are used in applications where researchers are willing to forgo the guarantee of global optimal FE in favor of computationally efficient algorithms that can be used in current and near future vehicles. Practical implementation derivation strategies in current vehicles include optimized rules based control [49], equivalent consumption minimization strategy [50], and model predictive control [51]. Lastly, stochastic derivation strategies also forgo a guarantee of global optimal FE in favor of a robustness to stochastic prediction errors. Stochastic derivation strategies include stochastic dynamic programming [47] and adaptive equivalent consumptions minimization strategy [48].

Prediction Error

Prediction errors applied to a predictive Optimal EMS is theorized to have a large impact [88] but has not been adequately studied [3,45]. There are five relevant studies that include some aspect of prediction error on a HEV Optimal EMS. But, none of these studies are strictly focused on general results regarding fuel economy from prediction errors applied to an Optimal EMS.

An early study considered the "cost of being wrong" when comparing a prediction-based Optimal EMS to charge-sustaining/charge-depleting EMS for PHEVs. They concluded that if the vehicle distance is less than predicted for the Optimal EMS, there is a significant FE loss [65]. This study suggests that prediction of the drive cycle length is important for an Optimal EMS in a PHEV, but no further conclusions can be drawn.

Another study used two stochastic Optimal EMS and applied one prediction error of a different drive cycle. It was demonstrated that FE results are approximately equivalent but no baseline FE results are shown [66]. This study has limited misprediction scope and because no baseline FE results are shown, there is no way to know if these strategies are better than a modern vehicle EMS.

Another group of researchers continued the use of a stochastic Optimal EMS and applied various levels of stochastic prediction error. They show that FE is degraded by stochastic mispredictions but are unable to find a correlation with the mean absolute percent error [67]. This study has limited applicability because it only uses stochastic prediction errors applied to a stochastic Optimal EMS.

A later study again uses a stochastic Optimal EMS but these researchers test their Optimal EMS against a large number of real world drive cycles. They were able to demonstrate FE improvements over the baseline EMS even when subject to drive cycle variations [68]. This is the most comprehensive study to date but it is only applicable to a stochastic Optimal EMS and there is no focus on the FE results from a globally Optimal EMS.

The last prediction error study investigated a real time implementable Optimal EMS subject to stochastic mispredictions. They computed the FE results for two different values of mean absolute deviation percentage and showed that FE improvements are lost at 6% mean absolute deviation percentage [69]. This study is limited in that only two mispredictions are analyzed and that the mispredictions are both stochastic.

A study that is often cited as providing insight about the aspects of prediction that are most important for an Optimal EMS needs mention. These researchers included various levels of prediction to determine a parameter for a predictive Optimal EMS [88], but their approach is strictly applicable to their chosen Optimal EMS. Additionally their study uses various levels of prediction information rather than investigating prediction error.

This research is unique in that it focuses on the effect of driving-derived prediction errors such as a mispredicted stopping event or an excess vehicle mass subjected to a globally Optimal EMS.

This research is intended to aid researchers and automotive industry professionals that are seeking to develop and implement a prediction-based Optimal EMS for FE improvements.

3.1.4 Research Novel Contributions

This research makes the following novel contributions to the HEV Optimal EMS body of knowledge: (1) dynamic programming is used to evaluate mispredictions, (2) driving-derived mispredictions are analyzed, (3) vehicle parameter mispredictions are analyzed, and (4) the dynamic programming solution matrix time state variable is converted to a distance state variable for improved misprediction robustness.

3.1.5 Organization of this paper

There are four important concepts that compose the methods of this research: expected and mispredicted drive cycle development (study 1), a validated vehicle model with expected and mispredicted parameters (study 2), the Optimal EMS derivation, and prediction error handling. Study 1 focuses on the FE impact of driving-derived velocity prediction errors, while study 2 focuses on the FE impact of real world vehicle parameter prediction errors. The FE results are compared using baseline control, perfect prediction optimal control, and mispredicted optimal control for every type of misprediction from study 1 and study 2. Relevant vehicle parameters for discussion are included and a comprehensive report of all vehicle parameters is included with this article as supplementary material.

3.2 Methods

To investigate the FE results from a predictive Optimal EMS, we define: drive cycle(s), the vehicle model, and the Optimal EMS. To analyze the FE results from prediction errors requires the addition of two more definitions: prediction error type and prediction error handling in the Optimal EMS.

3.2.1 Drive Cycle Development

To study the effect of driving-derived velocity prediction errors (study 1), an expected drive cycle was developed along with 14 drive cycles to serve as mispredictions.

The Expected Drive Cycle

To analyze the desired aspects of the Optimal EMS, a custom drive cycle with a second-by-second velocity trace is required that concentrates the features of interest into a short drive cycle. The required drive cycle features are:

- Short in length

- Urban driving conditions

- Capability to modify for multiple driving variations

A drive cycle which meets all of these criteria was chosen that starts from a parking lot in south Fort Collins, Colorado and ends at a Colorado State University research facility. A map of this drive cycle is shown in figure 3.1a and the associated velocity trace is shown in figure 3.1b.
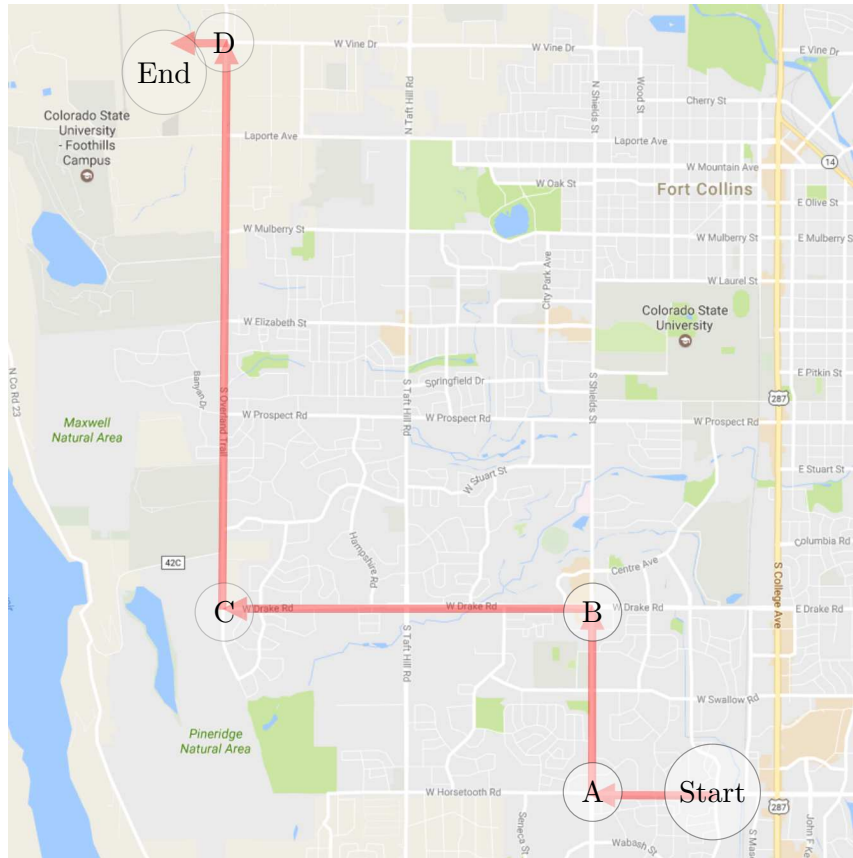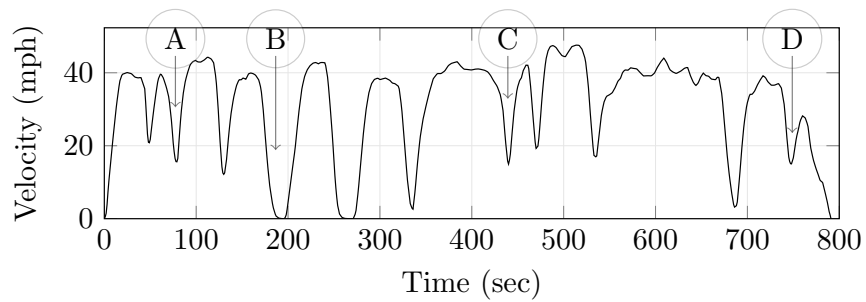
Figure 3.1: The 6.9 mile chosen drive cycle in Fort Collins, Colorado as shown from a Google Maps image (a) and a velocity trace (b).

Study 1: Mispredicted Drive Cycles

Study 1 focuses on vehicle velocity mispredictions which originate from driving-derived prediction errors along the route shown in figure 3.1, such as excess traffic or a sudden stopping

event. Four different types of mispredicted drive cycles were chosen: mispredicted stops (3 cases), mispredicted route changes (3 cases), mispredicted traffic levels (4 cases), and a compounded misprediction composed of all other types of mispredictions (4 cases). To isolate the mispredictions of stops, route changes, and traffic, the velocity trace was artificially modified so that only these mispredictions would exist in the drive cycle and ensuring the drive cycle preserves its overall distance. For the cases of compounded mispredictions, real driving data was recorded while driving the same route.

The stopping event mispredictions include 1, 2, or 3 mispredicted decelerations, pauses, and accelerations associated with having not predicted a stopping event such as a pedestrian in a crosswalk or a road obstruction. The route change mispredictions abruptly end the drive cycle at three different times. The traffic mispredictions adjust the velocity trace by a factor of 1.15, 0.85, 0.75, and 0.65 for the first 335 seconds of the 791 second drive cycle while maintaining equivalent drive cycle distance. For compounded mispredictions, there are differing levels of traffic along the drive cycle, different stoplight statuses, and one of the cases includes a wrong turn. Each of the drive cycle mispredictions is shown in figure 3.2.
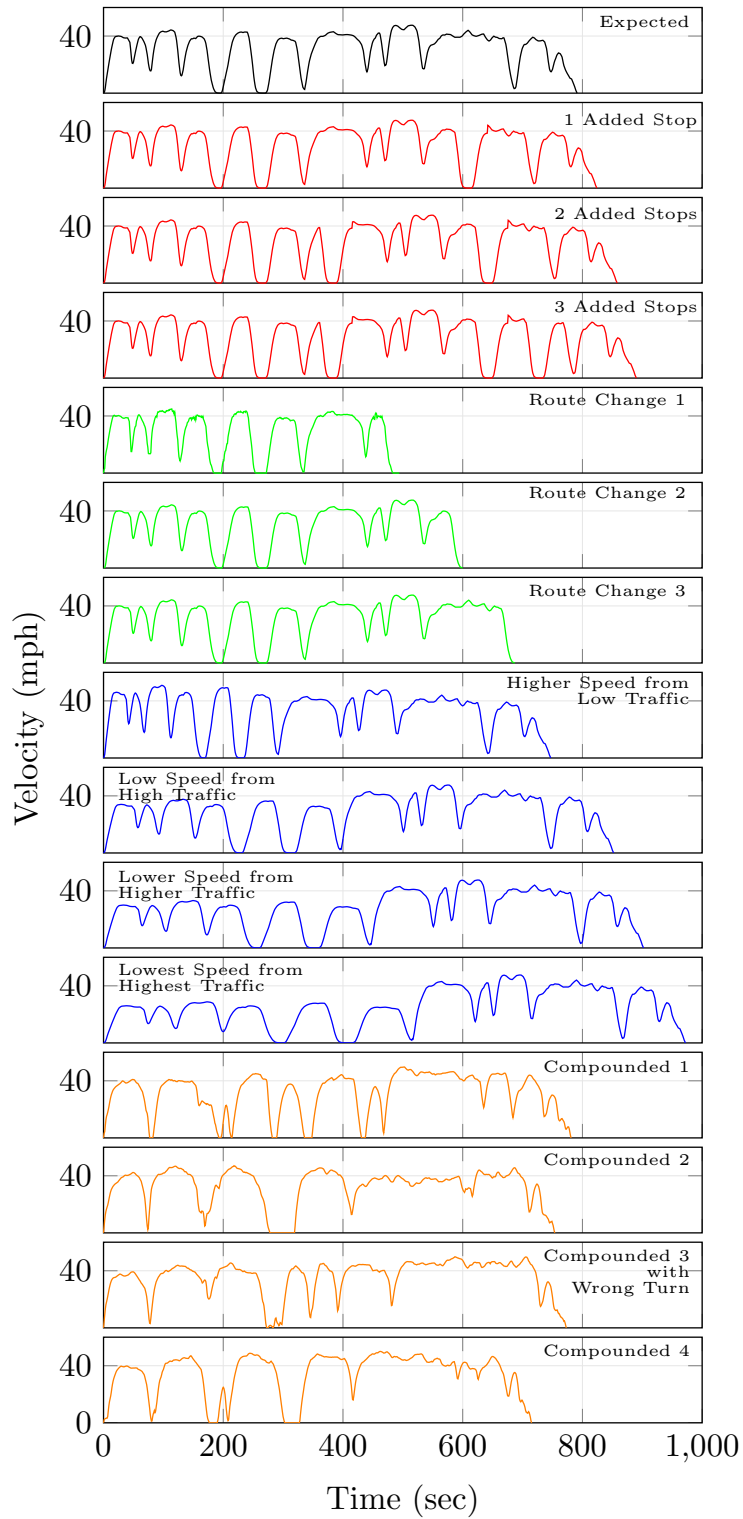
Figure 3.2: All of the drive cycles used for study 1.

3.2.2 Vehicle Model: 2010 Toyota Prius

(a)   **(b)**

Figure 3.3: Front (a) and rear (b) view of the 2010 Toyota Prius HEV simulated in studies 1 and 2.

The Toyota Prius is state of the art HEV technology and it was the first modern HEV [89]; even today it still has better FE than any other vehicle in its class [90]. Because of these reasons, a 2010 Toyota Prius is an ideal vehicle to demonstrate the potential FE improvements of the Optimal EMS.

To create the model of a 2010 Toyota Prius, the publicly available parameters shown in table 3.1 were used in the Autonomie vehicle modeling software.

Table 3.1: Table of significant model parameters that define the 2010 Toyota Prius (EM=electric motor, BSFC=brake specific fuel consumption).

Mechanical Parameters	
Vehicle Mass	1580.87 kg
Maximum Engine Power	73 kW
Engine BSFC map (g/kW·h)	$f(\text{Engine Torque, Engine Speed})$ [91]
Max Generator EM Speed	10,000 rpm
Max Traction EM Speed	13,500 rpm
Coeff. of Drag	0.259
Frontal Area	2.6005 m^2
Coeff. of Rolling Resistance	0.008
Final Drive Ratio	3.543
Ring Gear Number of Teeth	78
Sun Gear Number of Teeth	30
Wheel Radius	0.317 m
Battery Parameters	
Internal Resistance, Ω	0.373 Ω
Capacity	6.5 A·h
Open Circuit Voltage	219.7 V

Study 2: Mispredicted Vehicle Parameters

Of the parameters shown in table 3.1, several of them are subject to change due to daily driving scenarios. Study 2 assumes exact vehicle velocity prediction and seeks to analyze vehicle power mispredictions. The vehicle power mispredictions chosen for analysis include mass mispredictions, drag mispredictions, and rolling resistance mispredictions. The numbers used for each of the power mispredictions are shown in table 3.2 where the average vehicle power difference along the

same drive cycle was calculated from the output of Autonomie as

$$\text{Average Vehicle Power Difference} =$$

$$\text{Expected Parameter Average Vehicle Power}-$$

$$\text{Mispredicted Parameter Average Vehicle Power} \quad (3.1)$$

Vehicle mass mispredictions could come from extra passengers, cargo, or both. As a worst case scenario, the maximum cargo specification of 825 lbs (374 kg) from the 2010 Toyota Prius manual was used [92]. To provide a contrasting case, an elimination of an equivalent mass was used as an alternate prediction error.

Vehicle drag mispredictions could come from the addition of cargo outside the vehicle (roof rack), driving with the windows down, or even from unpredicted high winds. Research in this area suggests a loaded roof rack can cause a coefficient of drag increase of 44% and a frontal area load increase of 7% [93]. These results are dependent on the car and roof rack used for testing. As a worst case, a coefficient of drag increase of 50% and a frontal area increase of 38% was used. A similar low drag contrasting case of a coefficient of drag decrease of 50% and a frontal area of 38% was also analyzed. This low drag case also serves as a worst case prediction scenario.

Vehicle rolling resistance mispredictions could come from the over-inflated/under-inflated vehicle tires or from road conditions. A flat tire is known to cause a rolling resistance value to increase to 30 times its original value [94] and inflation pressures can cause rolling resistance changes of 50% [95]. A 100% increase in rolling resistance was analyzed as a misprediction as well as a 50% decrease.

Additional discussion in regard to changing vehicle parameters and justification for the ranges chosen can be found in the literature [96]. Note that these researchers identified these parameter mispredictions as being important to an Optimal EMS but never strictly studied them in future work.

Table 3.2: The modeling errors explored in study 2.

Vehicle Parameter	Coeff. of Drag	Frontal Area (m^2)	Mass Change (kg)	Coeff. of Rolling Resist.	Average Veh. Power Difference
Expected	0.259	2.6005	0	0.008	0%
Higher Mass	0.259	2.6005	+825	0.008	-26.2%
Lower Mass	0.259	2.6005	-825	0.008	26.6%
Higher Drag	0.3885	3.6005	0	0.008	-51.8%
Lower Drag	0.1295	1.6005	0	0.008	33.7%
Higher Rolling Resistance	0.259	2.6005	0	0.0016	-53.1%
Lower Rolling Resistance	0.259	2.6005	0	0.004	26.5%

Model Validation

Autonomie is a physics based vehicle FE model that has been demonstrated to show excellent correlation between real world operation of a 2010 Toyota Prius and a simulated 2010 Toyota Prius [97]. But, since the model of a 2010 Prius is not publicly available, the model of a 2010 Toyota Prius must be created by modifying the generic power split HEV model that comes preloaded in

Autonomie. To update the generic power split HEV model to a 2010 Toyota Prius, the parameters shown in table 3.1 were modified. Note that the BSFC map was created by matching values to data from the 2010 Toyota Prius in the public domain [91].

To validate the 2010 Toyota Prius Autonomie model, the resulting FE numbers were compared to the real world measured FE numbers from Argonne National Labs [98] over the three standard U.S. Environmental Protection Agency drive cycles as shown in table 6.1. Because the FE for each of the three drive cycles has less than 1.5% difference, the model was considered to be validated for further FE investigations.

Table 3.3: A comparison of the model simulated FE and physically measured FE for standard EPA drive cycles.

EPA Drive Cycle	Simulated Fuel Economy	Measured Fuel Economy [98]	Percent Difference
UDDS	75.4 mpg	75.6 mpg	0.3%
US06	45.9 mpg	45.3 mpg	-1.4%
HWFET	70.4 mpg	69.9 mpg	-0.7%

This validated model of a 2010 Toyota Prius provides the Baseline EMS which will be contrasted with various applications of an Optimal EMS in the results section.

3.2.3   Optimal Energy Management Derivation

Derivation of an optimal solution requires numerous iterations which is computationally costly for a model as detailed as Autonomie. Therefore, to derive the Optimal EMS, a simplified equation based power split model must be used. But, once the Optimal EMS has been calculated, it can be incorporated into Autonomie as an override of the "engine power demand" and "engine on" model parameters. A schematic of the context for optimal control derivation is shown in figure 3.4.

(a) Baseline EMS simulation — left column

Drive Cycle
Time
Velocity

Autonomie Model

Baseline Control
Actuation
Time
State of Charge
Engine Power

Calculate Performance
Fuel Consumption
State of Charge
Engine Power

Results
Fuel Economy
Final State of Charge

(a) Baseline EMS simulation

(b) Optimal EMS simulation — right column

Drive Cycle
Time
Velocity

Power Split Model

Optimal Control
Derivation
Time
State of Charge
Engine Power

Autonomie Model

Calculate Performance
Fuel Consumption
State of Charge
Engine Power

Results
Fuel Economy
Final State of Charge

(b) Optimal EMS simulation

Figure 3.4: Comparison of the simulations defined as Baseline EMS (a) and Optimal EMS (b).

Dynamic Programming Optimization Justification

Prediction errors in general have not been rigorously studied but prediction error applied to a globally Optimal EMS has not been studied at all. As mentioned in the introduction, of the five studies that address prediction error [65–69], none use a globally Optimal EMS to investigate specific types of driving-derived prediction error over a full drive cycle. The study of prediction error on a globally Optimal EMS is required because it establishes the FE difference from the absolute optimal FE. If it can be shown that driving-derived prediction error does not degrade FE

from a globally Optimal EMS, then development of any non globally Optimal EMS would be unnecessary.

DP provides a convenient method of evaluating mispredictions because, as a by-product of solution computation, it creates the globally optimal solution for all evaluated state variables while ensuring the constraints are met. This solution by-product is an optimal control matrix which serves as a lookup table to generate near optimal solutions for all feasible states of the chosen state variables. For mispredictions where the state variables are at new values, the optimal control matrix still produces a near optimal control. DP provides a unique ability to understand and quantify the FE results from prediction errors and it is well understood by other researchers.

Dynamic Programming Formulation

DP finds the optimal solution using backwards recursion, which avoids solutions that are not optimal as defined by the Bellman principle of optimality [99,100]. For every feasible state variable value, the optimal solution is stored. An appropriate DP scheme consists of a dynamic equation, a cost function, and state and control variable feasibility constraints

$$S(k+1) = S(k) + f_1(S, u, w, k)\Delta t \tag{3.2}$$

$$J = \sum_{k=0}^{N-1} f_2(S, u, w, k, \Delta t) \tag{3.3}$$

$$S_{\min}(k) \leq S(k) \leq S_{\max}(k) \qquad (k = 0, ...N) \tag{3.4}$$

$$u_{\min}(k) \leq u(k) \leq u_{\max}(k) \qquad (k = 0, ...N-1) \tag{3.5}$$

where S is the state, u is the control, w is the exogenous input, k is the timestep number, Δt is the timestep value, J is the cost, and N is the final timestep number.

For an HEV Optimal EMS derivation, the state is chosen to be the state of charge (SOC), the control is chosen to be the engine power, (P_{ICE}), the exogenous input is the vehicle velocity

(v), and the cost is chosen to be the fuel mass required (m_{fuel}). This formulation with the added feasibility constraints for a 2010 Toyota Prius yields the following modified equations

$$\text{SOC}(k+1) = \text{SOC}(k) + f_3(\text{SOC}, P_{\text{ICE}}, v, k)\Delta t \tag{3.6}$$

$$\text{Cost} = \sum_{k=0}^{N-1} m_{\text{fuel}} \tag{3.7}$$

$$\text{SOC}_{\text{min}} \leq \text{SOC}(k) \leq \text{SOC}_{\text{max}} \qquad (k = 0, ...N) \tag{3.8}$$

$$P_{\text{ICE,min}} \leq P_{\text{ICE}}(k) \leq P_{\text{ICE,max}} \qquad (k = 0, ...N-1) \tag{3.9}$$

This HEV Optimal EMS derivation can then be tailored to a 2010 Toyota Prius by deriving a power-split model.

2010 Toyota Prius Power-Split Model

The dynamic equation is derived using equations from the literature that describe a Toyota Hybrid System II [20, 101] and the parameters shown in table 3.1. The total force on the vehicle, F_{vehicle}, is

$$F_{\text{vehicle}} = C_{rr}mg + \frac{1}{2}C_d\rho_{\text{air}}v(k)^2 A_{\text{front}} + m\dot{v}(k) + mg\sin(\theta) \tag{3.10}$$

where C_{rr} is the coefficient of rolling resistance, m is the mass of the vehicle, g is the acceleration due to gravity ($9.81\ ^{m}/_{sec^2}$), C_d is the coefficient of drag, ρ_{air} is the density of air ($1.1985\ ^{kg}/_{m^3}$), v is the vehicle velocity, A_{front} is the frontal area, $\dot{v}$ is the vehicle acceleration (calculated using a numerical derivative), and θ is the elevation angle which is zero over the course of the drive cycle.

The power required by the vehicle, $P_{\text{vehicle}} = F_{\text{vehicle}}v(k)$, can come from either the engine or the battery, but excess engine power can also charge the battery. This can be expressed as

$$P_{\text{batt}} = F_{\text{vehicle}}v(k) - P_{\text{ICE}} \tag{3.11}$$

where P_batt is the battery power, P_ICE is the engine power. Note that when P_batt is negative, the battery is recharging.

The battery power shown in equation 3.11 does not account for the electric machine's efficiency. An overall efficiency map for a 2010 Toyota Prius is available in the literature [102] but the map changes as a function of voltage. It was found that incorporating a three dimensional interpolation function that would appropriately evaluate the efficiency maps was computationally prohibitive for the low level power-split model.

The change in the state of charge of the battery is given by $\frac{\mathrm{d}}{\mathrm{d}t}\text{SOC} = -I_\text{batt}/Q_\text{batt,o}$ where I_batt can be obtained by solving the quadratic electrical dynamic equation of the battery system of $P_\text{batt} = V_\text{oc}I_\text{batt} - R_\text{int}I_\text{batt}^2$ for the viable solution as $I_\text{batt} = \frac{V_\text{oc}-\sqrt{V_\text{oc}^2-4P_\text{batt}R_\text{int}}}{2R_\text{int}}$. Thus the change in state of charge of the battery is calculated as

$$\text{SOC}\,(k+1) = \text{SOC}\,(k) - \frac{V_\text{oc} - \sqrt{V_\text{oc}^2 - 4P_\text{batt}(k)R_\text{int}}}{2R_\text{int}Q_\text{batt,o}}\Delta t \tag{3.12}$$

where V_oc is the open circuit voltage, R_int is the internal resistance, and $Q_\text{batt,o}$ is the battery capacity.

Combining equations 5.2-5.3 produces the dynamic equation required in the DP algorithm

$$\text{SOC}\,(k+1) = \text{SOC}\,(k) - C_1 + C_2\sqrt{C_3 - C_4v(k) + C_5v(k)^3 + C_6\dot{v}(k)v(k) - C_7P_\text{ICE}} \tag{3.13}$$

where all C values are constants and are expressed as such for simplicity.

The cost function is derived by first obtaining a BSFC map through a cubic response surface [103] since a quadratic response surface would not match the structure of the BSFC map available in the public domain [91]. A BSFC cubic response surface has the form of

$$\text{BSFC} = A_1 + A_2\omega_\text{ICE} + A_3T_\text{ICE} + A_4\omega_\text{ICE}T_\text{ICE} + A_5\omega_\text{ICE}^2 + A_6T_\text{ICE}^2 +$$

$$A_7\omega_\text{ICE}T_\text{ICE}^2 + A_8\omega_\text{ICE}^2T_\text{ICE} + A_9T_\text{ICE}^3 \tag{3.14}$$

where all A values are constants, ω_{ICE} is the engine speed, and T_{ICE} is the engine torque. The surface developed is shown in figure 3.5. Once the BSFC response surface was developed, an ideal operating line can be computed that shows the minimum fuel consumption for any desired power (also shown in figure 3.5).
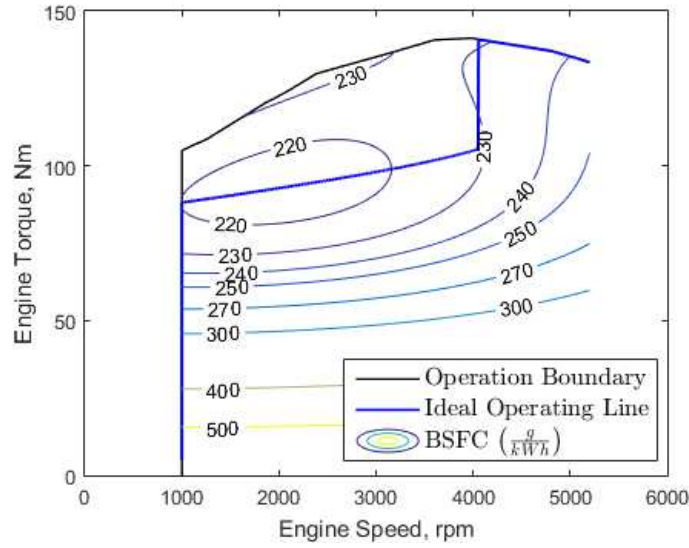
Figure 3.5: The approximated BSFC map response surface created.

For a specified power and desired minimal fuel consumption, the associated engine speed, engine torque, and fuel rate is fixed which is the concept of the ideal operating line discussed in the introduction. This idea is expressed by the following equation

$$\omega_{\text{ICE}} = f\left(P_{\text{ICE}}\right) \tag{3.15}$$

$$T_{\text{ICE}} = f\left(P_{\text{ICE}}\right) \tag{3.16}$$

$$m_{\text{fuel}} = f\left(P_{\text{ICE}}\right) \tag{3.17}$$

The functions in equation 3.17 could be expressed as an analytical function fit, but since DP uses discrete time, expression as a look up table is sufficient.

Note that it is not required to limit solutions to exist only along the ideal operating line; it is possible that overall system loss could be lessened by straying from the ideal operating line. Several test cases were completed which allow straying from the ideal operating line, but the solution for the Optimal EMS derived in the low level power-split model always ended up on the ideal operating line anyway. Significant computational savings were achieved by then only considering solutions along the ideal operating line.

A dynamic final state of charge value penalty function of

$$\text{Penalty} = W \left(\text{SOC}_f - S(N)\right)^2 ; \tag{3.18}$$

is also required where W is an arbitrary weight value which was selected to be 100,000 and $\text{SOC}_f = \text{SOC}_i = 50\%$.

The cost is then expressed as

$$\text{Cost} = \sum_{k=0}^{N-1} f_4 \left(P_{\text{ICE}}\right) + W \left(\text{SOC}_f - S(N)\right)^2 \tag{3.19}$$

Lastly, feasibility constraints must be incorporated into the model such as maximum ring gear speed, battery power, generator electric motor torque, generator electric motor speed, and generator electric motor power. It was found that the most limiting constraint was the generator electric motor speed which must be added to the DP formulation. The other constraints were incorporated in this research but are not shown due to their minimal effect.

To derive the maximum generator electric motor speed constraint, the following gearing relationship can be used

$$\omega_{\text{ICE}} = \omega_{\text{generator}} \frac{\rho}{1+\rho} + \omega_{\text{ring}} \frac{1}{1+\rho} \tag{3.20}$$

where $\rho = \frac{N_{\text{sun}}}{N_{\text{ring}}}$, $N_{\text{teeth,generator}} = 30$, and $N_{\text{teeth,ring}} = 78$. The ring gear speed is based on the vehicle speed as

$$\omega_{\text{ring}} = \frac{r_{\text{final drive}} v(k)}{R_{\text{wheel}}} \tag{3.21}$$

where $r_{\text{final drive}}$ is the final drive ratio and R_{wheel} is the wheel radius.

The constraint is then be expressed as

$$C_8 \left[f_5 \left(P_{\text{ICE}} \right) \right] + C_9 v(k) \leq C_1 0 \tag{3.22}$$

where all C values are constants.

Putting everything together, the dynamic programming formulation of the global EMS derivation for a 2010 Toyota Prius is

$$\text{SOC}\,(k+1) = \text{SOC}\,(k) - C_1 + C_2 \sqrt{C_3 - C_4 v(k) + C_5 v(k)^3 + C_6 \dot{v}(k) v(k) - C_7 P_{\text{ICE}}} \tag{3.23}$$

$$\text{Cost} = \sum_{k=0}^{N-1} f_4 \left(P_{\text{ICE}} \right) + W \left(\text{SOC}_f - \text{SOC}(N) \right)^2 \tag{3.24}$$

$$40\,\% \leq \text{SOC}(k) \leq 80\,\% \qquad (k = 0, ...N) \tag{3.25}$$

$$0\,\text{kW} \leq P_{\text{ICE}}(k) \leq 73\,\text{kW} \qquad (k = 0, ...N - 1) \tag{3.26}$$

$$C_8 \left[f_5 \left(P_{\text{ICE}} \right) \right] + C_9 v(k) \leq C_1 0 \tag{3.27}$$

where the following timestep, state, and engine power discretization values were used

$$\Delta t = 1\,\text{sec} \tag{3.28}$$

$$\Delta \text{SOC} = 0.001\% \tag{3.29}$$

$$\Delta P_{\text{ICE}} = 0.1\,\text{kW} \tag{3.30}$$

Optimal Control Model Validation

To validate this process, the Baseline EMS and the derived Optimal EMS were compared for three EPA cycles. The results are shown in table 3.4. The percent improvement numbers were calculated as

$$\text{Percent Improvement} = \frac{\text{Optimal FE} - \text{Baseline FE}}{\text{Baseline FE}} \tag{3.31}$$

where the FE is adjusted for differing SOC_f values according to the SAE J1911 "Recommended Practice for Measuring the Exhaust Emissions and FE of Hybrid-Electric Vehicles, Including Plug-in Hybrid Vehicles" standard [104].

Since there is a significant improvement in FE using the optimal control strategy implemented in Autonomie, the optimal control derivation technique is considered validated for further FE investigations. Globally Optimal EMS have been applied to these standard EPA cycles by numerous other researchers and the results in table 3.4 can also serve as validation for future researchers.

Table 3.4: A comparison of the baseline control FE and DP derived optimal control FE over three EPA drive cycles.

EPA Drive Cycle	Baseline Control Fuel Economy	Optimal Control Fuel Economy	Percent Improvement
UDDS	75.4 mpg	83.2 mpg	10.4%
US06	45.9 mpg	48.9 mpg	6.5%
HWFET	70.4 mpg	72.6 mpg	3.1%

Optimal Control with Mispredictions

A key aspect of this research is the evaluation of mispredictions using DP derived optimal control. DP provides an optimal control solution matrix which is valid for any state of charge and time during the drive cycle. The optimal control solution matrix for the expected drive cycle

(shown in figure 3.1b) was computed and is shown in figure 3.6. This matrix is used to evaluate all the mispredictions from study 1 and study 2. As a basis for comparison, the solution using the optimal control matrix for perfect prediction for each case was also computed.
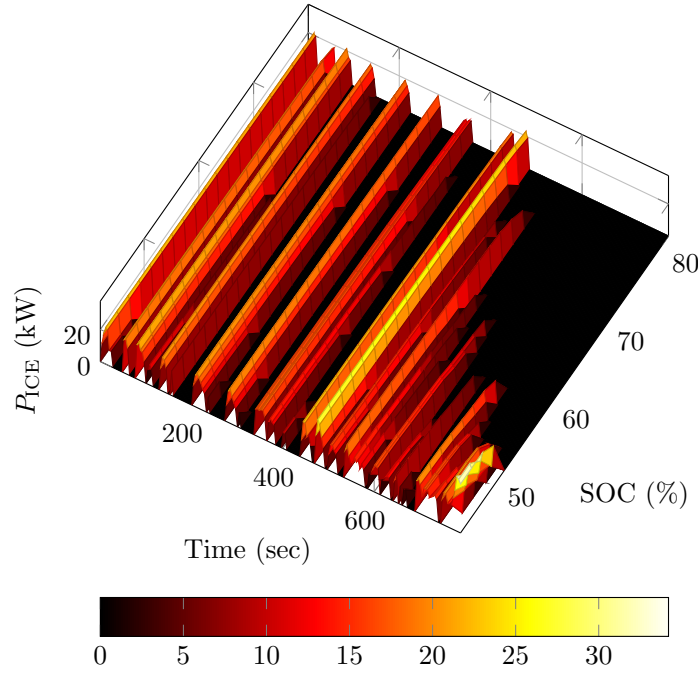
Figure 3.6: The optimal control matrix derived using DP for the expected drive cycle.

Drive cycle mispredictions are handled by converting the time state variable to a distance state variable numerically as distance $= \sum_{k=0}^{N} v(k)$ since all mispredictions occur over the same route. The mean absolute percent error (MAPE) applied to vehicle velocity has been defined in other prediction error research [67] as

$$\text{MAPE} = \frac{1}{N} \sum_{k=0}^{N} \frac{|\text{Actual Velocity} - \text{Predicted Velocity}|}{\text{Actual Velocity}} \tag{3.32}$$

and is under 20% in almost misprediction cases studied. Examples of the mispredictions when the time state variable is converted to a distance state variable are shown in figure 3.7.

For any state not in the design space, the Baseline EMS is employed.
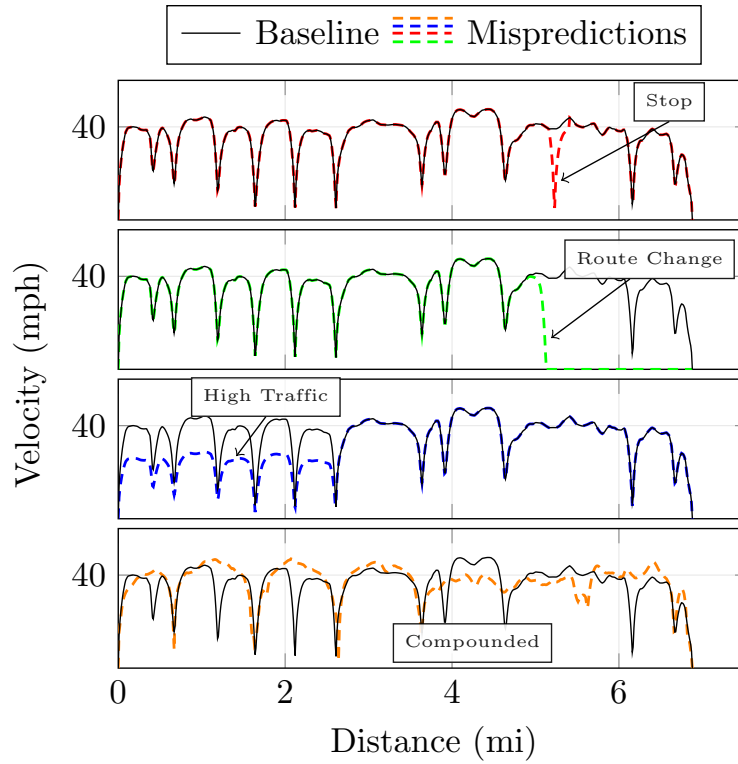
Figure 3.7: Examples of the drive cycles when time is converted to a distance for the velocity prediction errors associated with study 1.

3.3 Results and Discussion

The results are organized into subsections for study 1 and study 2. For each type of misprediction, FE results are shown for perfect prediction and misprediction (prediction of the expected drive cycle or prediction of the expected vehicle parameters). A discussion of the results from each instance of misprediction are shown with the relevant vehicle signals. Additional vehicle signals over each drive cycle are provided in the supplementary report.

3.3.1 Study 1: Optimal Energy Management Under Vehicle Velocity Mis-predictions
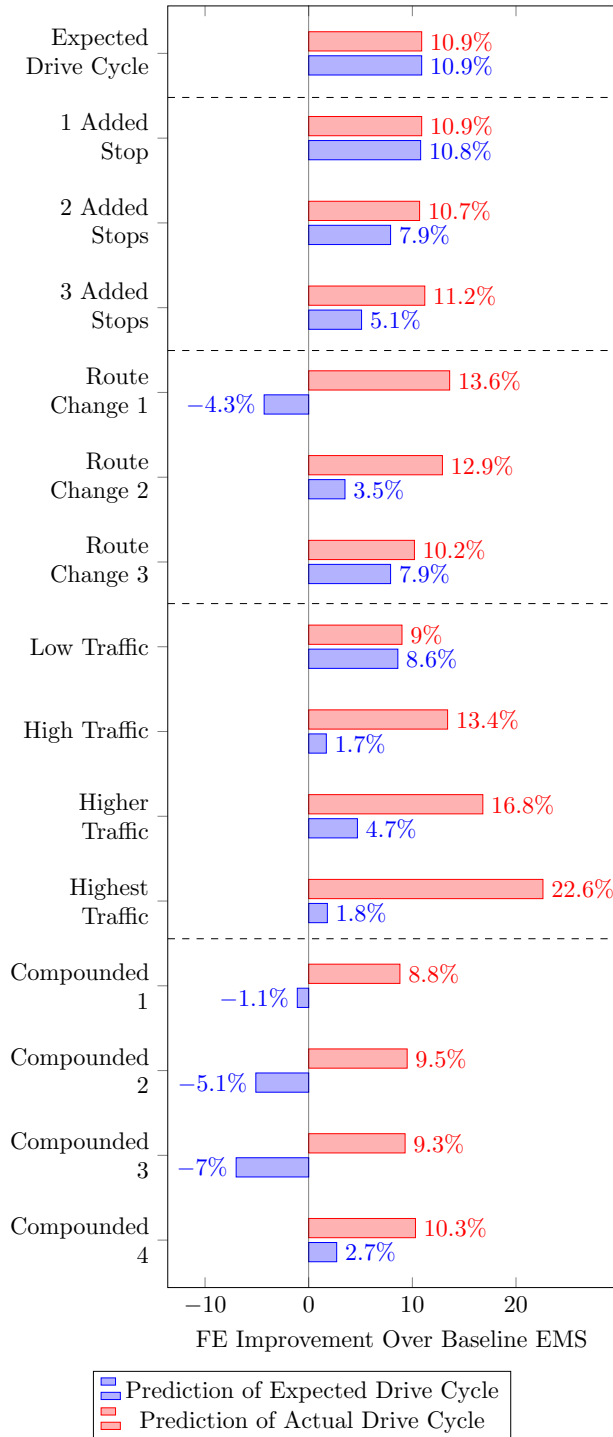
Figure 3.8: FE results that compare Optimal EMS using incorrect and correct drive cycle predictions (drive cycles shown in figure 3.2).

FE was improved over the 2010 Toyota Prius Baseline EMS in every case except for under a fast route change and compounded misprediction drive cycles. The FE numbers from study 1 shown in figure 3.8 motivates the following five results about globally Optimal EMS: (1) exact drive cycle prediction increases FE as expected from the literature, (2) FE gains are maintained under mispredicted stops, (3) FE gains may not be maintained under route-change mispredictions, (4) FE gains are maintained under mispredicted traffic, and (5) FE gains may not be maintained under compounded mispredictions.

Result 1: Exact Prediction Increases Fuel Economy

Figure 3.8 shows a 10.9% increase in FE if the exact drive cycle is predicted. This increase in FE over the Baseline EMS comes from four sources:

1. Elimination of low power engine operation (fig 3.9a)

2. Reduction of high power engine operation (fig 3.9b)

3. Reduction of battery charging at the beginning of the drive cycle (fig 3.10a and 3.10b)

4. Increase in battery charging at the end of the drive cycle (fig 3.10a and 3.10b)
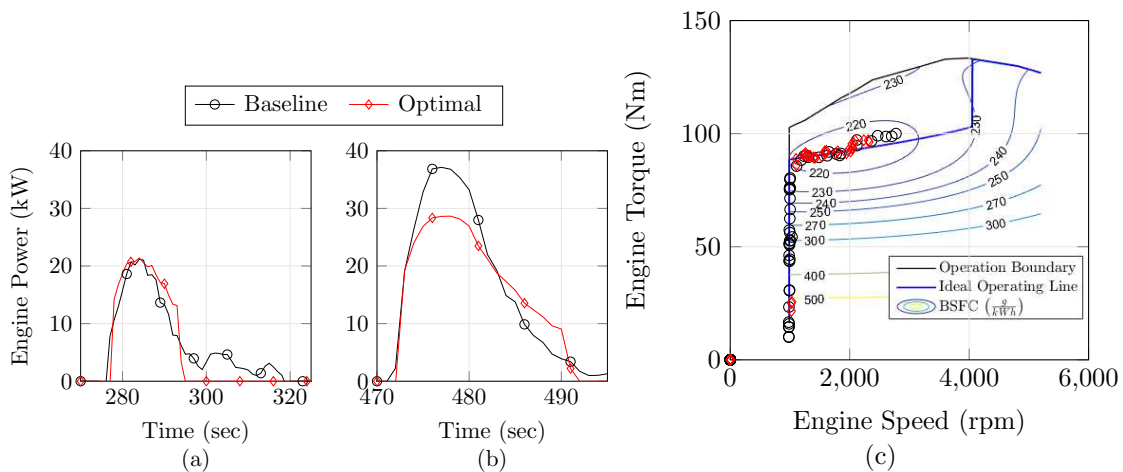
Figure 3.9: Low engine speed operation (a), high engine speed operation (b), and engine brake specific fuel consumption (BSFC) comparisons (c).

57

The elimination of low power engine operation and the reduction of high speed engine operation allows the engine to operate in a region on the brake specific fuel consumption map that has high efficiency, as shown in figure 3.9c. The Optimal EMS demonstrates the behavior shown in figures 3.9a and 3.9b over the entire drive cycle while maintaining the desired final state of charge and accumulates small decreases in fuel consumption which accumulate into a significant improvement in FE.
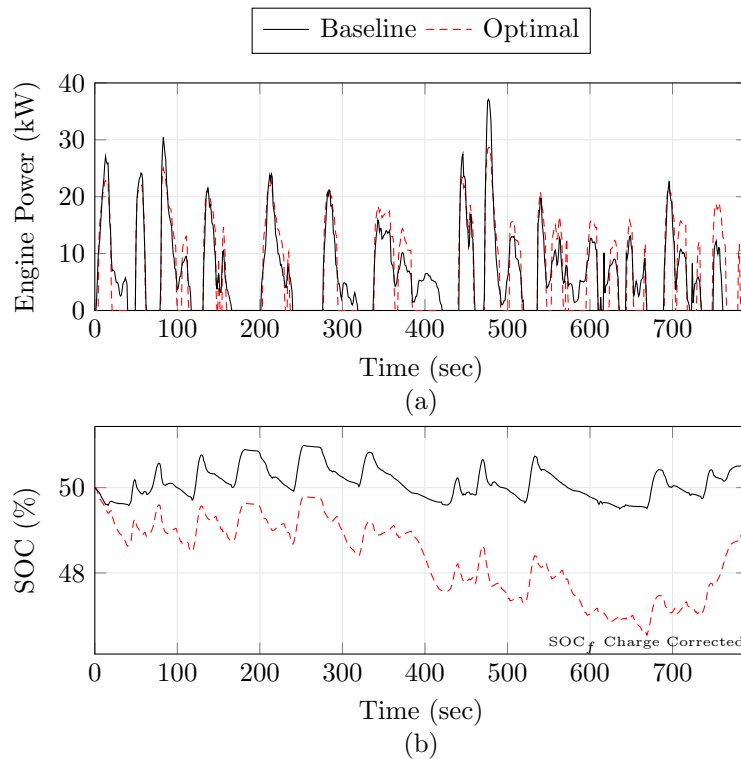
Figure 3.10: Comparison of Baseline EMS and Optimal EMS engine operation and state of charge results for the expected drive cycle.

The Optimal EMS increases FE through a reduction of battery charging at the beginning of the drive cycle and an increase in battery charging at the end of the drive cycle. This is accomplished through lowered peak engine power (closer to an optimal value) during the approximate first half of the drive cycle and increased peak engine power (closer to an optimal value) during the approximate second half of the drive cycle. Both of these engine power modifications result in an increase in engine efficiency as shown on the brake specific fuel consumption map in figure 3.9c.

Result 2: Fuel Economy Gains are Maintained Under Stop Misprediction

Related to the Baseline EMS, figure 3.8 shows a +10.8% (out of +10.9% possible) increase in FE if one stop is mispredicted, a +7.9% (out of +10.7% possible) increase in FE if two stops are mispredicted, and a +5.1% (out of +11.2% possible) increase in FE if three stops are mispredicted. This demonstrates that FE gains through the Optimal EMS are maintained under stop mispredictions because a FE increase is still achieved in every misprediction case that was studied.

Figure 3.11 shows the details of the "1 Added Stop" misprediction case. The actual and expected drive cycle differences are shown in figure 3.11b. When the stop is mispredicted, the Optimal EMS misapplies engine power as shown in figure 3.11c. This misapplication of engine power occurs because the Optimal EMS was derived assuming that the vehicle is traveling at 40 mph but the vehicle actually stops, remains stationary, and then accelerates. Overall, the engine power misapplication is a slight delay and does not affect fuel economy and state of charge significantly as shown in figures 3.8 and 3.11c.
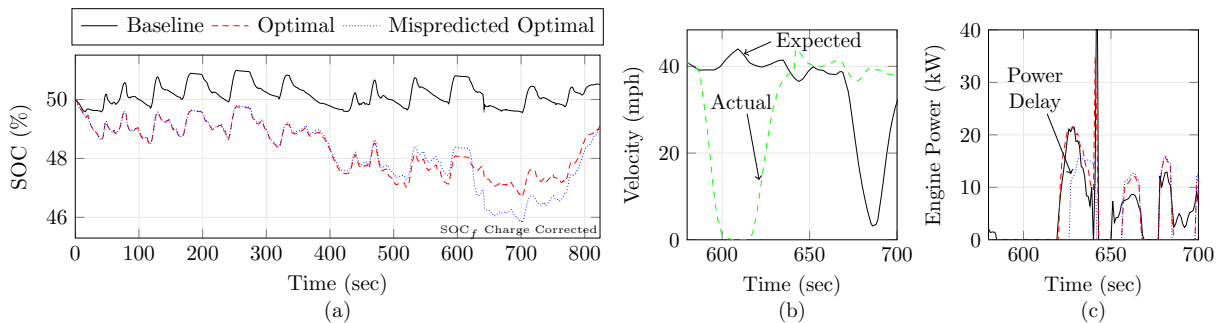
Figure 3.11: Baseline, optimal control, and mispredicted optimal control results for the "1 Added Stop" misprediction case.

Result 3: Fuel Economy Gains May be Lost from Route Change Misprediction

Related to the Baseline EMS, figure 3.8 shows a -4.3% (out of +13.6% possible) FE result if the drive cycle is the same as expected but then is suddenly ended shortly after it has begun (Route Change 1). This figure also shows a +3.5% (out of +12.9% possible) increase in FE if the drive cycle is suddenly ended midway through the predicted drive cycle, and a +7.9% (out of +10.2%

possible) increase in FE if the drive cycle is suddenly ended most of the way through the predicted drive cycle. This demonstrates that FE increases through the Optimal EMS may be decreased when a route change is mispredicted.

The Optimal EMS seeks to equate the state of charge at the beginning and the end of the drive cycle only. During the drive cycle, the optimization routine is only constrained by the physical maximum and minimum battery charge limitations. Therefore, when a route change is mispredicted, the battery state of charge could be excessively high or low which could result in a loss of battery state of charge adjusted FE. This battery state of charge discrepancy is shown in figure 3.12a, which presents results for "Route Change 1". Additionally, as can be seen in figure 3.12b, the mispredicted optimal control case seeks engine operation in anticipation of a forthcoming acceleration shown in figure 3.12a. But, since the acceleration shown in figure 3.12a is not realized, the FE is decreased.
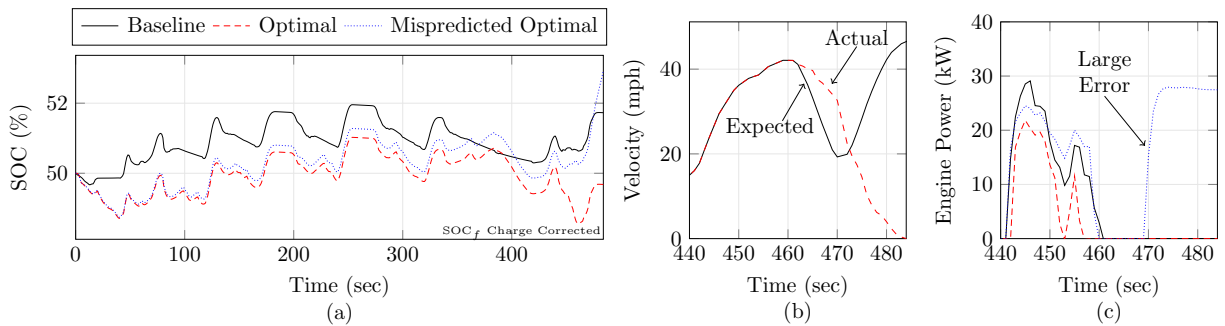
Figure 3.12: Baseline, optimal control, and mispredicted optimal control results for the "Route Change 1' misprediction case.

Result 4: Fuel Economy Gains are Maintained Under Traffic Misprediction

Related to the Baseline EMS, figure 3.8 shows an +8.6% (out of +9.0% possible) increase in FE if traffic levels are lower than expected (higher than expected vehicle speeds), a +1.7% (out of +13.4% possible) increase in FE if traffic is higher than expected (low vehicle speed), a +4.7% (out of +16.8% possible) increase in FE if traffic is significantly higher than expected (lower vehicle speed), and +1.8% (out of +22.6% possible) increase in FE if traffic is much higher

than expected (lowest vehicle speed). This demonstrates that the fuel economy gains from the Optimal EMS are maintained under traffic mispredictions because a FE increase is still achieved in every misprediction case with the caveat that if traffic is higher than predicted, there is a significant loss in *potential* FE improvements through the Optimal EMS.

For the "High Traffic" misprediction, the actual drive cycle is at speeds much lower than the predicted drive cycle as shown in figure 3.13b. This speed discrepancy results in the mispredicted Optimal EMS operating the engine at an excessively high power as shown in figure 3.13c. The higher than required engine power drives the battery state of charge up as shown in figure 3.13a. The Optimal EMS is still designed to end the state of charge at 50% so the state of charge is decreased over the second half of the drive cycle and a fuel economy improvement over the Baseline EMS is maintained.
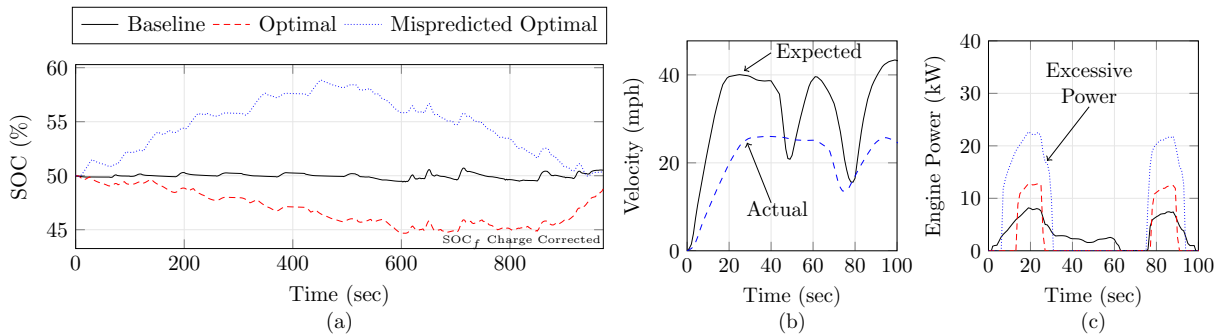
Figure 3.13: Baseline vs optimal control results for the "High Traffic" misprediction case.

Result 5: Fuel Economy Gains May be Lost from Compound Prediction Errors

A real world driven alternate drive cycle along the same route produces mispredicted stops, traffic, and potentially route changes. Figure 3.8 shows a -1.1% (out of +8.8% possible) FE result for an alternate drive cycle driven along the same route, a -5.1% (out of +9.5% possible) FE result for another alternate drive cycle driven along the same route, a -7.0% (out of +9.3% possible) FE result for an alternate drive cycle driven that includes a wrong turn but was intended to be driven along the same route, and a +2.7% (out of +10.3% possible) FE result for a fourth alternate drive cycle driven along the same route.

61

Despite the conversion of the time state variable to a distance state variable, the velocities are significantly different along the entire drive cycle as shown in figure 3.7. The sections with the most drastic velocity discrepancies as shown in figure 3.14b result in sections of high power engine operation at completely inappropriate points in the drive cycle as shown in figure 3.14c. Because of these large discrepancies in engine operation, the FE is worse than the Baseline EMS in almost every case of compounded prediction errors.
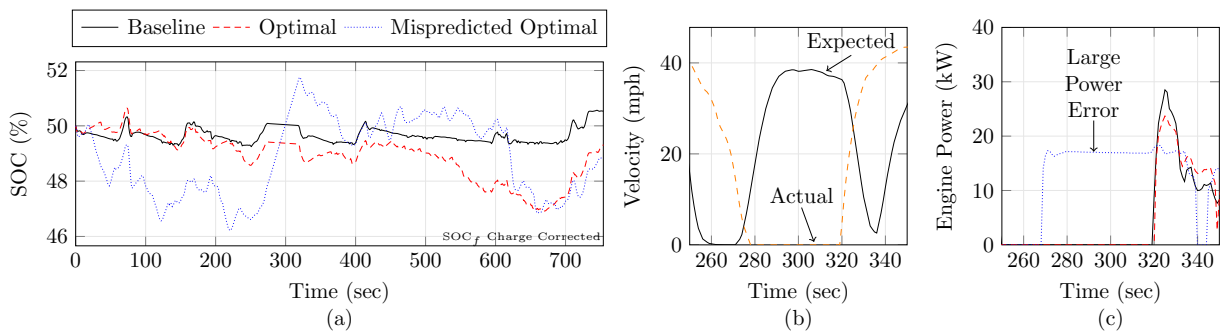
Figure 3.14: Baseline vs optimal control results for the "Compounded 2" misprediction case.

Study 1 Summary

The following results were obtained in study 1:

1. Fuel economy gains from the Optimal EMS are **maintained** under stop mispredictions

2. Fuel economy gains from the Optimal EMS are **maintained** under traffic mispredictions

3. Fuel economy gains from the Optimal EMS **may be lost** under route change mispredictions

4. Fuel economy gains from the Optimal EMS **may be lost** under compounded mispredictions

3.3.2 Study 2: Optimal Energy Management Vehicle Under Power Mispredictions
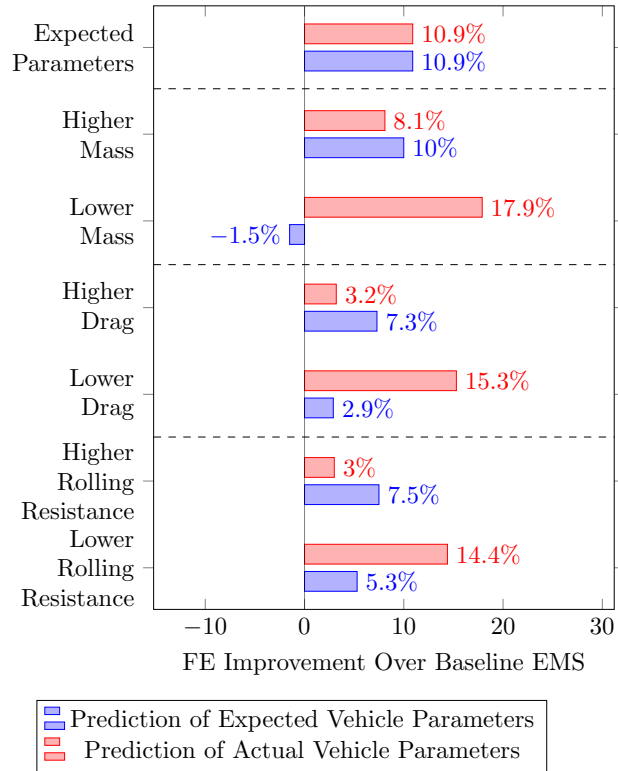
Figure 3.15: FE results that compare Optimal EMS using incorrect and correct vehicle parameter prediction (vehicle parameters shown in table 3.2).

FE was improved over the 2010 Toyota Prius Baseline EMS in every type of power misprediction except when the vehicle mass is severely under predicted ("Lower Mass" case) which is unlikely to occur in standard vehicle operation. The FE numbers from study 2 shown in figure 3.15 motivate the following two results: (1) FE gains are maintained under higher than expected vehicle power mispredictions and (2) FE gains are maintained under lower than expected vehicle power mispredictions.

Result 6: Fuel Economy Gains are Maintained Under Higher than Predicted Vehicle Power

Related to the Baseline EMS, figure 3.15 shows an +10.0% (out of +8.1% possible) FE result for a higher than expected vehicle mass, a +7.3% (out of +3.2% possible) FE result for a higher than

expected vehicle drag, and a +7.5% (out of +3.0% possible) FE result for a higher than expected rolling resistance.

When predicting vehicle power to be higher than actual vehicle power ("Higher Mass", "Higher Drag", and "Higher Rolling Resistance" cases), the Optimal EMS solution behaves in nearly the same as perfect prediction, except at a lower engine power, as seen in figure 3.16b. The result is a state of charge value well below 50% for the majority of the drive cycle as shown in figure 3.16a. The ending state of charge value is then significantly below the target value which results in a higher state of charge adjusted FE than the optimal solution based on the SAE J1711 standard [104].
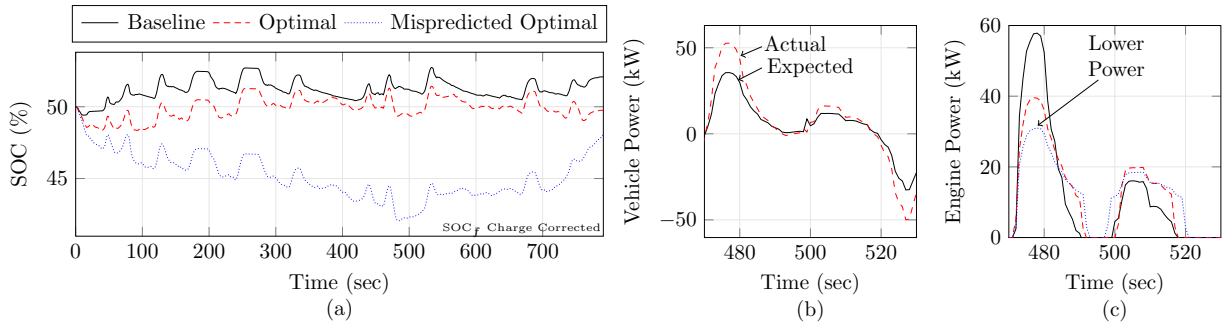
Figure 3.16: Baseline vs optimal control results for the "Higher Mass" misprediction case.

Result 7: Fuel Economy Gains are Maintained Under Lower than Predicted Vehicle Power

Related to the Baseline EMS, figure 3.15 shows a -1.5% (out of +17.9% possible) FE result for a lower than expected vehicle mass, a +2.9% (out of +15.3% possible) FE result for a lower than expected vehicle drag, and a +5.3% (out of +14.4% possible) FE result for a lower than expected rolling resistance.

When predicting vehicle power to be lower than actual vehicle power ("Lower Mass", "Lower Drag", and "Lower Rolling Resistance" cases), the Optimal EMS solution behaves in nearly the same as perfect prediction, except at a higher peak value as seen in figure 3.17b. The result is a state of charge value well above 50% for the majority of the drive cycle as shown in figure 3.17a.

The ending state of charge value is significantly above the target value which results in a lower state of charge adjusted FE than the optimal solution based on the SAE J1711 standard [104].
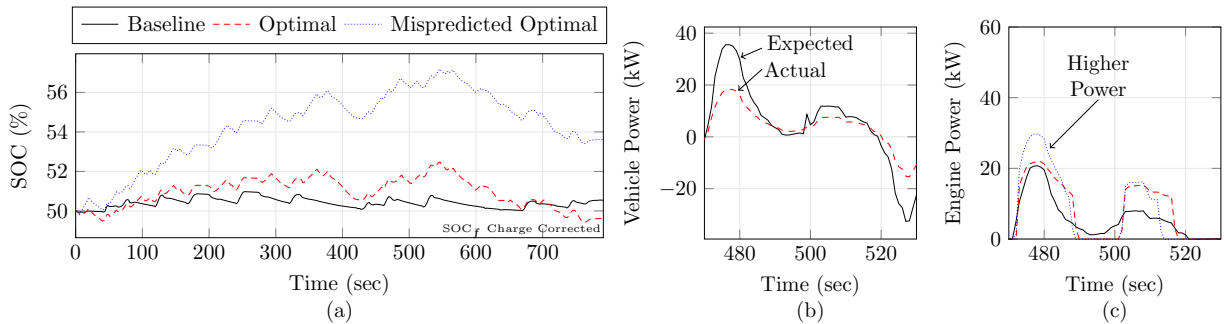
Figure 3.17: Baseline vs optimal control results for the "Lower Mass" misprediction case.

Study 2 Summary

The following results were obtained in study 2:

1. Fuel economy gains from the Optimal EMS are **maintained** under vehicle parameter mispredictions

2. Vehicle parameter mispredictions that result in **lower** average vehicle power result in a **higher** operating battery state of charge

3. Vehicle parameter mispredictions that result in **higher** average vehicle power result in a **lower** operating battery state of charge

3.4 Conclusions

In this study, an Optimal EMS with driving-derived mispredictions and vehicle power mispredictions was studied to quantify the fuel economy cost of misprediction. First, an expected drive cycle and fourteen drive cycle mispredictions were developed. Then, a validated 2010 Toyota Prius model was developed by updating the generic power-split HEV model in Autonomie with publicly available 2010 Toyota Prius data. Six cases of vehicle parameter mispredictions were also developed based on plausible values from the literature to investigate the effects of required

vehicle power mispredictions. A globally Optimal EMS derivation was developed using DP and an equation based model for the Toyota Hybrid System II used by the Toyota Prius. A misprediction analysis technique was developed using the optimal control solution matrix from DP and converting the time variable to a distance variable.

For many of the driving-derived mispredictions (stops, traffic, and vehicle power), a fuel economy improvement of the Optimal EMS over the Baseline EMS is maintained. For compounded mispredictions and route change mispredictions the fuel economy gains from the Optimal EMS may be lost. The results from studies 1 and 2 suggest that FE improvements over the Baseline EMS through a globally Optimal EMS are possible without perfect prediction.

Evaluating driving-derived mispredictions puts any alternate EMS into a more realistic context. The techniques presented in this research can be applied to an alternate EMS such as Equivalent Consumption Minimization Strategy (ECMS), adaptive Equivalent Consumption Minimization Strategy (a-ECMS), Stochastic Dynamic Programming (SDP), or Model Predictive Control (MPC). But, an EMS designed to be stochastically robust such as a-ECMS or SDP, may not maintain a FE improvement when subjected to certain driving-derived mispredictions because driving-derived mispredictions (mispredicted stops, route change, etc.) are not stochastic. The results from this study indicate that a globally Optimal EMS may provide the best fuel economy improvements even when mispredictions exist.

Future work can consider the application of driving-derived mispredictions to other Optimal EMS from the literature, sensors/signals/algorithms required for vehicle operation prediction, and implementability of an Optimal EMS in a modern vehicle operating in the current driving environment. An initial study using only current vehicle speed and GPS location shows promising fuel economy results from an Optimal EMS [105].

3.5 Chapter Conclusions

This section of the research effort has allowed us to address Research Question 1, which is restated here:

Research Question 1: What are the effects of different types of prediction errors on the fuel economy results enabled by predictive energy management?

Research Question 1 is associated with Hypothesis 1:

Hypothesis 1: Certain misprediction types will result in FE improvements being maintained while other misprediction types will result in a FE loss.

This research effort has provided support for this hypothesis. Through development of real world drive cycles that represent various types of misprediction, development of a dynamic programming algorithm that derives the globally Optimal EMS, and a high-fidelity 2010 Toyota Prius model, it has been determined that stop, traffic, and vehicle parameter mispredictions result in FE improvements being maintained while route changes and compounded mispredictions result in a FE loss. This informs prediction strategies since highly accurate predictions of the number of stops, traffic levels, and vehicle parameters are not required to improve FE with predictive energy management.

Chapter 4

Improved Fuel Economy through Acceleration Event Prediction Part 1: Optimal Control

This study investigates the FE impacts of acceleration event (AE) prediction within a drive cycle and involves development of an AE dataset, organization of the AE dataset, application of the dynamic programming algorithm, a high fidelity model of a 2010 Toyota Prius, a technique to identify characteristic AEs, and a technique to evaluate AE mispredictions with the optimal control matrix result from the dynamic programming algorithm. This research is part of an ongoing project funded by Toyota. David A. Trinko has also made significant contributions to this project by improving the vehicle model and expanding the study to include numerous organization schemes and results for each AE category. This monumental research effort is just now reaching the publication phase with a conference publication [106] and the recently submitted journal paper reproduced in this chapter [107].

4.1 Introduction

Advanced vehicle powertrain control strategies have the potential to improve fuel economy (FE) by up to 30%, but additional research is required before vehicle implementation can be realized [4]. An investigation of the trade-offs between prediction scope and the FE improvement result is required.

4.1.1 Fuel Economy Improvement Needs

Transportation accounts for approximately one third of worldwide energy consumption [108]. When this energy is generated from combustion engines, petroleum importing and exporting is required, air pollution is released, and global warming is exacerbated. On a per-country basis, petroleum consumption is often unbalanced from domestic production, creating the issue of energy

security and vulnerability to geopolitical stability [7] such as the 1973-1974 oil embargo on the United States [109]. The greenhouse gas emissions from transportation combustion engines [110] contribute significantly to the increasing global temperature which can severely inhibit animal and human life [111]. Transportation combustion engines also contribute to air pollution [87] which is the fourth-leading cause for premature death worldwide [16].

To combat these issues, countries from all over the world have implemented FE regulations [17, 112, 113] with many countries taking the initiative to ban gasoline and diesel powered vehicles outright between the years 2025 to 2040 [114–118]. In the U.S., FE is regulated by the Corporate Average Fuel Economy (CAFE) rules, first established in 1975, as well as other regulations such as the Environmental Protection Agency Clean Air Act [119], and the California Air Resources Board [120].

In 2009, the CAFE requirements were increased and research at the time showed that the increases could be met through improved vehicle design [121]. This CAFE increase affected model year vehicles from 2012-2016 with the 2016 requirement being an average fuel economy of 34.1 mpg for cars and light trucks [122]. This increase was projected to save up to 96 billion gallons of fuel and provide up to $170 billion in net societal benefits [123]. In 2011, the CAFE requirements were increased again affecting model year vehicles from 2017-2025 with the 2025 requirement being an average fuel economy of between 48.7 and 49.7 mpg for cars and light trucks [124]. This increase is projected to save up to 269 billion gallons of fuel and provide up to $483.2 billion in net societal benefits [125]. A review to determine the efficacy of meeting the 2022-2025 mpg standards was completed in 2016. This review notes that, on average, the automotive industry is over-complying with CAFE rules, a wide range of technologies exists for manufacturers to use to meet the 2022-2025 FE rules, and the 2022-2025 FE rules should not be adjusted [126, 127]. Despite these findings, the current CAFE rule effective date is being delayed [128] while the FE requirement is being reconsidered based on a perceived high cost to comply [129].

4.1.2 Optimal Energy Management to Increase Fuel Economy

Technologies used to increase FE for CAFE compliance include engine sizing, advanced engine control, friction/mass/drag reduction, and powertrain electrification [126]. But, there are numerous technologies that are not currently being utilized for CAFE compliance such as implementation of an optimal energy management strategy (Optimal EMS) which has demonstrated FE improvements of up to 30% for hybrid vehicles [130].

An Optimal EMS is the application of optimal control to vehicle powertrain operation with the objective of minimizing fuel consumption (maximizing FE). The earliest roots of optimal control can be traced back to the development of Calculus of Variations [131]. In the early 1960s, calculus of variations was modified to handle various constraints in an application known as Pontryagin's Minimization/Maximization Principle [132]. In the 1950s with the advent of the digital computer, a numerical scheme was invented known as dynamic programming (DP) [100]. These two methods are the main techniques still in use today to derive the globally optimal solution under the assumptions of discretization and they have been applied to numerous control problems [99]. To achieve a globally optimal control, knowledge of future events is required.

In the early 2000s, optimal control was applied to hybrid electric vehicles (HEVs) to determine the optimal usage of battery propulsive power versus engine propulsive power to produce the minimum fuel consumption, in other words, the Optimal EMS [32]. This foundational research focused on obtaining the globally optimal control through DP using 100% accurate prediction of an entire discretized drive cycle. Since then, researchers have investigated stochastically robust strategies [47, 48, 85, 133, 134] as well as fast computation strategies [49–51, 135, 136] which also require drive cycle predictions. The overall goal of HEV Optimal EMS research is to realize globally optimal FE from vehicle control. The main challenge with Optimal EMS implementation is the computational cost in processing sensor data to make predictions which are then used to derive the Optimal EMS [4]. As a subset of this general problem, this research investigates potential FE improvements from a DP derived Optimal EMS applied to *acceleration events (AE) only*.

4.1.3 Optimal Energy Management of Acceleration Events

Acceleration portions of driving require the most propulsive power and consume the most fuel relative to distance [137], thus they may represent the ideal place to apply optimal control. The proposed prediction requirement for optimal control of AEs is feasible since it can be accomplished using GPS location and speed limit information.

Initial research on AEs suggests that velocity and fuel consumption can be accurately modeled with sinusoidal and polynomial models that satisfy a zero jerk condition consistent with real world driving [138] but it is difficult to capture an inclusive set of AEs due to the variability introduced by obstacles such as roundabouts, intersections, and crossings for different vehicles' traffic conditions and road types [139, 140]. Additionally, substantial variations in driver behavior in regard to AEs results in significantly different fuel consumption rates [137] and many studies of AEs have become experimental and data-driven [141].

The goal of this study is to derive an Optimal EMS for general, real-world, AEs but then apply the Optimal EMS to many similar AEs thus eliminating the need for real-time calculations. This paper expands upon a previous research finding that FE improvements are possible for a DP derived Optimal EMS despite mispredictions [142] and is part one of two in this investigation. In part one of the study, a rigorous investigation of an Optimal EMS applied to AEs is undertaken. In part two of this study, the technique of Optimal EMS applied to AEs is implemented in several full drive cycles.

4.1.4 Novel Aspects/Unique Contributions of this Research

This research makes the following new and novel contributions to the HEV Optimal EMS body of knowledge:

1. Comprehensive analysis of thousands of AEs using an Optimal EMS

2. Feasibility investigation of applying precomputed AE Optimal EMS

3. Performance categorization of an Optimal EMS applied to AEs

4. Use of optimal control solutions that are a function of velocity which only works for monotonic drive segments

4.2 Methods

To understand the FE improvement potential of AE prediction, first a large database of real world AEs is extracted from real world drive cycles. These AEs are then organized into various categorization schemes. Next, two control methods are developed to implement in a model of a 2010 Toyota Prius: a baseline energy management strategy (Baseline EMS) and an Optimal EMS. Lastly, a custom battery state of charge (SOC) adjusted FE calculation technique is developed for AEs to ensure unbiased FE comparison.

4.2.1 Acceleration Event Dataset Development

Data was recorded from several 2010 Toyota Prius drivers in the California area. The data is composed of 384 drive cycles measured at at 10 Hz (0.1 second timesteps) with an average time length of 1086 seconds and an average velocity of 28.05 mph $\left(\frac{\text{miles}}{\text{hour}}\right)$. An example drive cycle is shown in Fig. 4.1.
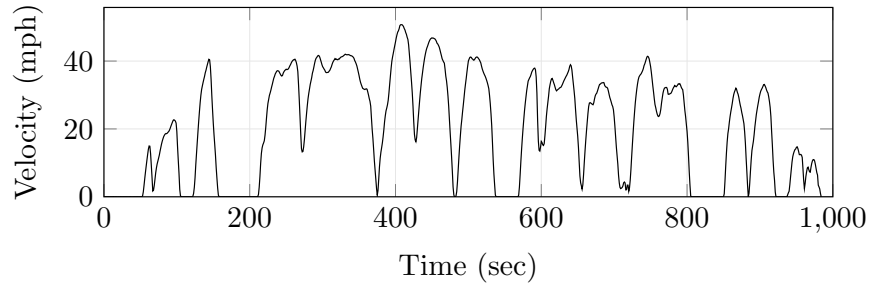
Figure 4.1: One of the drive cycles in the real world drive cycle data set.

AEs can be extracted by identifying sections of speed data where $v_j - v_{j-1} > 0$. But, for real-world accelerations, there are moments of steady or even decreasing speed within an AE and a two timestep evaluation will yield erroneous results. Additionally, the real world drive data has a high resolution and a strict equality evaluation for steady sections ($v_j - v_{j-1} = 0$) is insufficient. To

address these issues, AEs were extracted by searching for sections satisfying the following logic statement where $\wedge$ represents logical conjunction (i.e. an 'and' statement)

$$(v_j - v_{j-1}) \wedge (v_{j+1} - v_j) \wedge (v_{j+2} - v_{j+1}) \wedge (v_{j+3} - v_{j+2}) \leq 0.05 \text{ mph} \qquad (4.1)$$

If equation 4.1 is true, then this section of the drive cycle is labeled as an AE. From these extracted AEs, if they either start from a negative speed, last for one second or less, or only increase speed by 5 mph or less then they are ignored. A conceptual plot of the identification of AEs in an example drive cycle is shown in Fig. 4.2.
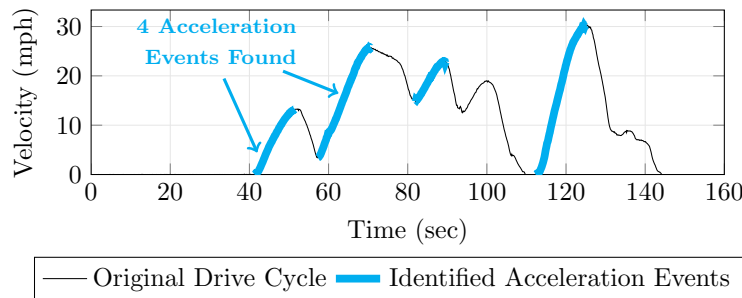
Figure 4.2: Example of the results from the AE extraction algorithm. Note that one AE is ignored for having a velocity increase less than 5 mph.

Using this process, 7,708 AEs are extracted from the 384 drive cycles for analysis. Next, each AE is prepended with 8 seconds of the initial velocity to ensure the vehicle is at steady state at the beginning of each AE and appended with 12 seconds of the final velocity to ensure the vehicle is at steady state at the end of each AE. An example of the resulting AE cycle is shown in Fig. 4.3.
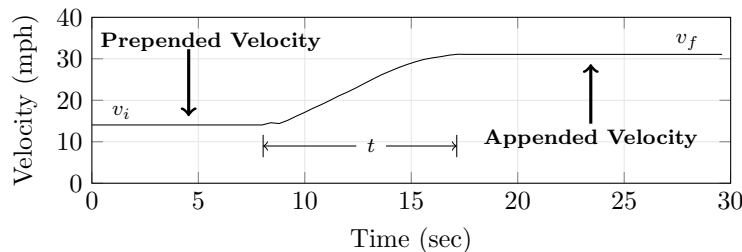
Figure 4.3: Example of prepending and appending constant velocity to each AE to ensure steady state.

The 7,708 AEs with the prepended and appended velocity states range from 22 seconds long to 76 seconds long and include speeds from 0 mph to 50 mph. To derive generalized improved control strategies, this dataset of AEs must now be categorized.

4.2.2 Acceleration Event Categorization

Three different AE categorization schemes were chosen for this analysis on the basis of principle component analysis applied to the dataset:

1. Starting velocity and ending velocity categorization; v_i, v_f

2. Time duration and ending velocity; t, v_f

3. Average acceleration and ending velocity; $\frac{v_f - v_i}{t}$, v_f

where the variables v_i, v_f, and t are shown in figure 4.3.

The first categorization scheme, starting velocity and ending velocity, is shown in Fig. 4.4. The x-axis shows the assigned AE category number, e.g. category 1, 2, 3, etc. The left y-axis shows the velocity range. For example category 1 captures all AEs that start at 0 mph and end at 7.8±1.5 mph. The right y-axis shows the number of AEs in the AE category, for example there are about 321 AEs in category 1 (starting around 0 mph and end around 7.8±1.5 mph). Overall, Fig. 4.4 shows there are a high number of low velocity AEs and a small number of high velocity AEs in the dataset.
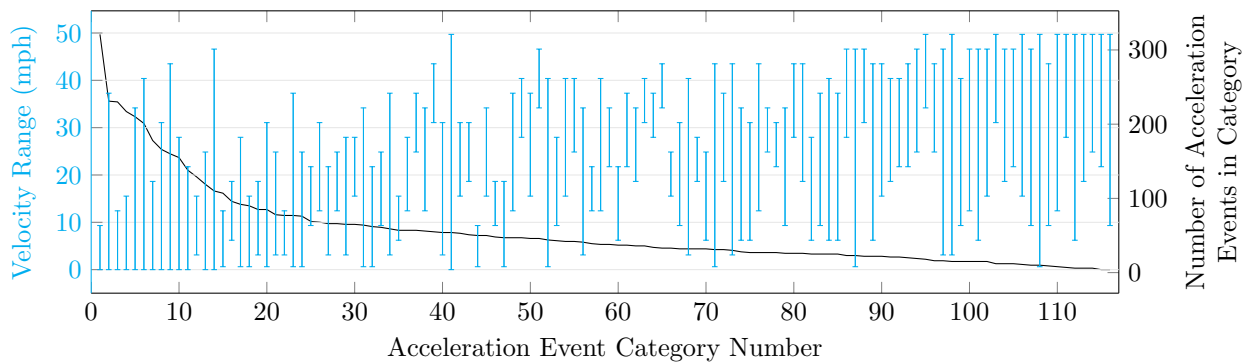
Figure 4.4: Plot showing the velocity range and the number of AEs in each category for the starting velocity and ending velocity categorization scheme.

The second categorization scheme, time duration and ending velocity, is shown in Fig. 4.5. The x-axis and right y-axis are consistent with first categorization scheme plot, Fig. 4.4. But now the left y-axis shows the ending velocity (as red X's) and the total time duration (as blue dots) of each category. For example, category 1 has a total time duration of 6.2±1.4 seconds and an ending velocity of 12.2±2.2 mph for which there are 274 AEs. Note that the total time duration is shown without prepended and appended velocity (Fig. 4.3) that is used to ensure steady state. Overall Fig. 4.5 shows that, in general, there is a high number of short duration AEs and a low number of long duration AEs in this dataset.
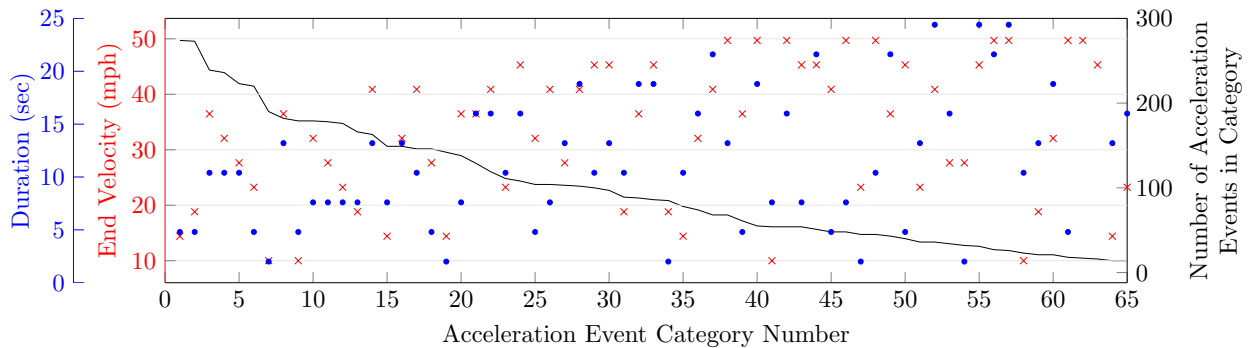
Figure 4.5: Plot showing total duration, end velocity, and the number of AEs in each category for the time duration and ending velocity categorization scheme.

The third categorization scheme, average acceleration and ending velocity, is shown in Fig. 4.6. The x-axis and right y-axis are consistent with the other two categorization scheme plots, Fig. 4.4 and 4.5. The left y-axis shows the ending velocity (as red X's) and the average acceleration (as blue dots) of each AE category. For example, AE category 1 has an average acceleration of about 0.11±0.01 g's (g-force) and an ending velocity of approximately 34.2±2.2 mph. Overall Fig. 4.6 shows that the majority of AEs in this dataset have a low magnitude.

75
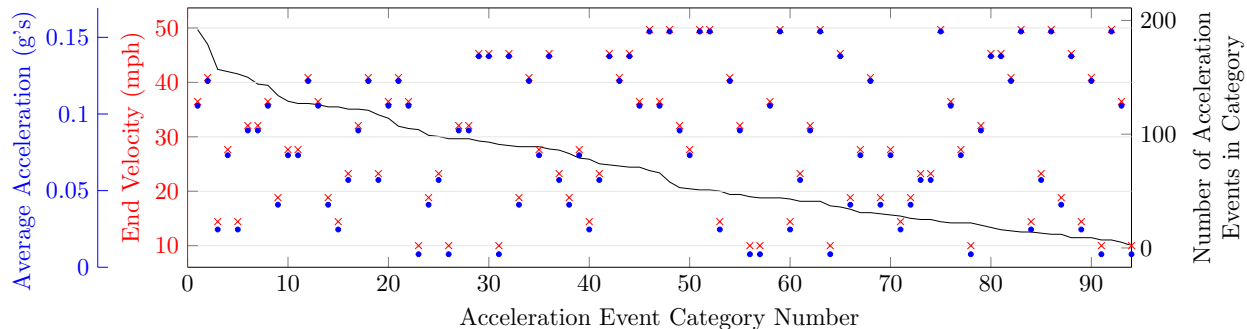
Figure 4.6: Plot showing average acceleration, end velocity, and the number of AEs in each category for the average acceleration and ending velocity categorization scheme.

4.2.3 Baseline Energy Management Strategy Development

The vehicle model chosen for analysis is a 2010 Toyota Prius because it is a popular and well documented vehicle. It also has the highest FE of any vehicle in its class (excluding electric vehicles) [143], implying that if a FE improvement can be demonstrated with this vehicle, it is likely that FE improvements for other vehicles will be higher. A 2010 Toyota Prius is shown in Fig. 4.7.

(a)   **(b)**

Figure 4.7: Front (a) and rear (b) view of the 2010 Toyota Prius hybrid electric vehicle simulated.

The Baseline EMS must be a high accuracy simulation of current real world vehicle FE performance. Additionally, to compare alternate control strategies over thousands of short segments of driving, such as AEs, the vehicle model must also have a low computational cost and high fidelity to model FE changes due to control systems changes.

To satisfy these requirements, a combination of a high fidelity vehicle model developed in the Autonomie modeling software is used with an equation-based power-split model. The Autonomie

modeling software has shown strong correlation with 2010 Toyota Prius physical vehicle operation [97]. The Autonomie model was used to derive the engine torque, engine speed, and engine power which was then implemented in the equation-based power-split model. FE and SOC with respect to time are then recorded.

To ensure that this model does not sacrifice FE prediction accuracy, a detailed model validation was conducted. The simulated FE from this model is validated against 2010 Toyota Prius FE data physically measured by Argonne National Laboratory [98]. The publicly available data is measured for the three standard U.S. Environmental Protection Agency (EPA) Drive Cycles: the city driving focused Urban Dynamometer Drive Schedule (UDDS), the highway driving focused Highway Fuel Economy Driving Schedule (HWFET), and the aggressive driving focused US06 cycle. All simulated FE was within 1.5% of the physically measured data as shown in Table 5.2. Additional, second-by-second, validation of engine speed and battery state of charge (SOC) for each of these drive cycles is shown in Appendix **??**.

Table 4.1: A comparison of simulated and measured fuel economy for standard EPA drive cycles.

EPA Drive Cycle	Simulated Fuel Economy	Measured Fuel Economy [98]	Percent Difference
UDDS	76.6 mpg	75.6 mpg	1.3%
HWFET	69.0 mpg	69.9 mpg	-1.4%
US06	44.9 mpg	45.3 mpg	-1.0%

The equation-based power-split model was developed using information from the literature [20, 91, 101, 102]. Each of the 7,708 AEs is input into the 2010 Toyota Prius Autonomie model and the engine torque, speed, and power output is recorded. For a given engine power, the required electric power can be determined by subtracting the total propulsive power requirement as

$$P_{\text{elec}} = F_{\text{prop}}v - P_{\text{ICE}} \tag{4.2}$$

where F_{prop} is determined from a force balance on the vehicle as

$$F_{\text{prop}} = m\dot{v} + C_{rr}mg + \frac{1}{2}C_d\rho_{\text{air}}v^2 A_{\text{front}} \tag{4.3}$$

where C_{rr} is the coefficient of rolling resistance, m is the mass of the vehicle, g is the acceleration due to gravity ($9.81 \ ^m/_{sec^2}$), C_d is the coefficient of drag, ρ_{air} is the density of air ($1.1985 \ ^{kg}/_{m^3}$), v is the vehicle velocity, A_{front} is the frontal area, and $\dot{v}$ is the vehicle acceleration (calculated using a numerical derivative). Note that the additional force component due to an elevation angle is not a part of this study.

The resulting battery SOC at the next timestep is then calculated as a numerical approximation by

$$\text{SOC}_{\text{new}} = \text{SOC} - \frac{V_{\text{oc}} - \sqrt{V_{\text{oc}}^2 - 4P_{\text{batt}}R_{\text{int}}}}{2R_{\text{int}}Q_{\text{batt,o}}}\Delta t \tag{4.4}$$

where V_{oc} is the open circuit voltage of 201.6 V, R_{int} is the battery internal resistance of 0.373 Ω, and $Q_{\text{batt,o}}$ is the battery capacity of 6.5 A·h.

The overall efficiency of the electrical components can then be captured using response surface fits [103] of data available in the literature [102]. Using the speed and torque, the electrical system efficiency is determined and applied as

$$P_{\text{batt}} = \frac{1}{\eta_{\text{elec}}}P_{\text{elec}} \tag{4.5}$$

where η_{elec} is a function of electric motor speed ω_{EM}, electric motor torque T_{EM}, generator speed ω_{gen}, and generator torque T_{gen}. The electric motor and generator efficiency maps are extracted from the Autonomie modeling software, shown in Figs. 5.4 and 5.5, which are used to compute η_{elec} as a function of the torques and speeds of the electric components.
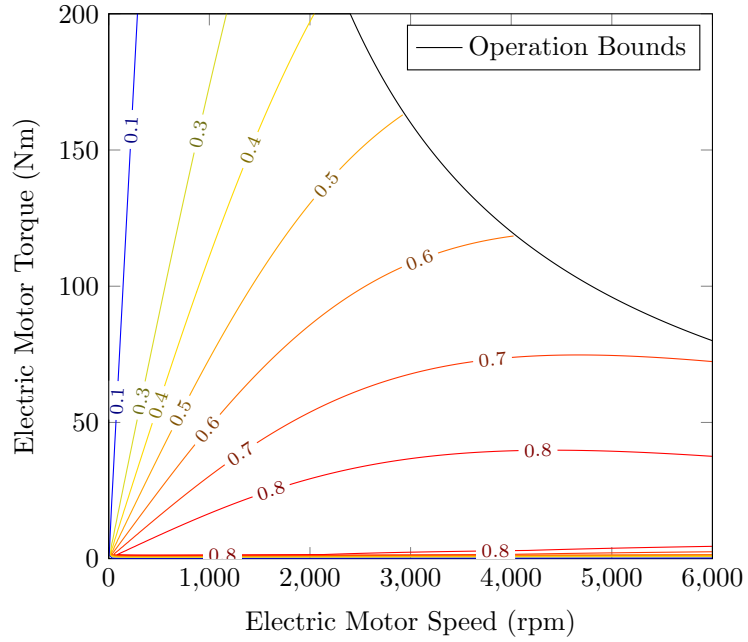
Figure 4.8: The electric motor map response surface.
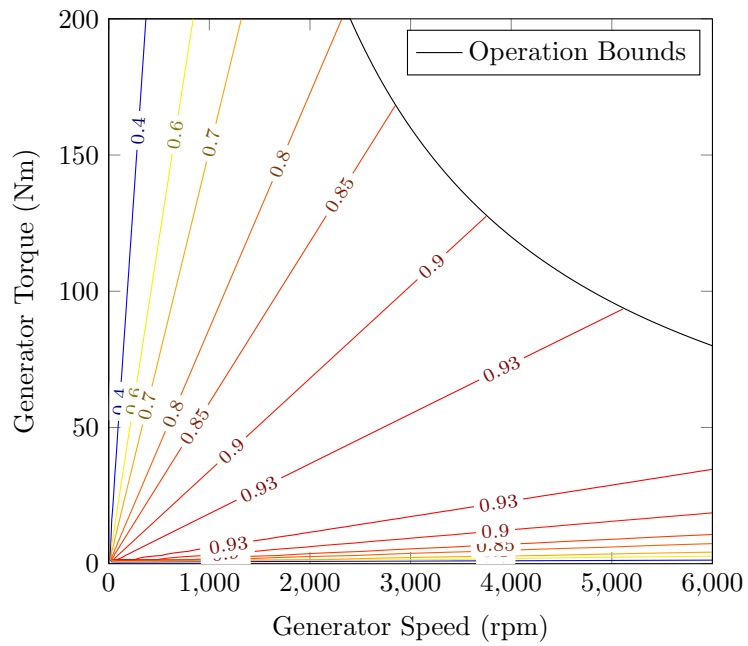
Figure 4.9: The generator response surface.

The fuel consumption is then obtained by first obtaining a Brake Specific Fuel Consumption (BSFC) map through a cubic response surface [103] since a quadratic response surface does not adequately match the structure of the BSFC map available in the public domain [91]. A BSFC cubic response surface has the form of

$$\text{BSFC} = A_1 + A_2\omega_{\text{ICE}} + A_3T_{\text{ICE}}+$$

$$A_4\omega_{\text{ICE}}T_{\text{ICE}} + A_5\omega_{\text{ICE}}^2 + A_6T_{\text{ICE}}^2+$$

$$A_7\omega_{\text{ICE}}T_{\text{ICE}}^2 + A_8\omega_{\text{ICE}}^2T_{\text{ICE}} + A_9T_{\text{ICE}}^3 \quad (4.6)$$

where all A values are fitted constants, ω_{ICE} is the engine speed, and T_{ICE} is the engine torque. The surface developed is shown in Fig. 5.6. Once the BSFC response surface is developed, the ideal operating line [37] can be computed which shows the minimum fuel consumption for any desired power (also shown in Fig. 5.6).

Figure 4.10: The approximated BSFC map response surface created.

Lastly, the engine, generator, and wheel speed are constrained according to

$$\omega_{ICE} = \omega_{gen}\frac{\rho}{1+\rho} + \omega_{ring}\frac{1}{1+\rho} \qquad (4.7)$$

$$P_{batt} = \omega_{gen}T_{gen} \qquad (4.8)$$

where $\rho = \frac{N_{sun}}{N_{ring}}$, $N_{teeth,generator} = 30$, and $N_{teeth,ring} = 78$ and is subject to operational speed limits of 13,500 rpm for the electric motor and 10,000 rpm for the generator. The ring gear speed is based on the vehicle speed as

$$\omega_{ring} = \frac{r_{final\ drive}v}{R_{wheel}} \qquad (4.9)$$

where $r_{final\ drive}$ is the final drive ratio of 3.267 and R_{wheel} is the wheel radius of 0.317 m.

4.2.4   Optimal Energy Management Strategy Development

Deterministic DP is used to derive the Optimal EMS. Previous research has shown that despite prediction errors, the DP derived control matrix results in maintained FE improvements [72]. This research investigates deriving an Optimal EMS using DP for a single AE in a category and applying the control matrix results to every other AE in the category.

The AE for which the Optimal EMS is derived is referred to as the "expected AE" and is an estimate of the most common AE within the category. As an example, category 1 in Fig. 4.4 has a starting velocity of 0 mph and an ending velocity of 7.8±1.5 mph. All of the AEs within category 1 are plotted in Fig. 4.11a. If the total duration of each of the AEs in category 1 is recorded, shown in Fig. 4.11b, it can be seen that a duration between 4.5 and 5 seconds is most common (this duration spans 40 occurrences). This implies that for category 1, a total duration of 4.5 to 5 seconds is an expected AE and all other durations are associated with "mispredictions". Note that only one AE is used to derive the Optimal EMS in the 4.5 to 5 second duration which is chosen at random. This ensures that only one Optimal EMS is used for every category.
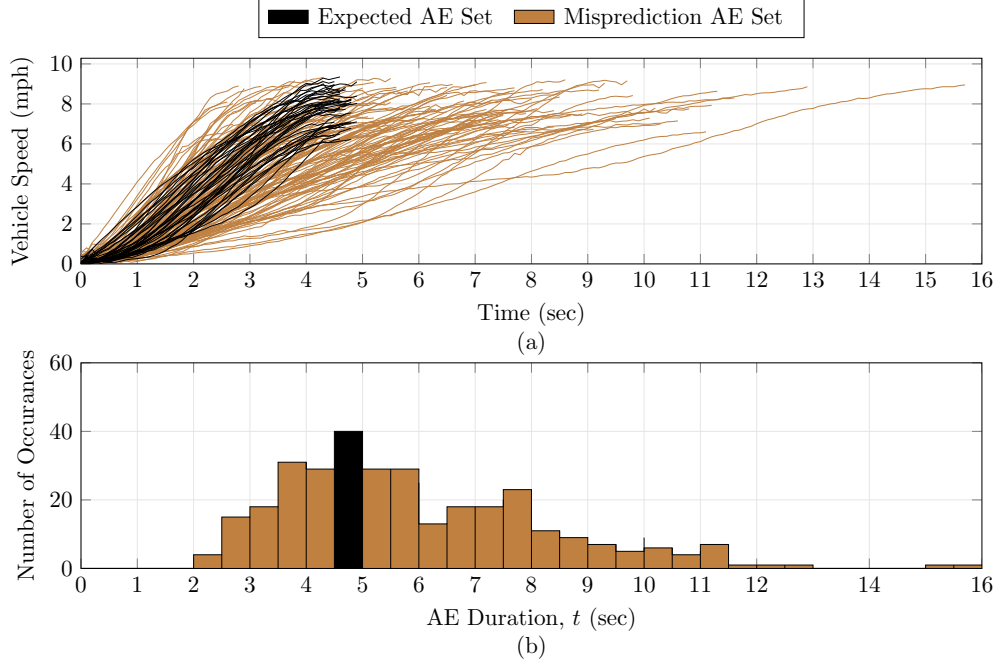
Figure 4.11: A visual representation of the characteristic AE selection process. The AEs with the most common total duration are labeled in black while all other AEs are shown in brown.

After the expected AE is determined for each category in each AE categorization scheme, the Optimal EMS can be derived using DP. DP finds the optimal solution using backwards recursion, which avoids solutions that are not optimal as defined by the Bellman principle of optimality [99, 100]. For every feasible state variable value, the optimal solution is stored. An appropriate DP scheme consists of a dynamic equation shown in Equation 4.10, a cost function shown in Equation 4.11, and state and control variable feasibility constraints shown in Equation 4.13:

$$S(k + 1) = S(k) + f_1(S, u, w, k)\Delta t \tag{4.10}$$

$$J = \sum_{k=0}^{N-1} f_2(S, u, w, k, \Delta t) \tag{4.11}$$

$$S_{\min}(k) \leq S(k) \leq S_{\max}(k) \qquad (k = 0, ... N) \tag{4.12}$$

$$u_{\min}(k) \leq u(k) \leq u_{\max}(k) \qquad (k = 0, ... N - 1) \tag{4.13}$$

where S is the state, u is the control, w is the exogenous input, k is the timestep number, Δt is the timestep value, J is the cost, and N is the final timestep number.

For an HEV Optimal EMS derivation, the state is chosen to be the battery state of charge (SOC), the control is chosen to be the engine power (P_{ICE}), the exogenous input is the vehicle velocity (v), and the cost is chosen to be the fuel mass consumed (m_{fuel}). This formulation with the added feasibility constraints of engine operation and battery SOC yields the following modified equations

$$\text{SOC}(k+1) = \text{SOC}(k) + f_3(\text{SOC}, P_{\text{ICE}}, v, k)\Delta t \tag{4.14}$$

$$\text{Cost} = \sum_{k=0}^{N-1} m_{\text{fuel}} \tag{4.15}$$

$$\text{SOC}_{\text{min}} \leq \text{SOC}(k) \leq \text{SOC}_{\text{max}} \qquad (k = 0, ...N) \tag{4.16}$$

$$P_{\text{ICE,min}} \leq P_{\text{ICE}}(k) \leq P_{\text{ICE,max}} \qquad (k = 0, ...N-1) \tag{4.17}$$

This HEV Optimal EMS derivation can then be tailored to a 2010 Toyota Prius using the equation-based power-split model described in section 4.2.3. The resulting DP formulation for a 2010 Toyota Prius is

$$\text{SOC}(k+1) = \text{SOC}(k) - C_1 + C_2\sqrt{C_3 - C_4 v(k) + C_5 v(k)^3 + C_6 \dot{v}(k)v(k) - C_7 P_{\text{ICE}}} \tag{4.18}$$

$$\text{Cost} = \sum_{k=0}^{N-1} f_4(P_{\text{ICE}}) + W(\text{SOC}_f - \text{SOC}(N))^2 \tag{4.19}$$

$$40\,\% \leq \text{SOC}(k) \leq 80\,\% \qquad (k = 0, ...N) \tag{4.20}$$

$$0\,\text{kW} \leq P_{\text{ICE}}(k) \leq 73\,\text{kW} \qquad (k = 0, ...N-1) \tag{4.21}$$

$$C_8[f_5(P_{\text{ICE}})] + C_9 v(k) \leq C_{10} \tag{4.22}$$

where C_1 through C_{10} are constants and W is an SOC target penalty weight set arbitrarily at 10,000. This process is described in more detail in the previous publication [72].

The following timestep, state, and engine power discretization values are used which were determined from a convergence test:

$$\Delta t = 0.4 \text{ sec} \tag{4.23}$$

$$\Delta \text{SOC} = 0.001\% \tag{4.24}$$

$$\Delta P_{\text{ICE}} = 0.1 \text{ kW} \tag{4.25}$$

The solution to this problem is an optimal control matrix which provides the minimum fuel consumption engine power for any feasible time and battery SOC during the AE. The optimal control matrix for a low velocity AE is shown in Fig. 4.12 and the optimal control matrix for a high velocity AE is shown in Fig. 5.10.
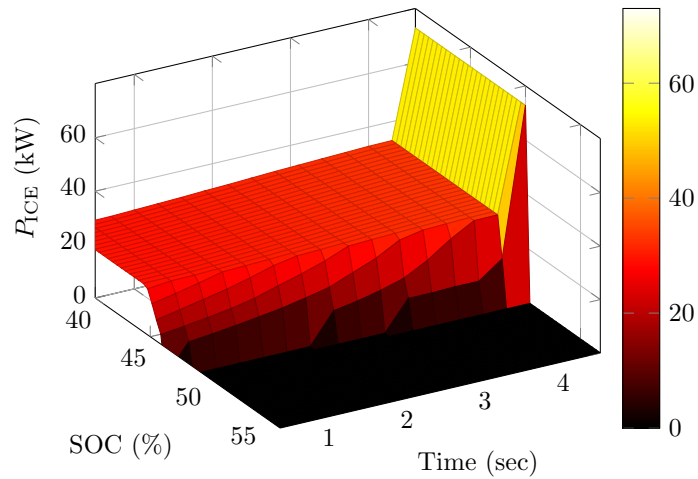
Figure 4.12: The optimal control matrix derived using dynamic programming for a low velocity acceleration event.

For example, if the battery SOC is 40% and the time since beginning the AE is 3 seconds, Fig. 4.12 shows that approximately 20 kW of engine power will provide the minimum fuel consumption solution (for a low velocity AE) while Fig. 5.10 shows that approximately 30kW of engine power will provide the minimum fuel consumption solution (for a high velocity AE).

84
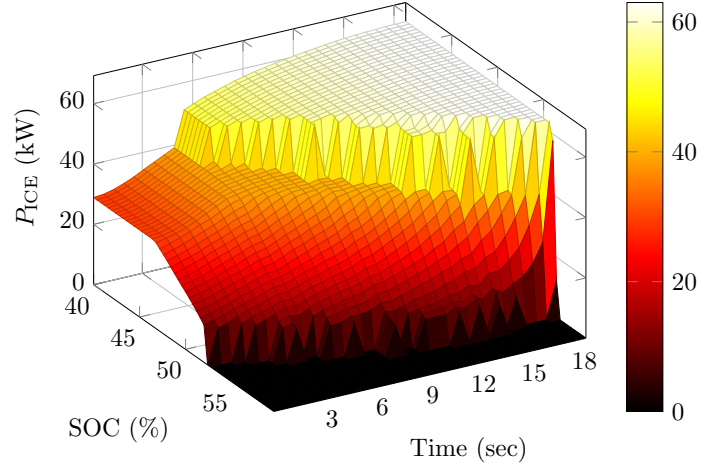
Figure 4.13: The optimal control matrix derived using dynamic programming for a high velocity acceleration event

4.2.5 Battery State of Charge Correction

When evaluating alternate control strategies it is likely that ending battery SOC (SOC_f) for each strategy will be different. For full drive cycles, the Society of Automotive Engineers (SAE) J1711 standard describes how to determine a corrected FE [104]. Unfortunately, this technique gives erroneous results when applied short sections of driving such as AEs.

SAE J1711 assumes a constant engine efficiency of 25% which is not appropriate for a large dataset of AEs since engine efficiency can be significantly different for different AEs. Additionally the FE results for AEs are very sensitive to the FE correction technique since the fuel consumption relative to full drive cycles is very low.

To address these issues, a FE correction technique was employed that is a slight modification to the SAE standard. Each relative increase in FE and SOC result for every AE within one category are plotted in Fig. 4.14, with relative increases defined as

$$\Delta\text{FE} = \text{FE}_{\text{Optimal EMS}} - \text{FE}_{\text{Baseline EMS}} \tag{4.26}$$

$$\Delta\text{SOC} = SOC_{f,\text{Optimal EMS}} - SOC_{f,\text{Baseline EMS}} \tag{4.27}$$
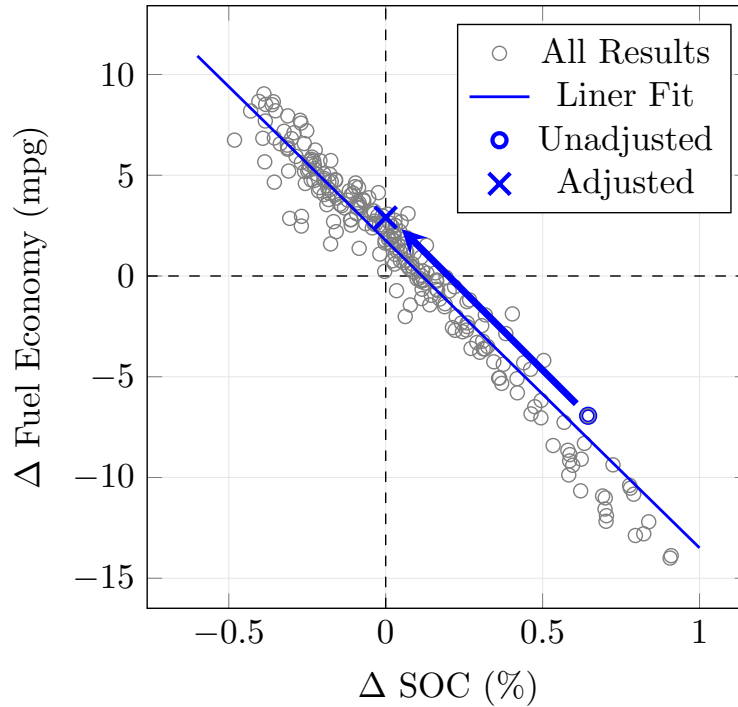
Figure 4.14: Illustration of SOC correction method.

Also shown in Fig. 4.14 is a linear fit of all of the AE results (shown in blue). The point where this blue line crosses the y-axis is the average FE improvement for all AEs in this category.

Individual AE results for this category are determined by tracing a point to where it crosses zero on the y-axis using the slope of the fit line. For example, the blue circle represents an AE with a SOC difference of 0.7% and a FE difference of -6%. The SOC adjusted FE improvement is 3% which can be seen by following the blue arrow to the blue X.

4.3   Results

The results include an investigation of the FE improvement mechanism, a FE improvement calculation for every AE in every AE category for each categorization scheme, and the impact of fewer or more AE categories on the overall FE improvement. Other impacts will be investigated in part 2 of this research which applies the control strategy outlined here to new full drive cycles.

4.3.1 Fuel Economy Improvement Mechanism

Applying the DP-derived Optimal EMS to AEs results in a FE improvement. For a low velocity AE, Fig. 5.12a compares the Baseline EMS and Optimal EMS engine operation points and shows that the Optimal EMS results in more efficient engine operation since the operation points are closer to the region of highest efficiency. For a high velocity AE, Fig. 5.12b compares the Baseline EMS and Optimal EMS engine operation points and shows that the Optimal EMS results in more efficient engine operation since the operation points are concentrated in the region of highest efficiency. Low velocity accelerations typically result in a FE improvement of approximately 5% while high velocity accelerations typically result in a FE improvement of approximately 2%[1].
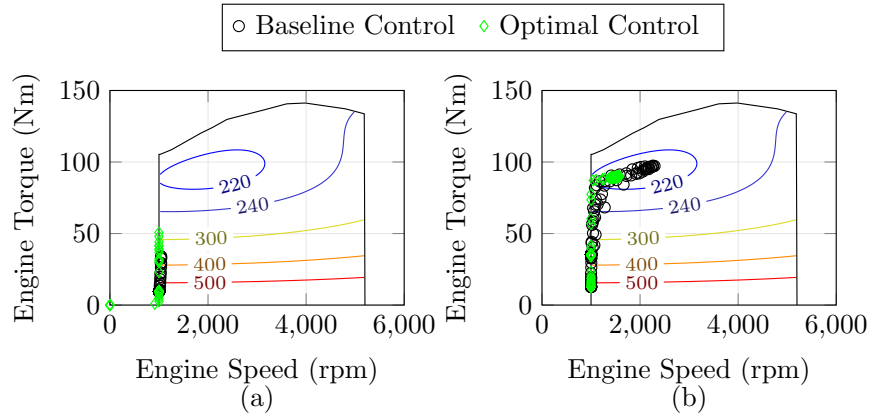
Figure 4.15: A comparison of baseline control and optimal control results for engine power (a) and engine operation (b).

4.3.2 Acceleration Event Categorization Scheme

Investigation of the overall FE improvement from each of the AE categorization schemes can be investigated next. The FE improvement was determined using equation 4.28 but the Optimal

---

[1]The FE improvement is calculated as

$$\text{FE Improvement} = \frac{\text{FE}_{\text{Optimal EMS}} - \text{FE}_{\text{Baseline EMS}}}{\text{FE}_{\text{Baseline EMS}}} \times 100\% \tag{4.28}$$

EMS was only derived for one expected AE in each category but was applied to every AE in the category.

In Fig. 4.16a, results for categories defined by starting and ending velocity are shown, sorted according to FE improvement. Fig. 4.16b shows that the highest FE improvement is achieved for low velocity accelerations, of which there are many instances in the driving dataset. This figure also shows a FE loss for high velocity accelerations, of which there are few instances in the driving dataset.
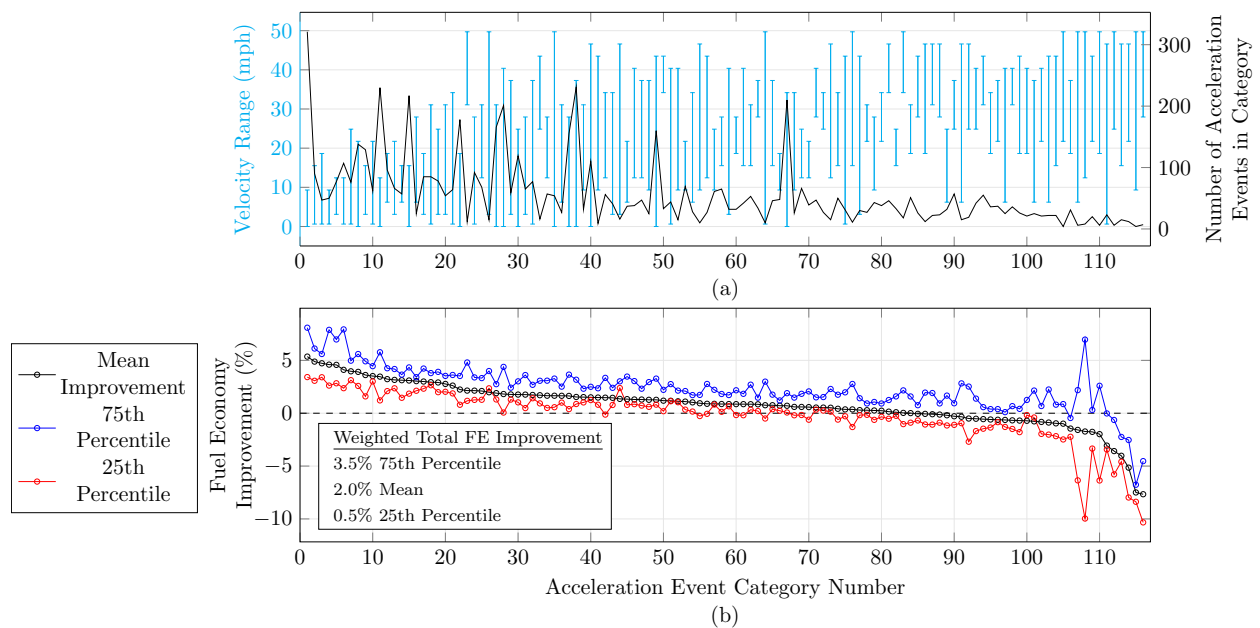
Figure 4.16: Plot comparing characteristic velocities to FE performance for each category, sorted by decreasing mean FE improvement.

In Fig. 4.17a, results for categories defined by time duration and end velocity are shown, sorted according to FE improvement. When correlating the results with the FE improvement shown in Fig. 4.17b, it can be seen that the largest FE improvements are for low velocity AEs that have a relatively long duration. Additionally, AEs with the longest duration tend to result in a general FE improvement. High velocity, short duration AEs give the lowest FE improvement.
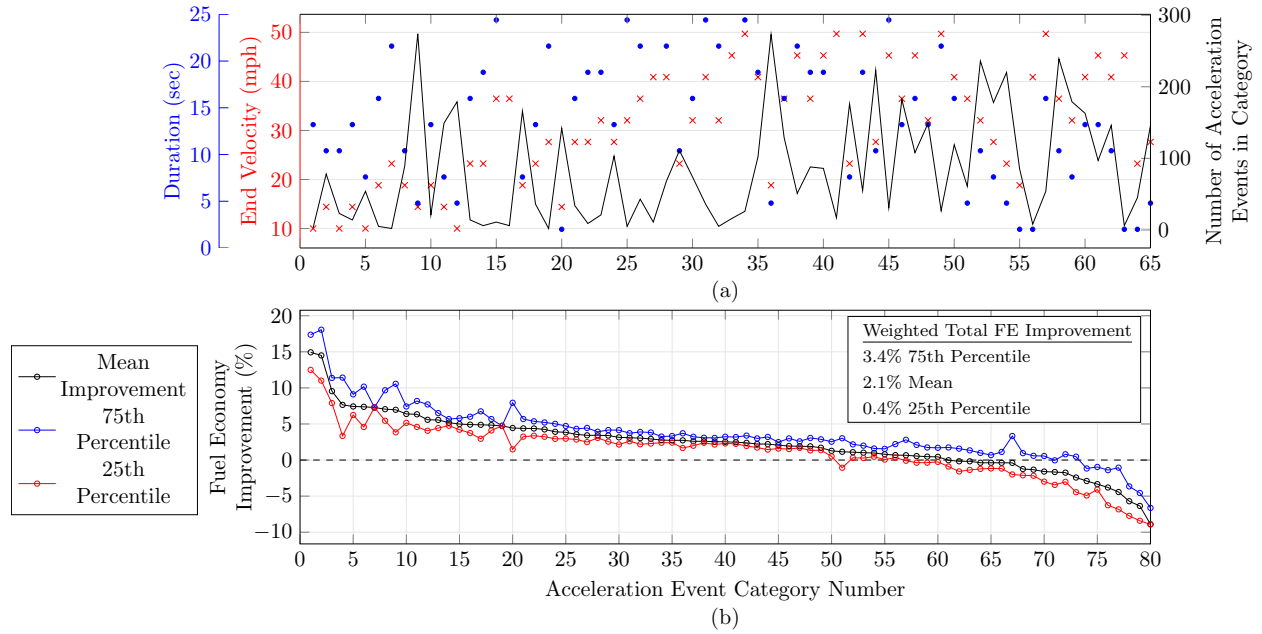
Figure 4.17: Plot comparing characteristic velocities to FE performance for each category, sorted by decreasing mean FE improvement.

In Fig. 4.18a, results for categories defined by average acceleration and end velocity are shown, sorted according to FE improvement. When correlating the results with the FE improvement shown in Fig. 4.17b, it can be seen that low magnitude low velocity AEs achieve the highest FE improvement. Additionally, high magnitude, high velocity AEs give the worst FE results.
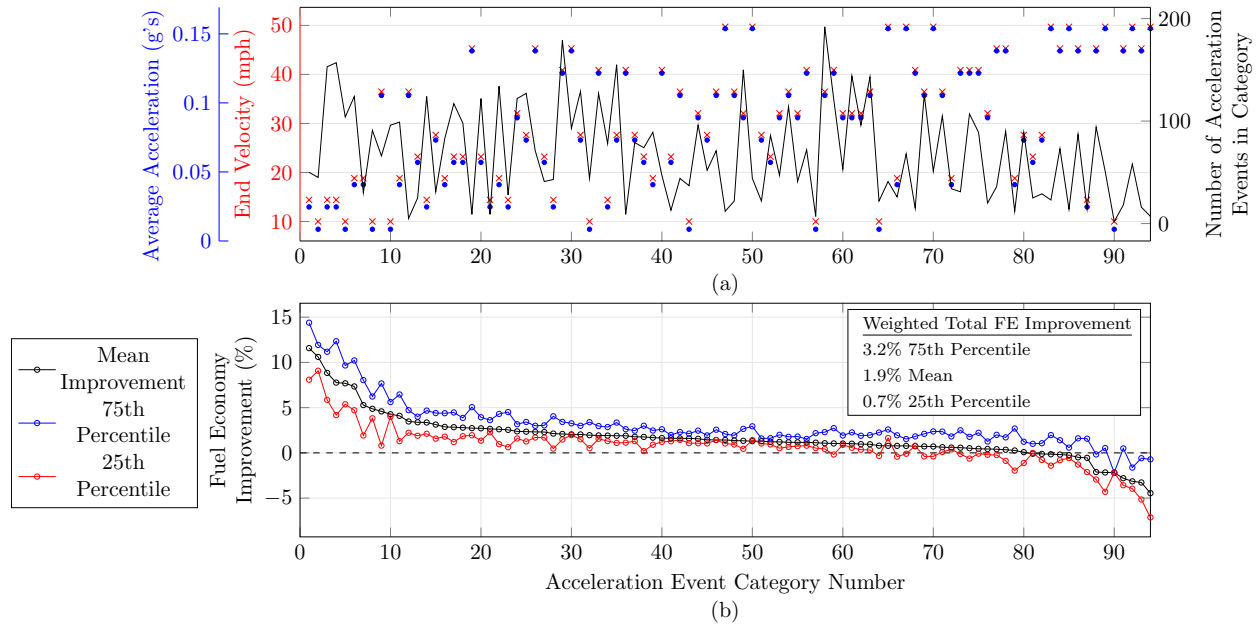
Figure 4.18: Plot comparing characteristic velocities to FE performance for each category, sorted by decreasing mean FE improvement.

In general each of the categorization schemes has a similar weighted total FE improvement (shown in the inset table in Figs. 4.16b, 4.17b, and 4.18b) with the duration and average acceleration categorization schemes have a higher overall variance than the starting velocity categorization scheme. It was also found that greater FE improvements are achieved when the actual AE duration is equal to or longer than the expected AE duration. This phenomenon may warrant investigation in future work.

4.3.3 Number of Acceleration Event Categories

Lastly, we investigate the tradeoff between FE improvement and the number of categories. With too few categories, the drive cycle data will have a large FE improvement variance and with too many categories the data is overfit and lacks generalization.

FE results for various numbers of starting velocity and ending velocity categories can be seen in Fig. 4.19. This figure shows that when few starting and ending speed categories are used, there is a large FE variance. This figure also shows that when 100s of starting and ending velocity

categories are used, the FE improvement is slightly higher, but we are approaching the point of an Optimal EMS derived for every single AE which results in an overfitting of data and a lack of generalization. For around 15 starting and ending categories there is a significant and robust FE improvement. This figure also shows that constraining the end velocity is more important than constraining the starting velocity. High numbers of end velocity categories (and therefore stronger constraints on end velocity error) result in robust FE improvements, with little regard to the number of start velocity categories; conversely, if there are few end velocity categories, no number of start velocity categories can produce reliable FE benefits.
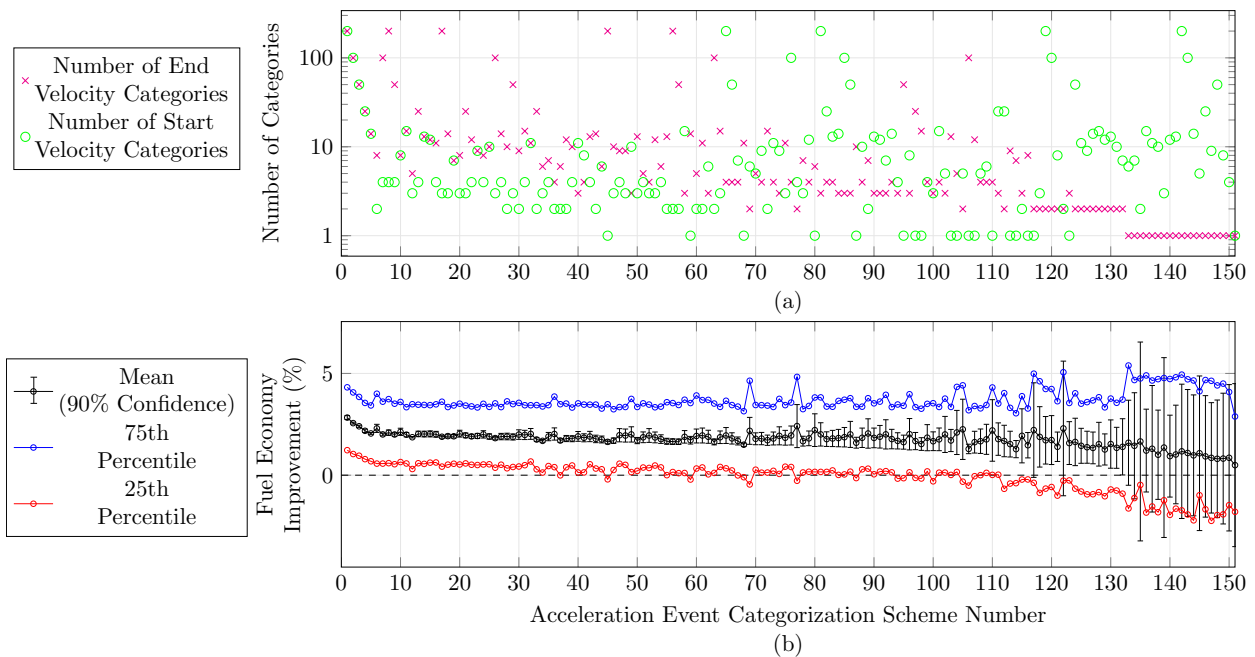
Figure 4.19: Plot comparing the number of starting and ending velocity categories to FE performance, sorted by decreasing mean FE improvement.

FE results for various numbers of time duration and ending velocity categories can be seen in Fig. 4.20. For few numbers of categories (e.g. AE categorization scheme number > 120) the variance in FE improvement is very large, but when 100s of categories are used the FE results are actually worse. Significant and robust FE improvement is achieved with approximately 10 time

duration and end velocity categories. Fig. 4.20 also shows that the end velocity error is more important to constrain than duration error.
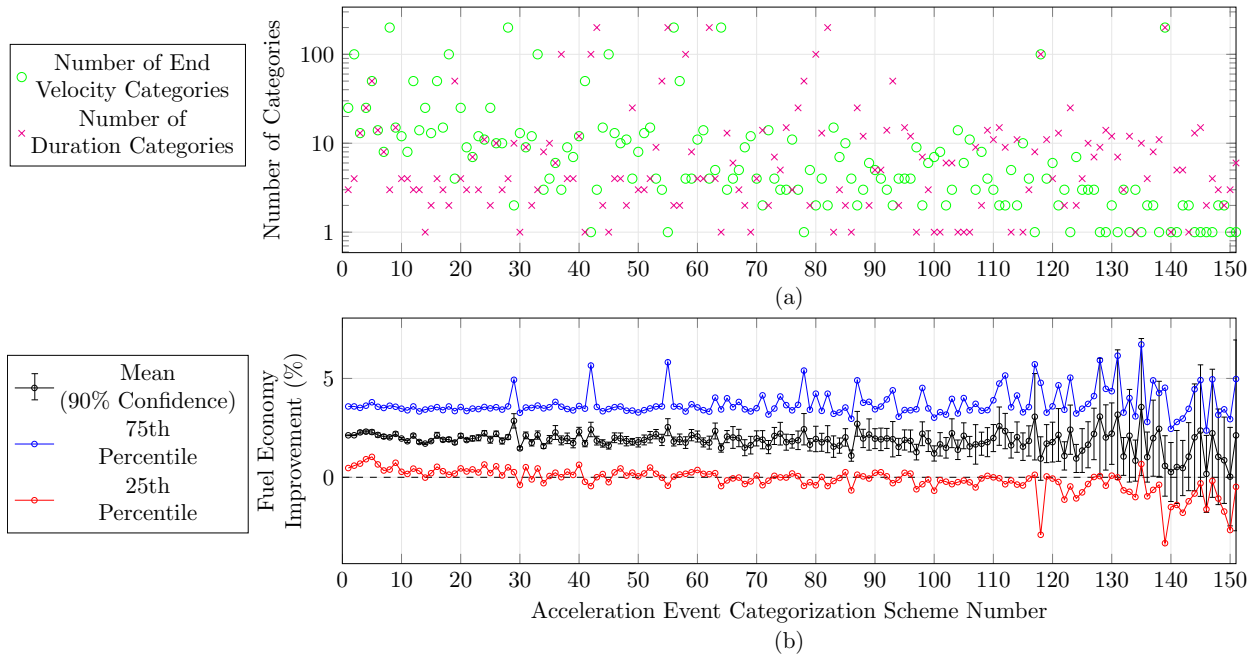
Figure 4.20: Plot comparing the number of duration and ending velocity categories to FE performance, sorted by decreasing mean FE improvement.

FE results for various numbers of time duration and ending velocity categories can be seen in Fig. 4.21. For few numbers of categories the variance in FE improvement is large, but with 100s of categories the FE results are actually worse. Fig. 4.21 also shows that end velocity error is more important to constrain than average acceleration error based on the similar relationship to the time duration categorization case.
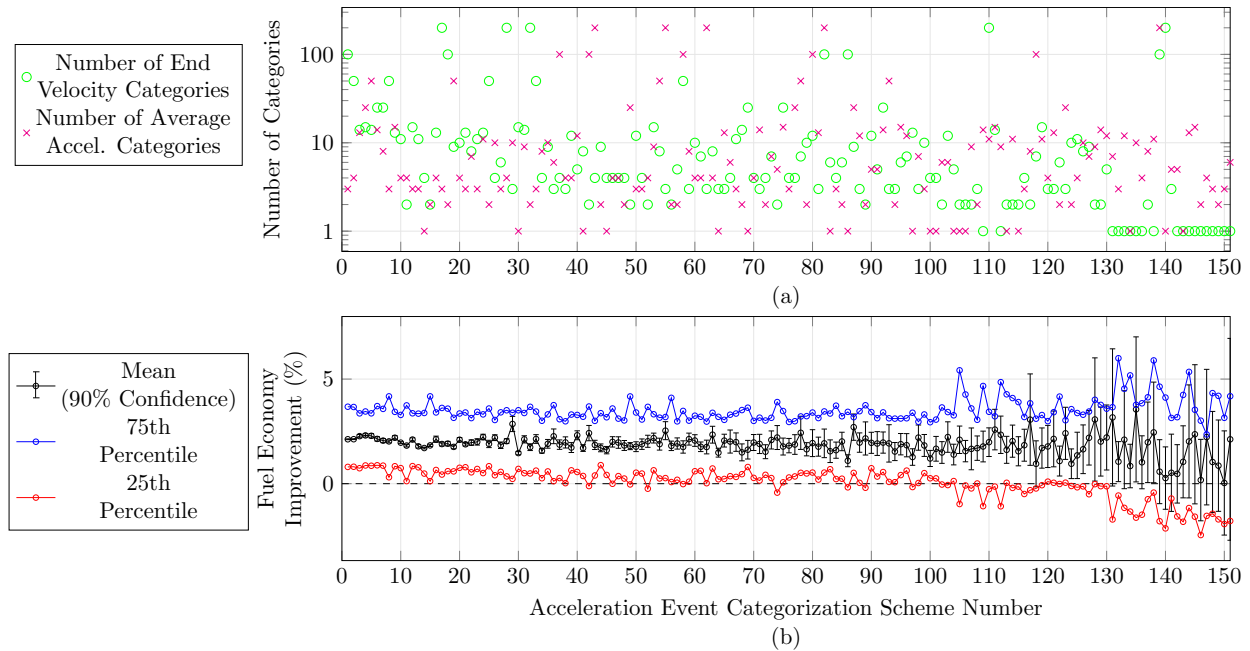
Figure 4.21: Plot comparing the number of average acceleration and ending velocity categories to FE performance, sorted by decreasing mean FE improvement.

Overall AE misprediction is most prone to end velocity error, reasonably prone to duration and acceleration error, and least prone to start velocity error. An categorization of AEs according to starting and ending velocity yields the largest FE improvements. This informs real world implementation of this technique.

4.4 Conclusion

In this study, a dataset of 7,708 AEs was extracted from 384 real world drive cycles. These AEs were organized according to multiple categorization schemes: end velocity and (1) starting velocity, (2) time duration, and (3) average acceleration. A Baseline EMS for a 2010 Toyota Prius was derived using a combination of the Autonomie modeling software and an equation-based power-split model which was rigorously validated against real world performance. An Optimal EMS was derived using DP for only the most common AE in each category, which expands upon a previous research finding that FE improvements are maintained for a DP derived Optimal EMS on a similar drive cycle [72]. The results show that FE improvements can be obtained because the

engine is operated at higher efficiency. The most significant and robust FE improvements can be obtained using starting velocity and ending velocity AE categorization with around 15 categories of each. Battery SOC impacts will be investigated in part 2 of this paper which applies the control strategy outlined here to full drive cycles.

Since a DP derived Optimal EMS can realize FE improvements for a variety of drive cycles, it may not be required to compute an Optimal EMS via DP in real time during vehicle operation. The Optimal EMS could be implemented as a look-up table thus making a real world Optimal EMS implementable with the limited computation power of vehicle controllers in use today. This FE improvement technique does not require new hardware to implement.

4.5   Chapter Conclusions

This section of the research effort has allowed us to partially address Research Question 2, which is restated here:

Research Question 2: *What level of prediction fidelity and scope is required to realize a fuel economy improvement through predictive energy management and potentially eliminate the need for real-time computation?*

Research Question 2 is associated with Hypothesis 2:

Hypothesis 2: *Implementing a general prediction solution for the acceleration portions of a drive cycle will result in FE improvements without the need for perfect prediction.*

This research effort has provided support for this hypothesis. Through development, organization, and organization discretization of AEs, it was determined that significant and robust FE improvements are possible. The limited AE prediction strategy can then be investigated within a drive cycle to further investigate the hypothesis.

Chapter 5

Improved Fuel Economy through Acceleration Event Prediction Part 2: Drive Cycle Application

This study investigates the FE impacts of AE prediction within a drive cycle and involves drive cycle development, application of the AE prediction control scheme discussed in Chapter 4 to full drive cycles, application of the dynamic programming algorithm to full drive cycle prediction as well as drive cycle AE prediction, and a high fidelity model of a 2010 Toyota Prius. This research is part of an ongoing project funded by Toyota. David A. Trinko has also made significant contributions to this project by improving the vehicle model and expanding the study to include improved drive cycle application techniques, and the analysis of more drive cycles. This monumental research effort is just now reaching the publication phase with a conference publication [106] and the recently submitted journal paper reproduced in this chapter [144]

5.1   Introduction

Advanced vehicle powertrain control strategies such as predictive optimal energy management can improve fuel economy (FE) by up to 30% but additional research is required before vehicle implementation can be realized. This is due to the complicated requirement of making future vehicle operation predictions and controlling the vehicle powertrain based on those predictions [4]. An investigation of the trade-offs between prediction scope versus the FE improvement result for a variety of drive cycles is required.

5.1.1   Fuel Economy Improvement Needs

Transportation provides significant economic benefits but is responsible for approximately one third of the global total energy consumption [108]. Generating this energy from petroleum fuel creates economic risks since petroleum reserves are finite and are not evenly distributed by country.

The European Union, the U.S., China, India, Japan and others are required to import petroleum thereby exposing themselves to high oil supply risk [7]. Meeting transportation energy needs through petroleum combustion generates significant air pollution from five of the six major air pollution constituents [87]. This air pollution has contributed to 6.5 million premature deaths across the world in 2012, making air pollution the fourth-leading cause for premature death world-wide [16]. Meeting transportation energy needs through petroleum combustion also generates greenhouse gas emissions and the transportation sector is the second largest contributor of these emissions [11, 110]. Greenhouse gas emissions have been linked to global warming which has major human health, ecosystem, and environmental impacts [111].

A new global policy that addresses these issues by limiting greenhouse gas emissions, known as the Paris Climate Agreement, has been signed by every country in the world [145, 146]. It is antic-ipated that the signing of this agreement will result in near future greenhouse gas emission reduc-tions [13, 147] but more aggressive greenhouse gas reduction solutions are required [13, 148, 149]. The U.S. initially helped establish the Paris Climate Agreement [150] but has since expressed a desire to leave the agreement to support government deregulation [151–153]. Despite this, indi-vidual states and cities within the U.S. have expressed that they will still uphold the requirements of the Paris Climate Agreement [154].

Improving vehicle FE is a major initiative for meeting the reduction in greenhouse gas emis-sions outlined in the Paris Climate Agreement which also, by extension, limits petroleum impor-tation and air pollution [14]. Because of the Paris Climate Agreement, many countries have FE related goals such as the 50% fuel economy improvement worldwide by 2050 challenges (50 by 50) [112, 155–158].

5.1.2 Drive Cycle Analysis

Drive cycles are a series of vehicle velocity versus time or distance data points. Over time, stan-dardized drive cycles have been developed that represent various types of driving which includes city driving, highway driving, and aggressive driving for small vehicles [159], heavy duty vehi-

cles [160], buses [161], and others. Current U.S. policy is to use a small number of city, highway, and aggressive drive cycles to represent the concept of operation [162] so vehicle performance can be evaluated [163]. Most researchers typically limit their concept of operations to one or two drive cycles [159, 161, 164–168]. But, new research has shown that to ensure robust operation over a variety of driving conditions, as many drive cycles as are available should be included in the study [169].

5.1.3   Optimal Energy Management to Increase Fuel Economy

Technologies used to increase FE include engine sizing, advanced engine control, friction/ mass/ drag reduction, and powertrain electrification [126]. But, there are numerous technologies that also have the potential to significantly improve FE, such as implementation of an optimal energy management strategy (Optimal EMS) which has demonstrated FE improvements of up to 30% for hybrid vehicles [130].

An Optimal EMS is the application of optimal control to vehicle powertrain operation with the objective of minimizing fuel consumption (maximizing FE). To achieve globally optimal control, knowledge of future events is required. In the early 2000s, optimal control was applied to hybrid electric vehicles (HEVs) to determine the optimal usage of battery propulsive power versus engine propulsive power to produce the minimum fuel consumption, in other words, the Optimal EMS [32]. This foundational research focused on obtaining the globally optimal control through DP using 100% accurate prediction of an entire discretized drive cycle.

5.1.4   Optimal Energy Management Implementation

Accurate prediction of an entire drive cycle and real time derivation of the Optimal EMS is difficult to achieve in modern and near-future vehicles due to limited understanding of prediction techniques and the high computational cost of Optimal EMS derivation [4]. To address these issues, researchers have begun investigating prediction techniques for use with an Optimal EMS [57–59, 61–63, 170, 171], real time Optimal EMS derivation strategies that may compromise

optimality [49–51, 135, 136], and stochastically robust Optimal EMS derivation strategies that may compromise optimality [47, 48, 85, 133, 134].

A potential solution to implementation of an Optimal EMS is to use a precomputed globally Optimal EMS rather than a real-time computed nonglobally Optimal EMS. This option did not seem feasible until recent research established that FE improvements are still achieved when a globally Optimal EMS is subjected to mispredictions [70–72]. Each precomputed, real-time, and stochastically robust Optimal EMS requires some form of prediction, but a correctly applied precomputed globally Optimal EMS eliminates the need for real-time computation and also eliminates the need for stochastic robustness [72, 106].

Prediction modeling is not within the scope of this research. Instead a limited prediction of acceleration events (AE), which are a small percentage of the total drive cycle, is assumed. Part one of this research has shown that prediction of only the start time of an AE, the approximate initial velocity (v_i) of the AE, and the approximate final velocity (v_f) of the AE are all that is required to realize a significant and robust FE improvement [107]. In part two of this research, this analysis is extended to investigate the total FE improvement and battery state of charge (SOC) impacts of this AE category precomputed Optimal EMS over a variety of drive cycles.

5.1.5 Novel Aspects/Unique Contributions of this Research

This research makes the following novel contributions to the Optimal EMS body of knowledge:

1. FE results of a precomputed Optimal EMS in a drive cycle, eliminating the need for real time calculations

2. FE results of AE prediction in a drive cycle reducing the scope of prediction required for an Optimal EMS

5.2 Methods

To determine the impact of AE category prediction in drive cycles, several steps are required. The first is to develop a set of drive cycles representing various styles of driving. Next four control

strategies are compared: (1) a baseline energy management strategy (Baseline EMS), (2) a full drive cycle prediction Optimal EMS, (3) an exact AE prediction Optimal EMS, and (4) a category AE prediction Optimal EMS. Comparing these control strategies will reveal the potential of a category AE prediction Optimal EMS.

5.2.1 Drive Cycle Development

To rigorously investigate the FE costs and benefits of AE prediction, numerous drive cycles are investigated. The drive cycles include standard Environmental Protection Agency (EPA) drive cycles as well as developed real-world drive cycles. All real-world drive cycles were recorded from the controller area network (CAN) bus of an instrumented vehicle using the CANoe software. The drive cycles can be divided into three categories: (1) city drive cycles, (2) highway drive cycles, and (3) aggressive drive cycles.

Four city drive cycles are analyzed. These include one city drive cycle recorded in Denver, Colorado, USA which drives directly through downtown with moderate traffic levels and one city drive cycle recorded in Fort Collins, Colorado, USA in low traffic conditions. Two EPA city drive cycles were also selected which include the Urban Dynamomoter Driving Schedule (UDDS) and the New York City Cycle (NYCC). These four city cycles are summarized in Table 5.3 and the velocity traces are shown in Fig. 5.1.

Three highway drive cycles and one aggressive drive cycle are also analyzed. The highway drive cycles include one drive cycle recorded in Denver, CO, USA, that transitions across two major highways and one drive cycle recorded on and around I-25 in Fort Collins, CO, USA. The last highway drive cycle used is the EPA's Highway Fuel Economy Test (HWFET). The aggressive drive cycle used is the EPA's US06 cycle. These four drive cycles are shown in Table 5.3 and the velocity traces are shown in Fig. 5.2.
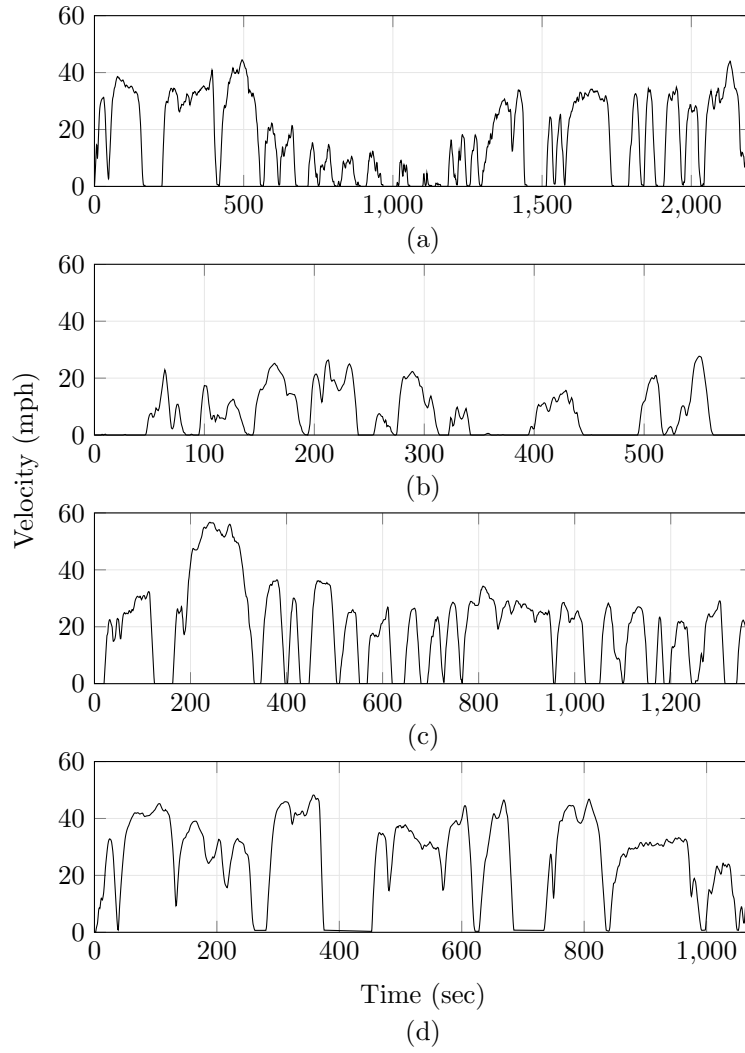
Figure 5.1: All of the city drive cycles analyzed which include the Denver City Cycle (a), the NYCC (b), the UDDS (c), and the Fort Collins City Cycle (d).
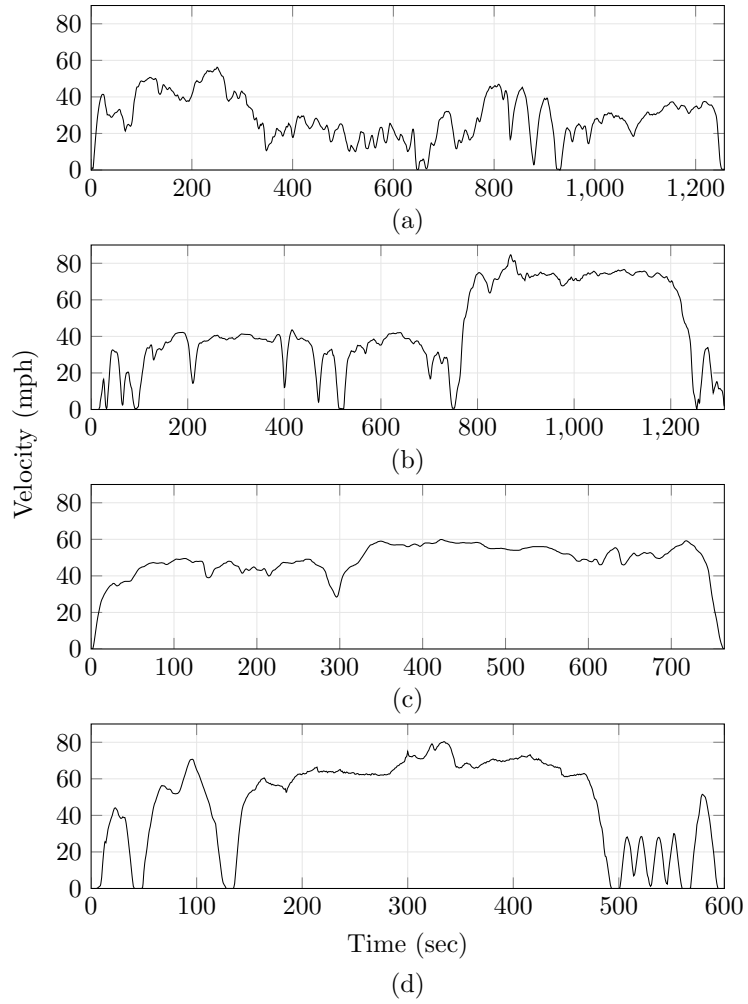
Figure 5.2: All of the highway drive cycles analyzed which include the Denver Highway Cycle (a), the Fort Collins Highway Cycle (b), and the HWFET (c). Also included is the aggressive drive cycle, the US06 (d).

Table 5.1: All drive cycles analyzed.

Drive Cycle Name	Drive Cycle Type	Source
Denver City	City	Real World
NYCC	City	EPA
UDDS	City	EPA
Fort Collins City	City	Real World
Denver Highway	Highway	Real World
Fort Collins Highway	Highway	Real World
HWFET	Highway	EPA
US06	Aggressive	EPA

5.2.2   Baseline Energy Management Strategy
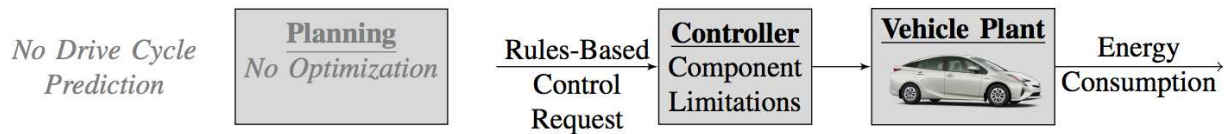
Figure 5.3: A conceptual diagram of how vehicle powertrain control is currently implemented, the Baseline EMS.

The Baseline EMS represents the current real world control of modern hybrid vehicles. The Baseline EMS controls the vehicle according to a set of rules and because of this, the a Baseline EMS is sometimes referred to as a "Rules-Based Control Strategy". The control conceptual diagram for the Baseline EMS is shown in Fig. 5.3. The vehicle model chosen for analysis is a 2010 Toyota Prius because it is a popular and well documented vehicle. This vehicle is shown in the "vehicle plant" subsystem of Fig. 5.3.

To model and compare the effects of alternate control strategies applied to short segments of driving, a responsive and high fidelity vehicle model is required. To satisfy this requirement, a combination of a high fidelity vehicle model developed in the Autonomie modeling software is used with an equation-based power-split model. The Autonomie modeling software has shown strong correlation with 2010 Toyota Prius physical vehicle operation [97] and is used to derive the engine torque, engine speed, and engine power. These inputs are then implemented in the equation-based power-split model with which FE and SOC with respect to time are calculated.

To ensure that this model does not sacrifice FE prediction accuracy, a detailed model validation was conducted. The simulated FE from this model is validated against 2010 Toyota Prius FE data physically measured by Argonne National Laboratory [98]. The publicly available data is measured for the three standard U.S. Environmental Protection Agency (EPA) Drive Cycles: UDDS, HWFET, and the US06. All simulated FE was within 1.5% of the physically measured data as shown in Table 5.2. Additional second-by-second validation of engine speed and battery state of charge (SOC) for each of these drive cycles is presented in [107].

Table 5.2: A comparison of simulated and measured fuel economy for standard EPA drive cycles.

EPA Drive Cycle	Simulated Fuel Economy	Measured Fuel Economy [98]	Percent Difference
UDDS	76.6 mpg	75.6 mpg	1.3%
HWFET	69.0 mpg	69.9 mpg	-1.4%
US06	44.9 mpg	45.3 mpg	-1.0%

The equation-based power-split model was developed using information from the literature [20, 91, 101, 102]. Each drive cycle is input into the 2010 Toyota Prius Autonomie model and the engine torque, speed, and power output is recorded. For a given engine power, the required electric power can be determined by subtracting the total propulsive power requirement as

$$P_{\text{elec}} = F_{\text{prop}} v - P_{\text{ICE}} \qquad (5.1)$$

where F_{prop} is determined from a force balance on the vehicle as

$$F_{\text{prop}} = m\dot{v} + C_{rr}mg + \frac{1}{2}C_d\rho_{\text{air}}v^2 A_{\text{front}} \qquad (5.2)$$

where C_{rr} is the coefficient of rolling resistance, m is the mass of the vehicle, g is the acceleration due to gravity $(9.81\ ^m/_{sec^2})$, C_d is the coefficient of drag, ρ_{air} is the density of air $(1.1985\ ^{kg}/_{m^3})$, v is the vehicle velocity, A_{front} is the frontal area, and $\dot{v}$ is the vehicle acceleration (calculated using a numerical derivative). Note that the additional force component due to an elevation angle is not a part of this study.

The resulting battery SOC at the next timestep is then calculated as a numerical approximation by

$$\text{SOC}_{\text{new}} = \text{SOC} - \frac{V_{\text{oc}} - \sqrt{V_{\text{oc}}^2 - 4P_{\text{batt}}R_{\text{int}}}}{2R_{\text{int}}Q_{\text{batt,o}}}\Delta t \qquad (5.3)$$

where V_{oc} is the open circuit voltage of 201.6 V, R_{int} is the battery internal resistance of 0.373 Ω, and $Q_{\text{batt,o}}$ is the battery capacity of 6.5 A·h.

The overall efficiency of the electrical components can then be captured using response surface fits [103] of data available in the literature [102]. Using the speed and torque, the electrical system efficiency is determined and applied as

$$P_{\text{batt}} = \frac{1}{\eta_{\text{elec}}}P_{\text{elec}} \qquad (5.4)$$

where η_{elec} is a function of electric motor speed ω_{EM}, electric motor torque T_{EM}, generator speed ω_{gen}, and generator torque T_{gen}. The electric motor and generator efficiency maps are extracted from the Autonomie modeling software, shown in Figs. 5.4 and 5.5, which are used to compute η_{elec} as a function of the torques and speeds of the electric components.

The fuel consumption is then obtained by first deriving a Brake Specific Fuel Consumption (BSFC) map through a cubic response surface [103] since a quadratic response surface does not adequately match the structure of the BSFC map available in the public domain [91]. A BSFC cubic response surface has the form of
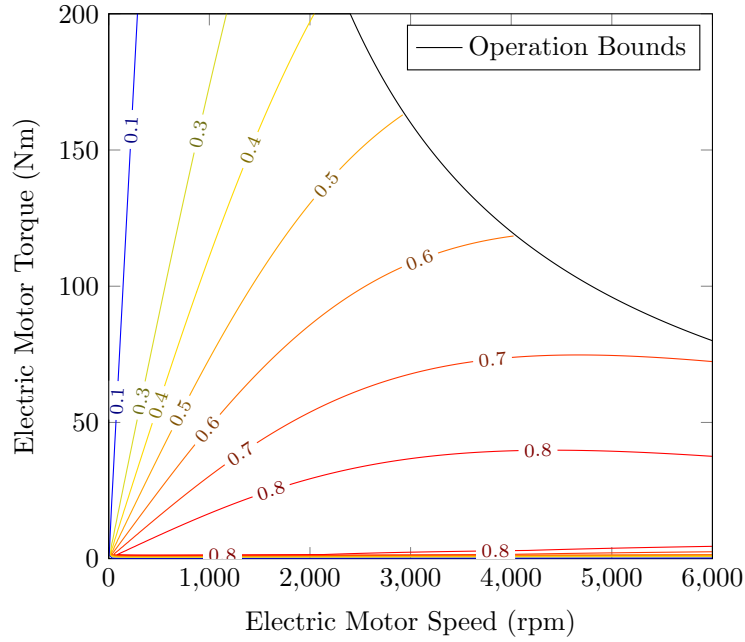
Figure 5.4: The electric motor map response surface.
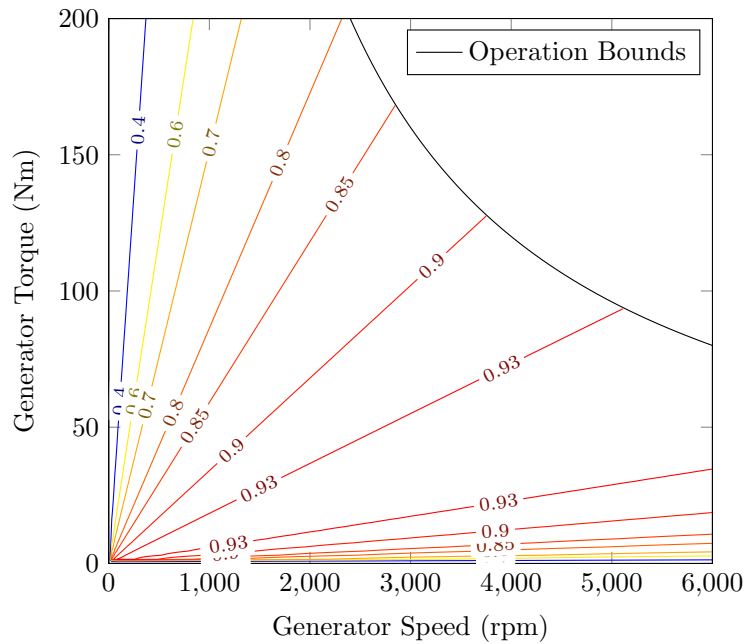
Figure 5.5: The generator response surface.

$$\text{BSFC} = A_1 + A_2 \omega_{\text{ICE}} + A_3 T_{\text{ICE}} +$$

$$A_4 \omega_{\text{ICE}} T_{\text{ICE}} + A_5 \omega_{\text{ICE}}^2 + A_6 T_{\text{ICE}}^2 +$$

$$A_7 \omega_{\text{ICE}} T_{\text{ICE}}^2 + A_8 \omega_{\text{ICE}}^2 T_{\text{ICE}} + A_9 T_{\text{ICE}}^3 \quad (5.5)$$

where all A values are fitted constants, ω_{ICE} is the engine speed, and T_{ICE} is the engine torque. The surface developed is shown in Fig. 5.6. Once the BSFC response surface is developed, the ideal operating line [37] can be computed which shows the minimum fuel consumption for any desired power (also shown in Fig. 5.6).
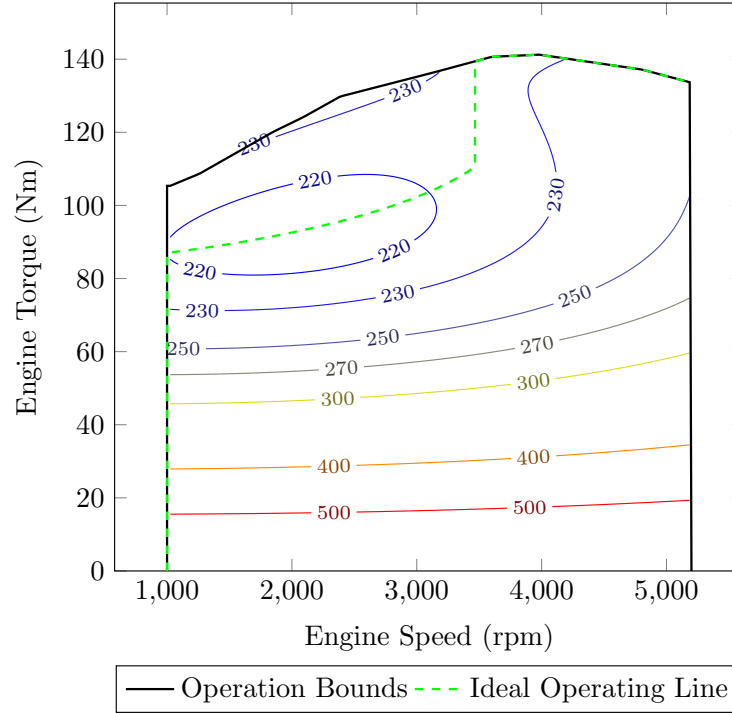
Figure 5.6: The BSFC map response surface created.

Lastly, the engine, generator, and wheel speed are constrained according to

$$\omega_{\text{ICE}} = \omega_{\text{gen}} \frac{\rho}{1+\rho} + \omega_{\text{ring}} \frac{1}{1+\rho} \tag{5.6}$$

$$P_{\text{batt}} = \omega_{\text{gen}} T_{\text{gen}} \tag{5.7}$$

where $\rho = \frac{N_{\text{sun}}}{N_{\text{ring}}}$, $N_{\text{teeth,generator}} = 30$, and $N_{\text{teeth,ring}} = 78$ and is subject to operational speed limits of 13,500 rpm for the electric motor and 10,000 rpm for the generator. The ring gear speed is based on the vehicle speed as

$$\omega_{\text{ring}} = \frac{r_{\text{final drive}} v}{R_{\text{wheel}}} \tag{5.8}$$

where $r_{\text{final drive}}$ is the final drive ratio of 3.267 and R_{wheel} is the wheel radius of 0.317 m.

5.2.3 Optimal Energy Management Strategy: Perfect Full Drive Cycle Prediction
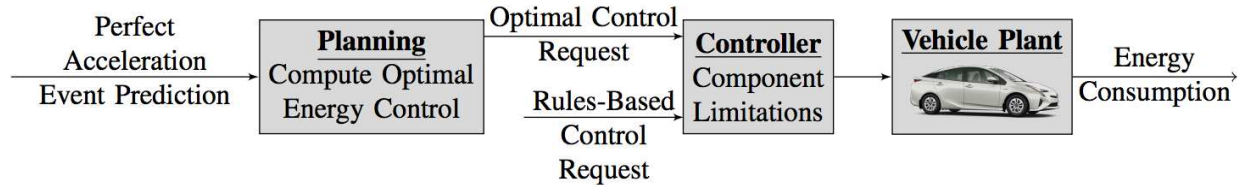
Figure 5.7: A conceptual diagram of how globally optimal vehicle powertrain control is implemented, the globally Optimal EMS.

Deterministic DP is used to derive the globally Optimal EMS for a fixed drive cycle. This is an important and relevant data point to put other FE improvement results in perspective. Although it is not expected that AE prediction will provide nearly the same result as full drive cycle prediction, it will be beneficial to understand the portion of the FE improvement that can be gained from AE prediction. The control conceptual diagram for this globally Optimal EMS is shown in Fig. 5.7.

DP finds the optimal solution using backwards recursion, which avoids solutions that are not optimal as defined by the Bellman principle of optimality [99,100]. For every feasible state variable value, the optimal solution is stored. An appropriate DP scheme consists of a dynamic equation, a cost function, and state and control variable feasibility constraints. Applying this to engine control of a 2010 Toyota Prius results in the following equations

$$\text{SOC}\,(k+1) = \text{SOC}\,(k) - C_1 + C_2\sqrt{C_3 - C_4 v(k) + C_5 v(k)^3 + C_6 \dot{v}(k)v(k) - C_7 P_{\text{ICE}}} \quad (5.9)$$

$$\text{Cost} = \sum_{k=0}^{N-1} f_1\left(P_{\text{ICE}}\right) + W\left(\text{SOC}_f - \text{SOC}(N)\right)^2 \quad (5.10)$$

$$30\ \% \leq \text{SOC}(k) \leq 80\ \% \qquad (k = 0, ...N) \tag{5.11}$$

$$0\ \text{kW} \leq P_{\text{ICE}}(k) \leq 73\ \text{kW} \qquad (k = 0, ...N-1) \tag{5.12}$$

$$C_8 \left[f_2 \left(P_{\text{ICE}} \right) \right] + C_9 v(k) \leq C_{10} \tag{5.13}$$

where Equation 5.9 is the dynamic equation, Equation 5.10 is the cost function, and Equation 5.13 shows the state and control feasibility constrains. The state variable is the battery state of charge (SOC), the control variable is the engine power (P_{ICE}), the exogenous input variable is the velocity (v) and its time derivative (acceleration $\dot{v}$), the cost is the fuel mass consumed (m_{fuel}), C_1 through C_{10} are constants, and W is an SOC target penalty weight set arbitrarily at 10,000. The remaining variables describe time discretization where k is the timestep number and N is the final timestep number.

The solution to this problem is an optimal control matrix which provides the minimum fuel consumption engine power for any feasible time and battery SOC during the AE. An example of the optimal control matrix for the Fort Collins city drive cycle is shown in Fig. 5.8. For example, at a time of 430 seconds,an engine power of 27 kW is required for almost every feasible value of battery SOC, which results in the the minimum fuel consumption solution.
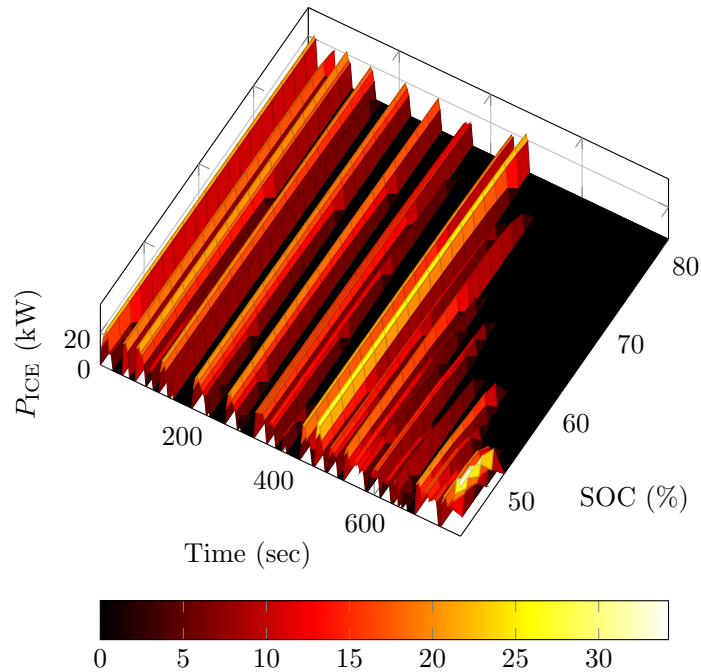
Figure 5.8: The optimal control matrix derived using dynamic programming for a full drive cycle.

5.2.4 Optimal Energy Management Strategy: Perfect Acceleration Event Prediction
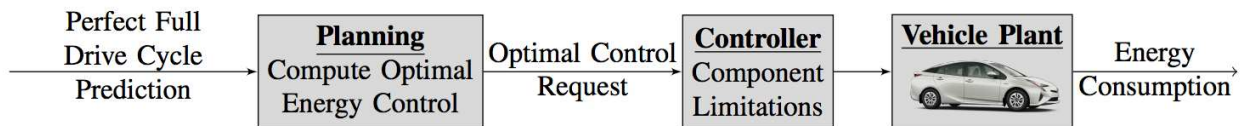
Figure 5.9: A conceptual diagram of how optimal vehicle powertrain control is implemented in acceleration events only.

Deterministic DP is also used to derive the Optimal EMS for each AE in each drive cycle. This is also an important and relevant data point to put the new AE control FE improvement results in perspective. The goal of designing alternate AE control strategies is to show that the new control strategy achieves nearly the same result as perfect prediction of the actual AE in the drive cycle. The control conceptual diagram for this Optimal EMS is shown in Fig. 5.9.
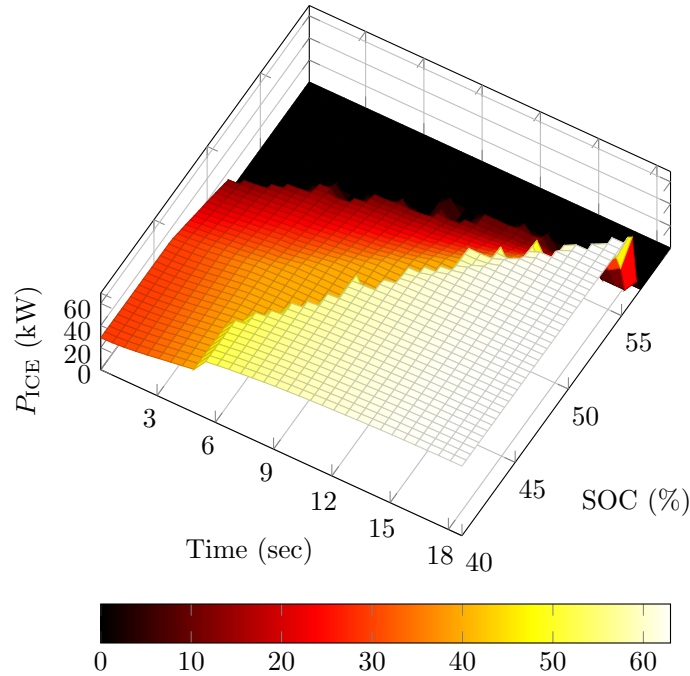
Figure 5.10: The optimal control matrix derived using dynamic programming for a high velocity acceleration event

Derivation of an Optimal EMS for AEs follows the same procedure outlined in section 5.2.3, except the exogenous input is not the entire drive cycle, just the AE. The DP algorithm is run for each AE in each drive cycle. An example result of the optimal control matrix is shown in Fig. 5.10. For example, this figure shows that if battery SOC is 40% and 3 seconds have elapsed since beginning the AE, 30kW of engine power will provide the minimum fuel consumption solution.

Fig. 5.9 shows how perfect AE prediction is implemented in each drive cycle. During portions of driving that are not AEs, the Baseline EMS is employed (rules-based control). As an example, if a drive cycle consists of an AE followed by steady state followed by an AE, then the control strategy is an Optimal EMS for the first AE, the control strategy then reverts to the Baseline EMS for the steady state portion, and then switches to an Optimal EMS for the second AE.

This was realized in simulation by first running the vehicle model with the Baseline EMS, removing portions of control that take place during an AE, and implementing the Optimal EMS for

each AE that seeks a final SOC value, SOC_f, to be coincident with the SOC_f from the Baseline EMS.

5.2.5 Optimal Energy Management Strategy: Acceleration Event Category Prediction
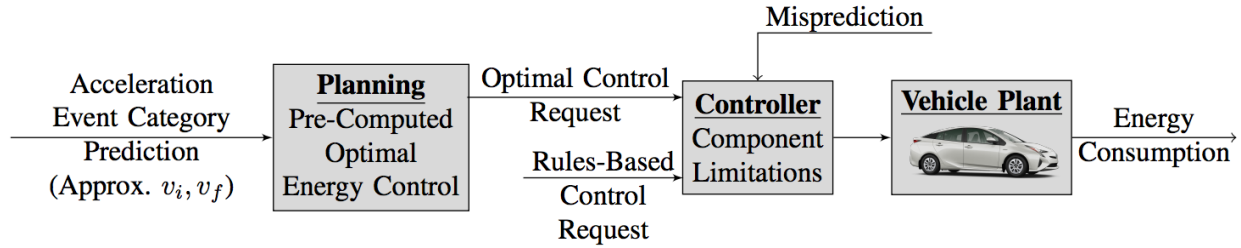
Figure 5.11: A conceptual diagram of how the proposed acceleration event optimal vehicle powertrain control is implemented.

Previous research has shown that FE is improved despite mispredictions when using a DP derived control matrix [72]. Part one of this research investigated an AE categorization scheme to take advantage of this result. A dataset of 384 real world drive cycles was used to extract 7,708 AEs. Note that this dataset does not include any of the drive cycles analyzed for this study. Significant and robust FE improvements were obtained for a categorization scheme consisting of 15 end velocity categories and 10 starting velocity categories for which one Optimal EMS was derived for each category [107]. This overall control strategy can now be tested on a variety of AEs in independent drive cycles.

Fig. 5.11 shows how AE prediction categorization is implemented for each drive cycle. During portions of driving that are not AEs, the Baseline EMS is employed (rules-based control). Implementing this control strategy in each drive cycle, results in sections of applying a precomputed Optimal EMS and sections of applying the Baseline EMS. For example, if a drive cycle starts with an AE, the Optimal EMS for an associated AE category is implemented. Once the AE ends, the Baseline EMS is implemented. Then, if a second AE is identified, the Optimal EMS for an asso-

ciated AE category can be applied once this second AE starts. After the second AE, the Baseline EMS is implemented again. This process continues for the duration of the drive cycle. Because the optimal solution is defined for all feasible states of the vehicle, different values of battery SOC are automatically accounted for and adjusted. Battery SOC for this control strategy may vary significantly from the Baseline EMS as the drive cycle progresses.

The major advantage of this control strategy is that Optimal EMS calculations are not computed in real time. The Optimal EMS is essentially implemented as a look-up table thus making it compatible with the current abilities of vehicle powertrain controllers.

5.3   Results

To compare and understand each of these control strategies, a comparison of the FE and the drive cycle characteristics is required as well as a time trace of the drive cycle, FE, and battery SOC. This time trace is presented for a representative case of city driving, highway driving, and for the aggressive driving cycle. A time trace for all other drive cycles is shown in Appendix C.

5.3.1   Fuel Economy Improvement Comparison

Four control strategies are required to properly analyze the results of the proposed AE categorization control strategy: (1) the Baseline EMS, (2) the globally Optimal EMS from perfect full drive cycle prediction, (3) the Optimal EMS from perfect AE prediction, and (4) the proposed AE categorization prediction. Note that second control strategy, the globally Optimal EMS from perfect full drive cycle prediction, is the maximum possible FE that can be achieved from an Optimal EMS. The third control strategy, the Optimal EMS from perfect AE prediction, is the maximum possible FE that can be achieved from only AE prediction with an Optimal EMS. These four control strategies are then reduced to three FE results by calculating the FE improvement over the Baseline EMS as $\mathrm{FE_{New\ Control} - FE_{Baseline\ EMS}}/\mathrm{FE_{Baseline\ EMS}} \times 100\%$.
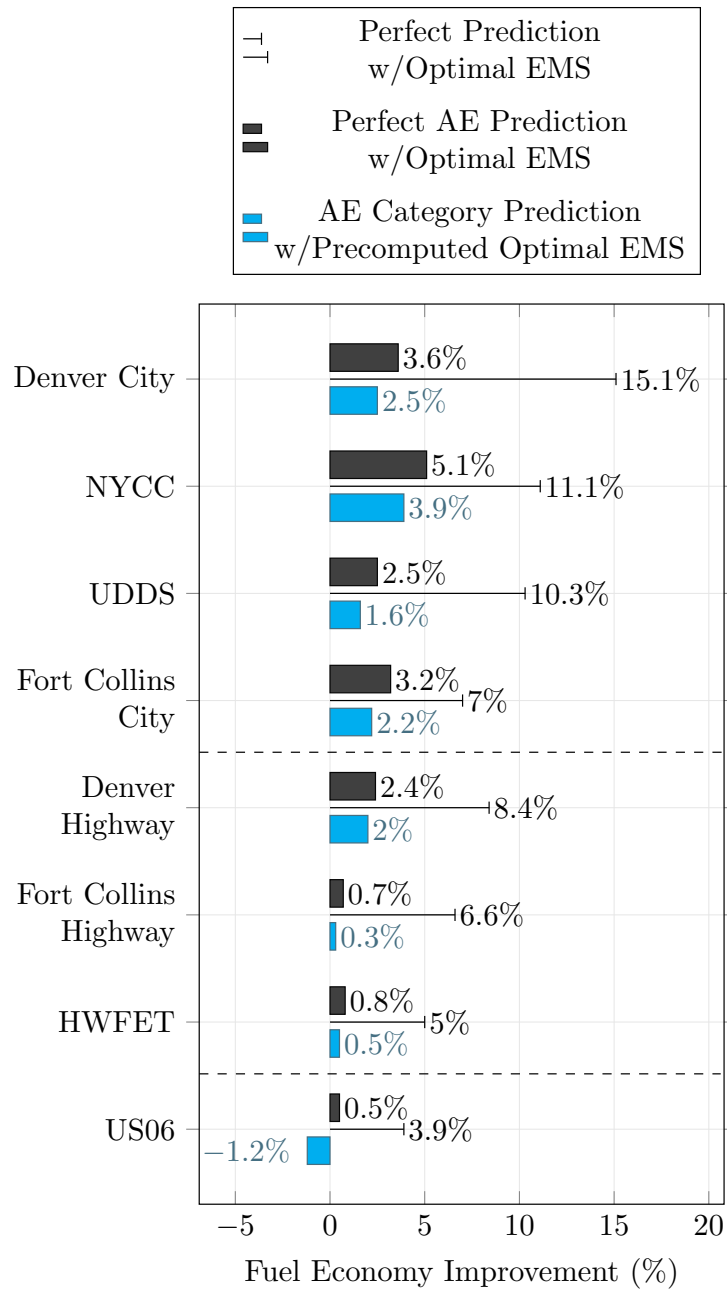
Figure 5.12: All FE results shown as a percentage improvement over the Baseline EMS FE. Note that all Optimal EMS are derived using DP.

Fig. 5.12 shows the FE results for all control strategies for all drive cycles. As expected, perfect full drive cycle prediction results in a significant FE improvement ranging from 3.9% for the US06 cycle up to 15.1% for the Denver City Cycle. Perfectly predicting every AE in each drive cycle results in a sizable FE improvement ranging from 0.5% for the US06 drive cycle up to 5.1% for the

Table 5.3: All drive cycles analyzed.

Drive Cycle	Number of AEs	AE Portion of Drive Cycle	Average v for AEs
Denver City	28	18%	15.3 $^m/_{sec}$
NYCC	13	18%	14.9 $^m/_{sec}$
UDDS	22	22%	17.4 $^m/_{sec}$
Fort Collins City	19	23%	20.5 $^m/_{sec}$
Denver Highway	18	20%	23.4 $^m/_{sec}$
Fort Collins Highway	11	13%	18.2 $^m/_{sec}$
HWFET	4	10%	23.4 $^m/_{sec}$
US06	12	26%	25.7 $^m/_{sec}$

NYCC drive cycle. Predicting only the AE category and applying a precomputed Optimal EMS can result in significant FE improvements but the results span a 1.2% FE loss for the US06 drive cycle up to a 3.9% FE improvement for the NYCC drive cycle.

Table 5.3 compares some characteristics of each drive cycle. The Fort Collins Highway Cycle and the HWFET cycle have the fewest AEs and thus AEs only compose 13% and 10% of the drive cycle respectively. The Denver City Cycle, the NYCC drive cycle, and the UDDS drive cycle have the smallest AE average velocity. The US06 drive cycle has a small number of AEs and the highest AE average velocity.

By comparing Fig. 5.12 and Table 5.3, trends can be discovered regarding large FE improvement cases. Fig. 5.12 shows that the Denver City Cycle, the NYCC, the UDDS, the Fort Collins City Cycle, and the Denver Highway Cycle all have a large FE improvement from AE category prediction with a precomputed Optimal EMS. And Table 5.3 shows that these drive cycles have a large number of AEs and the AE average velocity is low. Therefore, for drive cycles with lots of low velocity AEs, category prediction with a precomputed Optimal EMS provides a significant FE improvement.

Other trends can also be discovered by comparing Fig. 5.12 and Table 5.3 relating to small FE improvement cases. Fig. 5.12 shows that the Fort Collins Highway and the HWFET drive cycles result in the lowest FE improvement for AE category prediction with a precomputed Optimal EMS. Table 5.3 shows that these drive cycles do not have many AEs and the HWFET has high velocity

AEs. Therefore, using an AE category prediction with a precomputed Optimal EMS does not provide a significant FE improvement for drive cycles without many AEs.

Lastly the FE loss scenario can be understood by comparing Fig. 5.12 and Table 5.3. Fig. 5.12 shows a 1.2% FE loss for the US06 drive cycle when AE category prediction with a precomputed Optimal EMS is used. Table 5.3 shows that this drive cycle has a significant amount of AEs, but the AEs are at a significantly higher velocity. This is important because high velocity AEs typically result in a FE loss due to the original dataset used to precompute the Optimal EMS not including many high velocity AEs [107].

In general, AE category prediction with a precomputed Optimal EMS results in half to 90% of the FE improvement from perfect AE prediction. This strategy does not require real-time computations and requires very limited predictions. The FE improvement results from perfect AE prediction compared to full drive cycle prediction are dependent on how many AEs are in the drive cycle. But, for drive cycles with a large number of AEs, the FE improvement can be significant for a relatively low prediction requirement. For example, 18% of the NYCC drive cycle is composed of AEs, but half of the maximum FE improvement can be realized by only predicting AEs.

5.3.2 Drive Cycle Results
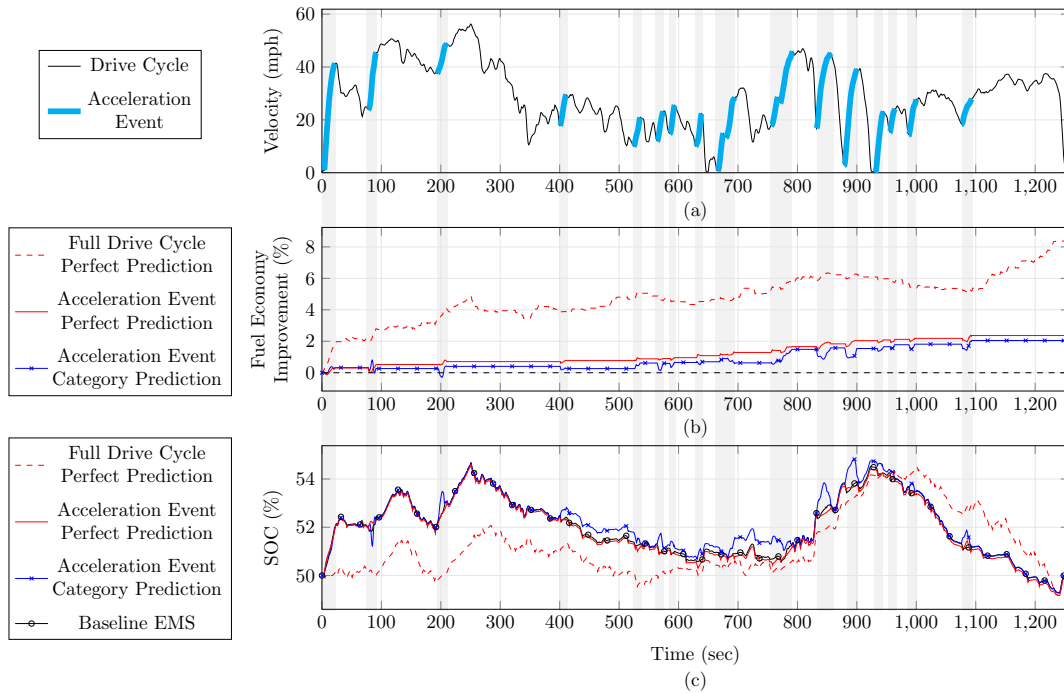
Figure 5.13: The Denver Highway Cycle which shows a close correlation between AE category prediction and perfect AE prediction.

The FE results shown in Fig. 5.12 can be further explored by investigating the second-by-second engine operation and battery SOC for each AE in each drive cycle. There are three unique FE results: (1) nearly the same FE improvement from AE category prediction and perfect AE prediction, (2) an overall FE improvement but a reduction when compared to perfect AE prediction, and (3) a FE loss when compared to the Baseline EMS. A representative drive cycle from each of these results will be presented and discussed. All additional drive cycles are shown in Appendix **??**. Details as to how FE is improved are presented and discussed in the previous study [107].
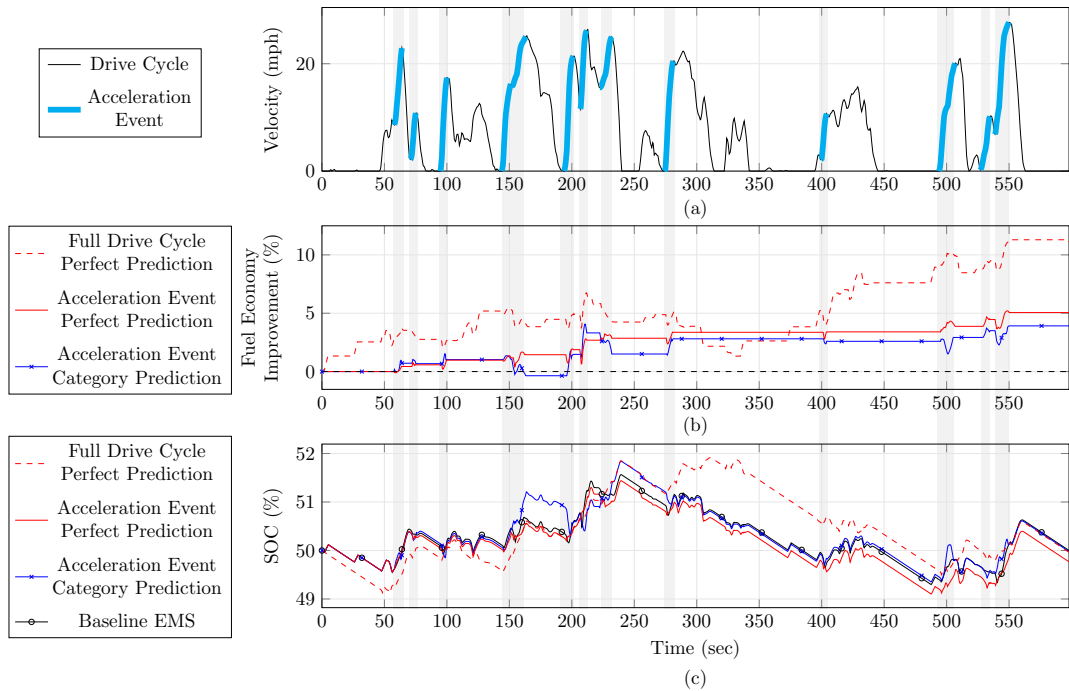
Figure 5.14: The NYCC drive cycle which shows a similar correlation between AE category prediction and perfect AE prediction.
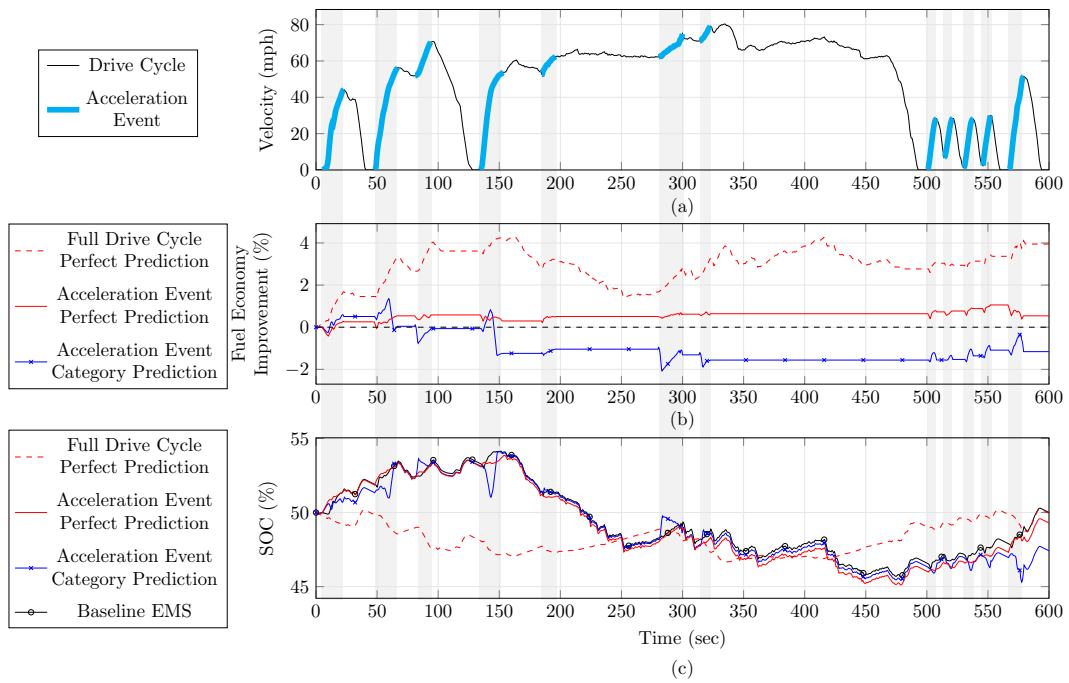
Figure 5.15: The Us06 drive cycle which worse results between AE category prediction and perfect AE prediction.

The drive cycle that results in nearly the same FE improvement from AE category prediction and perfect AE prediction is the Denver Highway drive cycle. As shown in Fig. 5.12, perfect AE prediction results in a 2.4% FE improvement while AE category prediction results in a 2.0% FE improvement. The velocity trace for this drive cycle with AEs identified is shown in Fig. 5.13a. Figs. 5.13b and 5.13c show a second-by-second FE improvement and battery SOC results along the drive cycle. For full drive cycle prediction, there is a significant SOC excursion compared to the Baseline EMS but also a significant FE improvement. Perfect AE prediction and AE category prediction provide nearly the same overall FE improvement, but there are significant differences in individual AE operation. For example, the AE that starts at 847 seconds results in more fuel consumption for AE category prediction and a banking of battery SOC. These differences even out over the drive cycle.

One drive cycle that results in an overall FE improvement but a reduction when compared to perfect AE prediction is the NYCC drive cycle. As shown in Fig. 5.12, perfect AE prediction results in a 5.1% FE improvement while AE category prediction results in a 3.9% FE improvement. The velocity trace, AE identification, second-by-second FE results for each control strategy, and battery SOC are shown in Fig. 5.14. For each control strategy there is a significant FE improvement with limited SOC excursion. Additionally when comparing perfect AE prediction and AE category prediction, the overall FE improvements are similar but results for each AE can vary. For example, the AE that starts at 145 seconds results in more fuel consumption but SOC banking which is evened out once the next AE starts,

The drive cycle that results in a FE loss when compared to the Baseline EMS is the US06 drive cycle. As shown in Fig. 5.12, perfect AE prediction results in a 0.5% FE improvement while AE category prediction results in a 1.2% FE loss. The velocity trace, AE identification, second-by-second FE results for each control strategy, and battery SOC are shown in Fig. 5.15. Minimal FE improvements are achieved for each perfectly predicted AE, but for category AE prediction, FE losses are frequent. For example, AEs at 50 seconds, 90 seconds, 140 seconds, etc. results in FE losses. This indicates that the Optimal EMS derived for this category does not adequately

capture aggressive driving. In other words, the AE dataset used to derive the Optimal EMS must be inclusive of current driving habits or FE losses are possible.

5.4   Conclusion

In this study, four EPA drive cycles and four real world drive cycles were used which represent city driving, highway driving, and aggressive driving. Four control strategies to be tested on each drive cycle were also developed. The vehicle model used is a 2010 Toyota Prius and was designed to be responsive to alternate control inputs. The first control strategy is designed to be representative of the current vehicle operation, where the engine operation was determined in the Autonomie modeling software and then implemented in an equation-based power-split model and validated against real world vehicle operation. The second control strategy is the globally Optimal EMS derived using full drive cycle prediction with DP. The third control strategy is perfect prediction of all AEs within each drive cycle with the Optimal EMS derived using DP. The final control strategy is built from part one of this research and is a look-up table of an Optimal EMS for a similar AE predicted from each drive cycle. Results show a FE improvement of between half to 90% of perfect AE prediction which in turn represents one fourth to half of the FE improvement results of full drive cycle prediction. But FE losses are possible if the AEs used to derive the Optimal EMS are not representative of current driving habits.

FE improvements for all types of driving are possible using an Optimal EMS derived using DP for a similar AE within a drive cycle, with the largest FE improvements possible for city driving. This indicates that real-time calculation of an Optimal EMS may not be necessary and perhaps sacrificing optimality for fast computation may be the wrong approach to improving vehicle FE with a predictive Optimal EMS. Overall, the demonstrated FE improvement from prediction of only AEs and applying a precomputed Optimal EMS further progresses the implementability of an Optimal EMS in modern vehicles.

5.5 Chapter Conclusions

This section of the research effort has allowed us to partially address Research Question 2, which is restated here:

Research Question 2: *What level of prediction fidelity and scope is required to realize a fuel economy improvement through predictive energy management and potentially eliminate the need for real-time computation?*

Research Question 2 is associated with Hypothesis 2:

Hypothesis 2: *Implementing a general prediction solution for the acceleration portions of a drive cycle will result in FE improvements without the need for perfect prediction.*

This research effort has provided additional support for this hypothesis. Through implementation of a limited AE prediction control strategy and with comparison to other optimal control strategies it was determined that significant and robust FE improvements can be realized. This demonstrates that predictive energy management can be implemented over short segments of driving and that an optimal control derived for a similar driving segment can be used to improve FE thus eliminating the need for real time computations. This significantly improves the feasibility of predictive energy management implementation.

Chapter 6

Enabling Prediction for Optimal Fuel Economy Vehicle Control

This study investigates the potential of using only current vehicle technology to make predictions for use in predictive energy management. It involves gathering real outputs from current vehicle technology, using these output to train an artificial neural network to make vehicle speed predictions, using the prediction with a dynamic programming algorithm, a high fidelity model of a 2010 Toyota Prius, and comparing this control strategy to perfect prediction optimal control strategies. This research is the result of a collaboration with Jordan A. Tunnell in the electrical and computer engineering department who assisted with the operation and recording of the vehicle technology. His research has focused on the technology detection algorithms where my research has focused on how the information can be used to improve FE. His research paper [172] and my research paper [173], reproduced here, have been accepted and will be published in April 2018.

6.1   Introduction

There is a global need to increase automotive vehicle fuel economy (FE). An increase in FE would result in global decreases in energy consumption [6], petroleum importation costs [8, 10], greenhouse gas emissions [11], and air pollution [87]. A reduction of greenhouse gas emissions reduces the effects of climate change [111], while a reduction in air pollution reduces human deaths associated with air pollution [174]. Because of these issues, governments around the world have imposed various FE requirements that automotive manufacturers are required to meet [17]. A key technology to ensure FE compliance is vehicle electrification [18]. Hybrid electric vehicles (HEV) and plug-in hybrid electric vehicles (PHEV) are able to realize FE improvements due to the powertrain efficiency improvements enabled through intelligent use of mechanical power from the engine and electric power from the battery [175].

121

However, there is also a global need to improve vehicle safety. In the United States, 90% of vehicle crashes are due to driver error [176]. This has fostered significant development in commercially implemented driver assistance technology, known as Advanced Driver Assistance Systems (ADAS), over the past 30 years [21] that focus on safety [177]. ADAS sensing is achieved through a variety of sensors including cameras, radar, and ultrasonic detection [1]. A conceptual diagram of the potential sensing abilities of ADAS is shown in Figure 1. Note that connected and autonomous vehicle (CAV) technology further improves safety issues but has not currently experienced widespread commercial adoption [5].
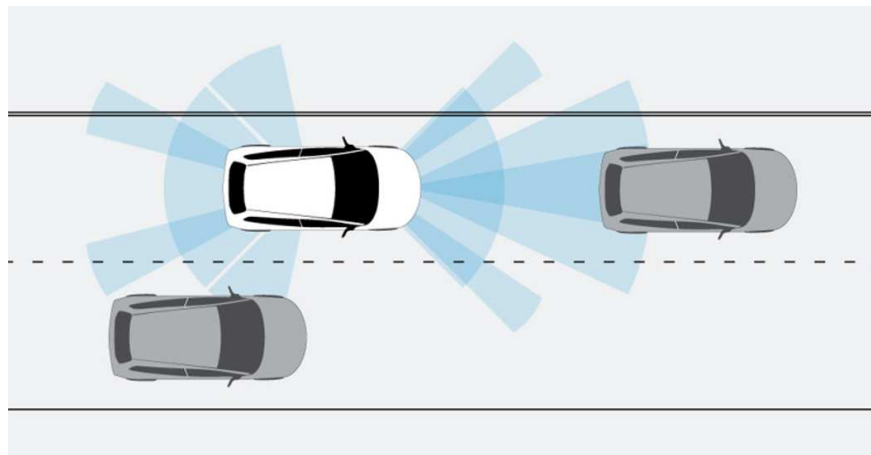
Figure 6.1: A conceptual image of the sensing capabilities and scope of modern ADAS using a variety of sensors [**?**, 1].

In addition to the advancement of ADAS technologies, travel time technology has also improved significantly in recent years. Travel time calculations are currently used in routing software and programmable street signs shown in Figure 2. The travel time monitoring system records vehicles through a variety of sensors including Bluetooth, magnetic detectors, and cell phone signal monitoring and stores results in a database used by local state departments of transportation (DOT) [2]. Travel time information has widespread commercial adoption and is publically available.

(a)	**(b)**
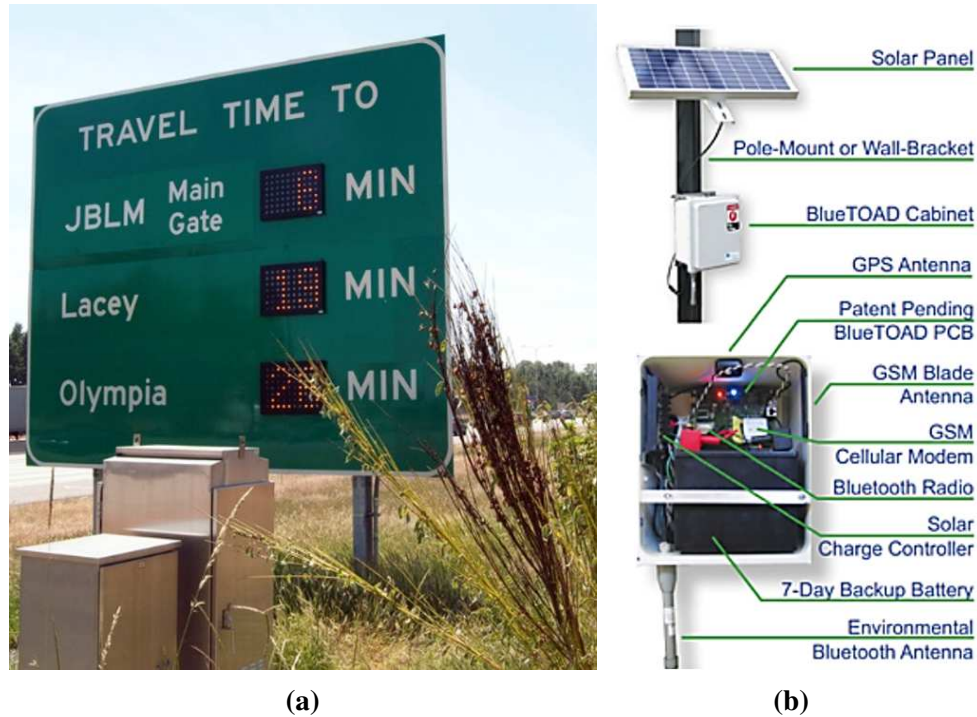
Figure 6.2: A conceptual image of the travel time calculation technology in deployment (a) and the basics of the sensing systems (b) [2].

The global need for increased FE and the trend of increasing sensing capabilities in the automotive industry have led to the development of improved vehicle control strategies. These strategies have the largest FE improvement in HEVs and PHEVs due to the optimization of engine power usage and battery power usage. For a fixed route, this can be accomplished through driver feedback to promote efficient driving habits (Eco-driving) [30, 178] as well as through optimal powertrain control to improve the powertrain efficiency [20]. Recent research suggests that the highest FE improvements are possible when Eco-driving is combined with optimal powertrain control [130]. The research in this paper is focused on improving FE through optimal powertrain control, which is typically discussed as an Optimal Energy Management Strategy (Optimal EMS). For a globally optimal solution, an Optimal EMS must have perfectly accurate vehicle speed information along the entire route, then a computationally costly calculation must be made through either dynamic programming (DP) [32, 179] or Pontryagin's minimization principle [46, 180, 181]. To reduce the prediction requirement researchers have developed an alternative non-globally Optimal EMS that

is stochastically robust using stochastic dynamic programming [47, 133, 182] and adaptive equivalent consumption minimization strategy [48, 134, 183]. To reduce the high computational cost, a non-globally Optimal EMS that is real time computable is realizable through optimized rules-based control [49, 76], model predictive control [51, 135, 184, 185], and equivalent consumption minimization strategy [50, 186–188]. But, despite the development of numerous alternate Optimal EMS, DP remains the overwhelming favorite due to its ease of use and that it provides the globally optimal control [45].

An existing research gap for commercial implementation of an Optimal EMS is the development of any type of prediction for use in an Optimal EMS [3]. From the limited research that does exist, initial results show that incorporation of traffic information improves prediction quality [57, 61] and that an artificial neural network may provide the most robust predictions [60]. Additionally, recent research suggests that using 15-30 second prediction windows may yield the best FE results when sensors and signals are limited [62]. None of these studies use ADAS technologies to enable prediction.

In this study, we seek to enable prediction for use in an Optimal EMS using a database of similar drive cycles [58, 60, 62, 63] but with the addition of commercially available ADAS and travel time technology. This novel incorporation of ADAS and travel time technology is then used to generate predictions for use in an Optimal EMS. A comparison of the FE improvements for each type of sensor-enabled prediction is the end result.

6.2 Methods

To analyze the effectiveness of various prediction scenarios, a baseline energy management strategy (Baseline EMS) and an Optimal EMS must be compared on city and highway focused drive cycles. The Baseline EMS should be reflective of the current standard and be validated against real world data. The Optimal EMS is composed of multiple subsystems, which include drive cycle prediction, Optimal EMS derivation, and Optimal EMS vehicle implementation.

6.2.1 Drive Cycle Development

Existing research in the prediction component of an Optimal EMS has been successful when a rigorous database of predictable drive cycles is used. Applications for this strategy include delivery or pick-up drive cycles or low traffic drive cycles. In order to make predictions difficult and demonstrate the potential of the prediction scheme, we seek to use high traffic and long drive cycles developed in a big city. We also seek to analyze and understand the application differences for city-focused driving and highway-focused driving.

The first drive cycle used is a city-focused drive cycle. Two of the busiest roads in Denver, CO USA were selected for the drive cycle, one of which passes directly through downtown. This downtown Denver drive cycle (shown in Figure 3) is ten miles long and was driven four times.

The second drive cycle used is a highway focused drive cycle. To complicate this drive cycle, it was modified to take place over two separate interstates and include a city driving portion at the end. The final drive cycle (shown in Figure 4) is also ten miles long and was driven four times. There are varying levels of traffic on each interstate for each drive cycle.

6.2.2 Baseline Energy Management Strategy Simulation

A 2010 Toyota Prius is selected as the vehicle model due to its commercial prevalence and that it has the highest FE in its class. The model used to represent the Baseline EMS is consistent with previous research in that it is a modification of the publically available 2004 Toyota Prius in the Autonomie modeling software to represent a 2010 Toyota Prius [72]. The Autonomie modeling software has demonstrated strong correlation with real world testing and is generally accepted as the standard among industry and research professionals.

The vehicle model must be validated against real world data. Table 1 shows the simulated FE over the industry standard U.S. Environmental Protection Agency (EPA) drive cycles of the Urban Dynamometer Driving Schedule (UDDS) drive cycle, the Highway Fuel Economy Test (HWFET) drive cycle, and the US06 drive cycle. A change in battery state of charge values must be taken in to account according to the SAE J1711 industry standard [104] and the adjust FE can
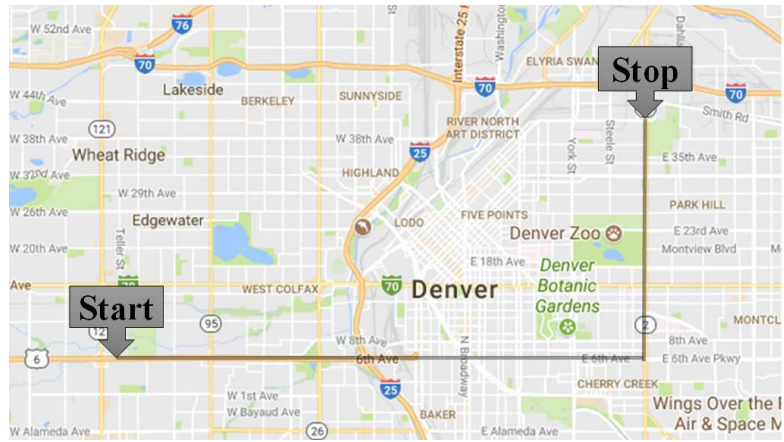
(a)
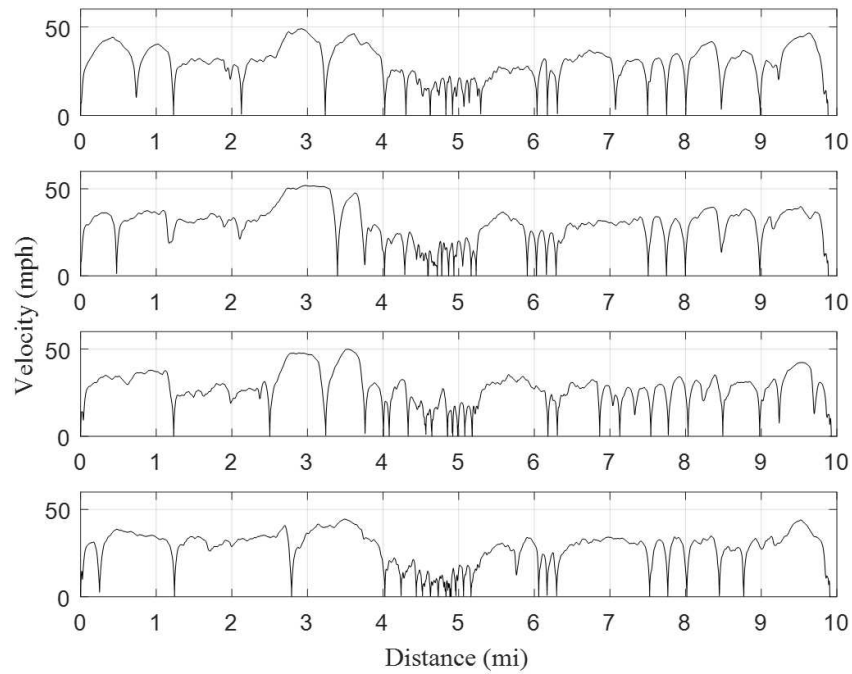
(b)

(c)

Figure 6.3: The city-focused drive cycle that passes through downtown in Denver, CO USA source: Google Maps (a), the velocity with respect to time of each of the four times the drive cycle was driven (b), and images of various driving encounters during the drive cycle (c).

(a)
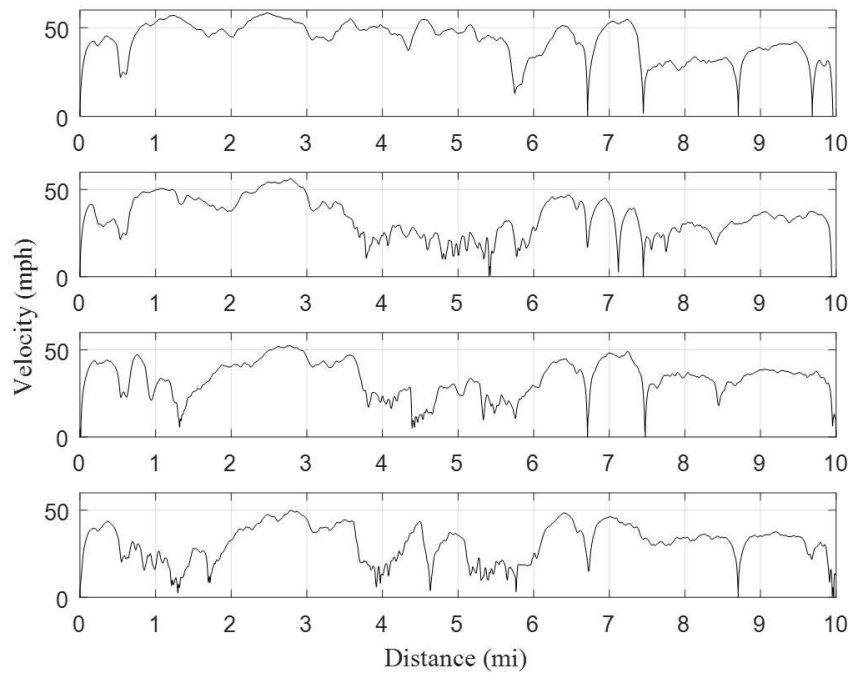
(b)

(c)

Figure 6.4: The highway-focused drive cycle that passes through two interstates in Denver, CO USA source: Google Maps (a), the velocity with respect to time of each of the four times the drive cycle was driven (b), and images of various driving encounters during the drive cycle (c).

| (a) | (b) |
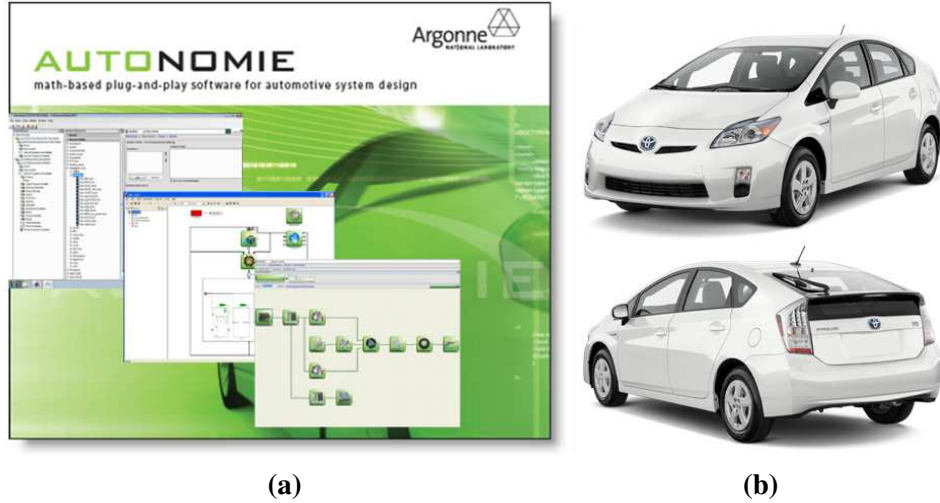
Figure 6.5: The high-fidelity Autonomie modeling software (a) was used to model the real world performance of a 2010 Toyota Prius (b).

be reported. These numbers can then be compared to real world measured values from Argonne National Labs [98]. When the numbers are compared, the simulation FE is within 3% of all of the physically measured FE numbers and the Baseline EMS is considered validated.

Table 6.1: Simulated and measured FE for the 2010 Toyota Prius HEV model developed using Autonomie.

EPA Drive Cycle	Simulated Fuel Economy	Measured Fuel Economy [98]	Percent Difference
UDDS	75.4 mpg	75.6 mpg	0.3%
US06	45.9 mpg	45.3 mpg	-1.4%
HWFET	70.4 mpg	69.9 mpg	-0.7%

6.2.3 Optimal Energy Management Strategy Simulations

Implementation of an Optimal EMS has been recently reviewed [4] and it was determined that a systems-level viewpoint consistent with autonomous vehicle control best captures Optimal EMS implementation. This system includes subsystems for drive cycle prediction (perception), derivation of the Optimal EMS (planning), and implementation of the Optimal EMS in the vehicle.

This systems-level viewpoint is shown in Figure 6. The perception, planning, and vehicle plant subsystems can be developed and investigated independently, but the FE results are dependent on full system implementation and analysis.

Figure 6. The systems-level viewpoint of the optimally controlled vehicle model with subsystems for perception, planning, and a vehicle plant [4].

Perception Subsystem Model

The perception subsystem utilizes outputs of the sensors and signals to generate a prediction of future vehicle operation. The commercially available sensors and signals chosen for the study were

- GPS Coordinates

- Current Vehicle Velocity

- ADAS Detection Ground Truth

- Travel Time Data

Each of these inputs is recorded independently and do not have a direct relationship to one another. Conceptually, GPS data locates the vehicle in the current drive cycle, which allows prediction of the upcoming drive speed based on previous drive cycles. ADAS detection serves to identify points of interest along a drive cycle that may affect unique driver behavior such as red traffic lights, slowing vehicles, or pedestrians in the road. Travel time data provides information about average vehicle velocities in 1-2 mile increments.

All of these inputs are recorded using 1 second timesteps and synchronized by atomic time. The GPS coordinates and current vehicle speed were recorded from the Controller Area Network (CAN) bus directly from the vehicle during the drive cycle. The ADAS detection ground truth (ground truth defined as a set of measurements that are provided by direct observation) was identified from recorded footage from the drive cycle using a camera, shown in Figure 7. The average

<div align="center">(a)   (b)</div>

Figure 6.6: The camera used to record the drive cycle (a) and an example of the camera output (b).

travel time data along the drive cycle was recorded from the Colorado Department of Transportation (DOT).

The ADAS ground truth detection did not include the typical detection objectives that are required for safety focused ADAS implementation. Based on previous research identifying aspects of real-world driving that are most important for prediction [72], it was determined that the ADAS detection objective should only include identification of the state of the traffic light, identifying vehicle speed changes from the vehicle directly in front, identification of stop sign location, and identification of turn lanes. An analysis of automated ADAS detection algorithms and a comparison to ADAS ground truth is available in a separate article [172]. ADAS usage has the advantage of providing detailed drive cycle prediction information for the upcoming 1-100 seconds.

Travel time data in the Denver area does not provide drive cycle prediction details. Instead, it provides approximate drive cycle speeds for the entire drive cycle before the trip has begun. These traffic levels for the entire drive cycle have demonstrated accuracy, as shown in Figure 8, but traffic information may not be as important for an Optimal EMS [72].
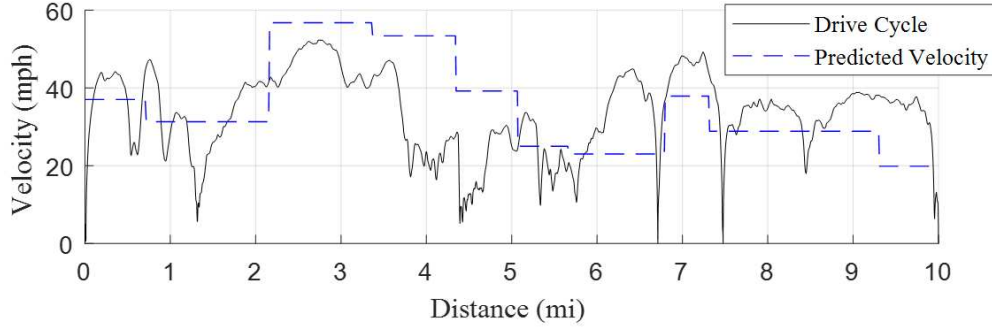
Figure 6.7: Drive cycle predictions possible using travel time data for the highway-focused Denver drive cycle.

There are numerous methods to combine outputs from sensors and signals to generate a vehicle velocity prediction but initial research suggests that an artificial neural network may provide the best results [60]. For time series predictions used in control of dynamic systems, Nonlinear Autoregressive Neural Networks are typically used [189] since they have been demonstrated to be effective [190]. To predict future velocity using the sensor and signal outputs, a nonlinear autoregressive neural network with external input (NARX) is required. This neural network predicts future values of the vehicle velocity, $v(t)$, from past values of the vehicle velocity, $v(t-1)$, and from past values of each of the sensors and signals, $x(t-1)$. This network can be written mathematically as

$$v(t) = f\left[v(t-1), ..., v(t-d), x(t-1), ..., (t-d)\right] \tag{6.1}$$

where d is a time delay. Due to the success of neural networks, there are numerous toolboxes that can be used to design custom neural networks. Since other aspects of the Optimal EMS system must interface with the Autonomie Simulink model, the neural network was designed and implemented in Matlab. NARX networks were trained to predict both the Denver downtown drive cycle and the Denver highway drive cycle using three of the alternate versions of the drive cycle to be analyzed. After comprehensively studying the effect of all NARX parameters on the average FE results, it was found that 3 feedback delays, 1 hidden layer, 1 input delay, scaled conjugate gradient

131

training, 90% data training, 2% data validation, and 8% data testing provided the best results. An overall conceptual diagram of the perception subsystem model is shown in Figure 9. The output of the perception subsystem is a prediction of vehicle velocity from which an Optimal EMS can be determined in the planning subsystem model.
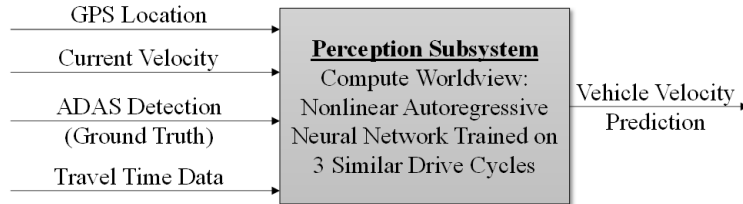
Figure 6.8: Details of the perception subsystem shown in Figure 6 that shows ADAS, GPS and Average Traffic Data as an input to a NNARX perception model to generate a vehicle velocity prediction.

Planning Subsystem Model

The planning subsystem model receives a prediction of the future vehicle operation as an input, determines the globally optimal control using dynamic programming (DP) and issues a control request to the vehicle model. The DP formulation for an HEV Optimal EMS derivation uses the battery state of charge (SOC) as the state variable, the engine power (P_{ICE}) as the control variable, the vehicle velocity (v) as the external input, and the total mass of fuel required (m_{fuel}) as the cost function. This HEV Optimal EMS derivation can then be tailored to a 2010 Toyota Prius by using a power-split vehicle architecture relationship between these variables. A detailed description of this process can be found in previous research [72]. The final form used to derive the optimal control is

$$\text{SOC}\left(k+1\right) = \text{SOC}\left(k\right) - C_1 + C_2\sqrt{C_3 - C_4 v(k) + C_5 v(k)^3 + C_6 \dot{v}(k)v(k) - C_7 P_{\text{ICE}}} \quad (6.2)$$

$$\text{Cost} = \sum_{k=0}^{N-1} f_1\left(P_{\text{ICE}}\right) + W\left(\text{SOC}_f - \text{SOC}(N)\right)^2 \quad (6.3)$$

$$40\ \% \le \text{SOC}(k) \le 80\ \% \qquad (k = 0, ...N) \tag{6.4}$$

$$0\ \text{kW} \le P_{\text{ICE}}(k) \le 73\ \text{kW} \qquad (k = 0, ...N-1) \tag{6.5}$$

$$C_8 \left[f_2 \left(P_{\text{ICE}} \right) \right] + C_9 v(k) \le C_{10} \tag{6.6}$$

where C_{1-10} are constants, k is an arbitrary timestep, N is the final timestep, and W is a penalty weighting factor set at 10,000. SOC_f is the desired final state of charge of the battery. This value is typically set at 50% to encourage typical charge sustaining behavior of an HEV. Electric drivetrain component efficiencies were added to improve the fidelity of the Optimal EMS derivation from the previous publication [72].

The solution of the DP algorithm is a cost-to-go matrix, which is used to derive the optimal control decision matrix. This algorithm can be used to derive the globally Optimal EMS which assumed 100% accurate prediction data (shown in Figure 10) for the entire drive cycle as well as an Optimal EMS derived using time limited prediction data.
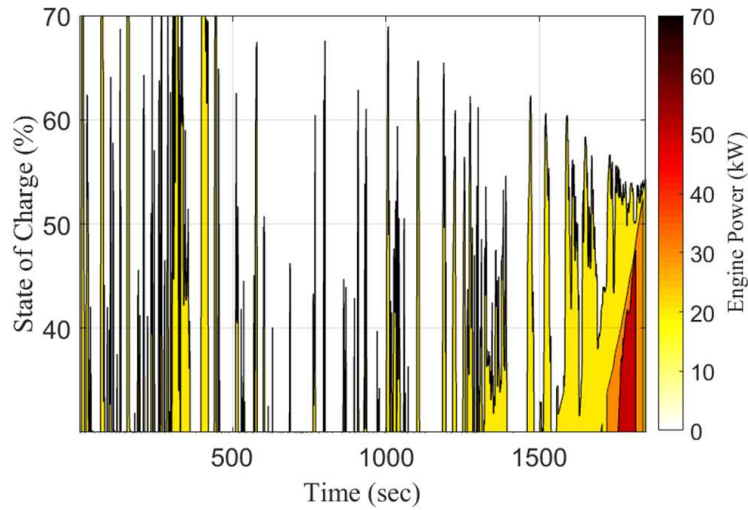
Figure 6.9: The Optimal EMS solution for 100% accurate prediction of the downtown Denver drive cycle.

Results from existing research demonstrate that a 15 or 30 second prediction window is an ideal tradeoff between prediction accuracy and FE improvement potential [62]. Because ADAS technology provides near term prediction data such as identification of a red light or a slowing

133

vehicle, a 15 second prediction window was used. An example of the Optimal EMS from 100% accurate prediction of a 15 second window that is then updated and actuated on a second by second basis is shown in Figure 11.

The technique used for sensing and prediction is a 15 second prediction that is recomputed every second. This implies that an Optimal EMS is calculated for every 15 second window but only the first second of operation is used. Thus, the key metric is not overall drive cycle prediction accuracy but a 15 second prediction accuracy for every second of the drive cycle. Therefore, presenting intermediate drive cycle results concerning velocity prediction accuracy does not provide meaningful insight. For a discussion on velocity prediction error analysis refer to other work [62, 171].
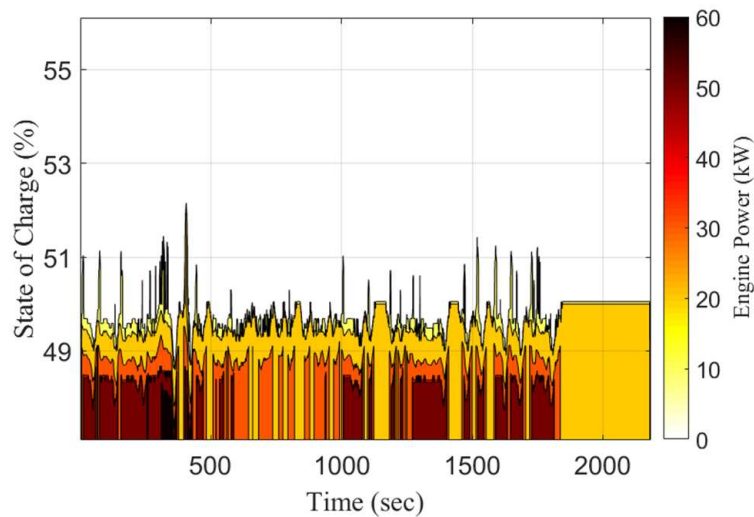
Figure 6.10: The Optimal EMS solution of a 15 second window within the first downtown Denver drive cycle for 100% accurate prediction (a) and sensor and signal output prediction (b).

An overall conceptual diagram of the planning subsystem model is shown in Figure 12. The output of the planning subsystem is the Optimal EMS decision matrix, which provides the optimal engine power for any feasible timestep and battery state of charge, also known as a 2-D lookup table. This output is then used in the vehicle to actuate the Optimal EMS.
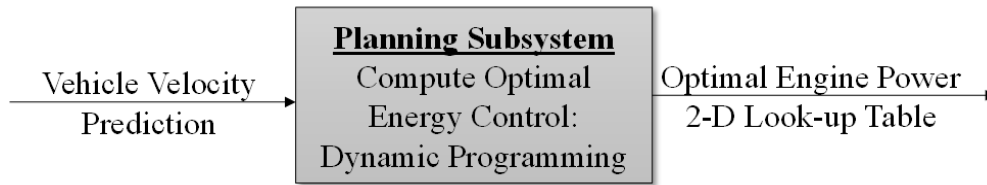
Figure 6.11: Details of the planning subsystem shown in Figure 6 that shows generation of a globally optimal solution for the provided vehicle velocity prediction.

Vehicle Subsystem Model

The input to the vehicle model is the Optimal EMS control request and disturbances attributed to misprediction. The vehicle model used is a modified version of the baseline 2010 Toyota Prius Autonomie model that allows the desired engine power to be overwritten. This model includes a running controller, which enforces individual component operation limitations. The recorded output of this model can be any variable inherent in the Autonomie software. Of particular interest is the fuel consumption, achieved engine power, and battery state of charge. These results can then be compared to the same outputs from Baseline EMS simulation. An overall conceptual diagram of the vehicle subsystem model is shown in Figure 12. The main output of the vehicle subsystem is achieved charge adjusted FE which can be calculated according to the current SAE standard [104].

Figure 13. Details of the vehicle plant subsystem shown in Figure 6 that received the modified control request and implements it with the vehicle running control for FE measurements.

6.3   Results

There are several important data points required to gain insight into the prediction capabilities that are possible using the commercially available sensors and signals discussed. The first relevant data point is the globally Optimal EMS solution, which provides the FE improvement that is possible with 100% accurate prediction of the entire drive cycle. This data point is important because it identifies the absolute FE improvement ceiling. Next, since the chosen sensors and signals are being used to provide 15 second predictions, the 100% accurate 15 second prediction data point

is required (prediction window optimal). This data point identifies the ceiling of the detection capabilities of the chosen sensors and signals in the 15 second window.

Next, to understand the relative importance of the chosen signals, three comparisons can be made Prediction using GPS and current velocity Prediction using GPS, current velocity, and ADAS Prediction using GPS, current velocity, ADAS, and travel time (traffic) information For each of these prediction types, a unique NARX must be trained and implemented. The achieved FE improvement can then be compared to the ceiling value for 15 second prediction as well as the global ceiling. FE improvements are calculated as

$$\text{Percent Improvement} = \frac{\text{FE}_{\text{Optimal}} - \text{FE}_{\text{Baseline}}}{\text{FE}_{\text{Baseline}}} \tag{6.7}$$

To obtain information about general behavior of this technique, a unique NARX was trained using three drive cycle datasets and was then tested on the fourth drive cycle. This leads to four results from the four city drive cycles (for example: train using city drive cycles 1, 2, 3 then test on city drive cycle 4; train using city drive cycles 2, 3, 4 then test on city drive cycle 1; etc.) and four results from the four highway drive cycles. This implies that results cannot be "cherry-picked" and that the final results will be representative of overall behavior of this technique.

6.3.1 City-Focused Drive Cycle

For the city-focused drive cycle, the FE results are shown in Figure 14, the engine operation is shown in Figure 15, and the battery state of charge results are shown in Figure 16.
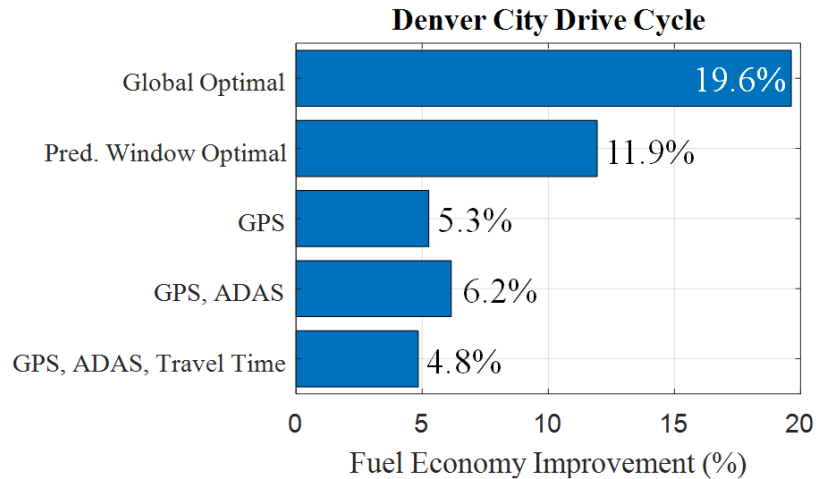
Figure 6.12: Average FE improvement results for the four Denver downtown drive cycles.

The Baseline EMS for the city-focused Denver drive cycle was able to achieve 58.7 mpg on average, which was improved significantly by the globally Optimal EMS to 70.2 mpg; a total percent improvement of 19.6% as shown in Figure 14. Figure 14 also shows an 11.9% improvement for 15 second perfect prediction and a 5.3% FE increase for prediction using only GPS and current velocity. There is a 6.2% FE increase when using GPS, current velocity, and ADAS, which is the largest non-perfect prediction result. Lastly, there is a 4.8% FE increase when using GPS, current velocity, ADAS, and travel time information which is less than when travel time information is not included.
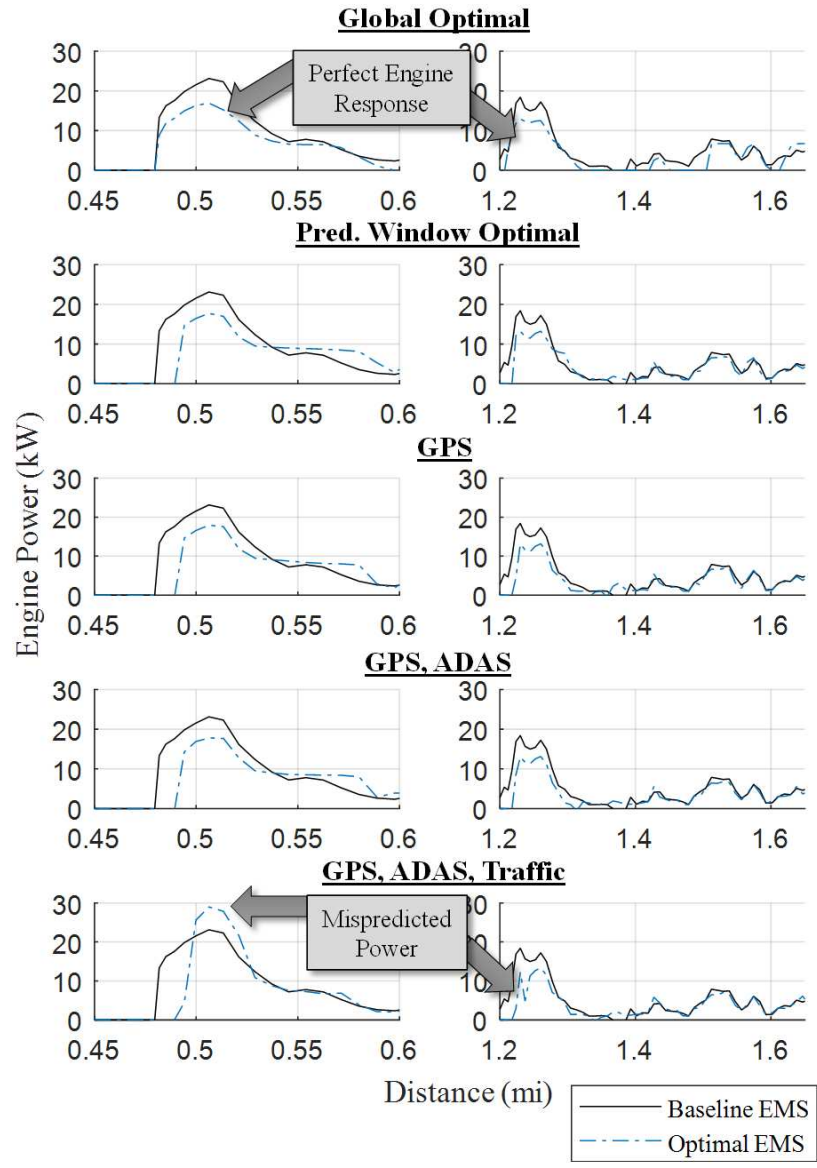
Figure 6.13: Engine power comparison for a Denver downtown drive cycle.

These results suggest that for city-focused driving, travel time information does not provide enough resolution to aid in prediction. In fact, excess or inaccurate information may hinder the prediction quality and thus the FE gain. Figure 15 shows two instances for which the addition of travel time data caused significant mispredictions of the engine power that was required. Meanwhile, the other prediction scenarios follow the prediction window optimal solution very closely. Figure 15 also shows the benefit of full drive cycle prediction since the global Optimal EMS is able

to leverage operation over the entire drive cycle. A drawback of the globally Optimal EMS is that the battery state of charge varies significantly over the drive cycle as shown in Figure 16. This may be due to the low cost of increasing battery charge in general since most optimal solutions follow a similar trajectory [72]. The Baseline EMS (shown in black) executes charge banking for the first half of the drive cycle while the globally Optimal EMS charge depletes over the first half of the drive cycle to realize a FE improvement but still is able to end the drive cycle at the same value of final state of charge. All other cases use 15 second prediction windows and are constrained to end the 15 second prediction window at 50% state of charge. The result over the full drive cycle is a rigid charge sustaining operation that may improve battery longevity. The final FE numbers are computed using charge corrections [104].
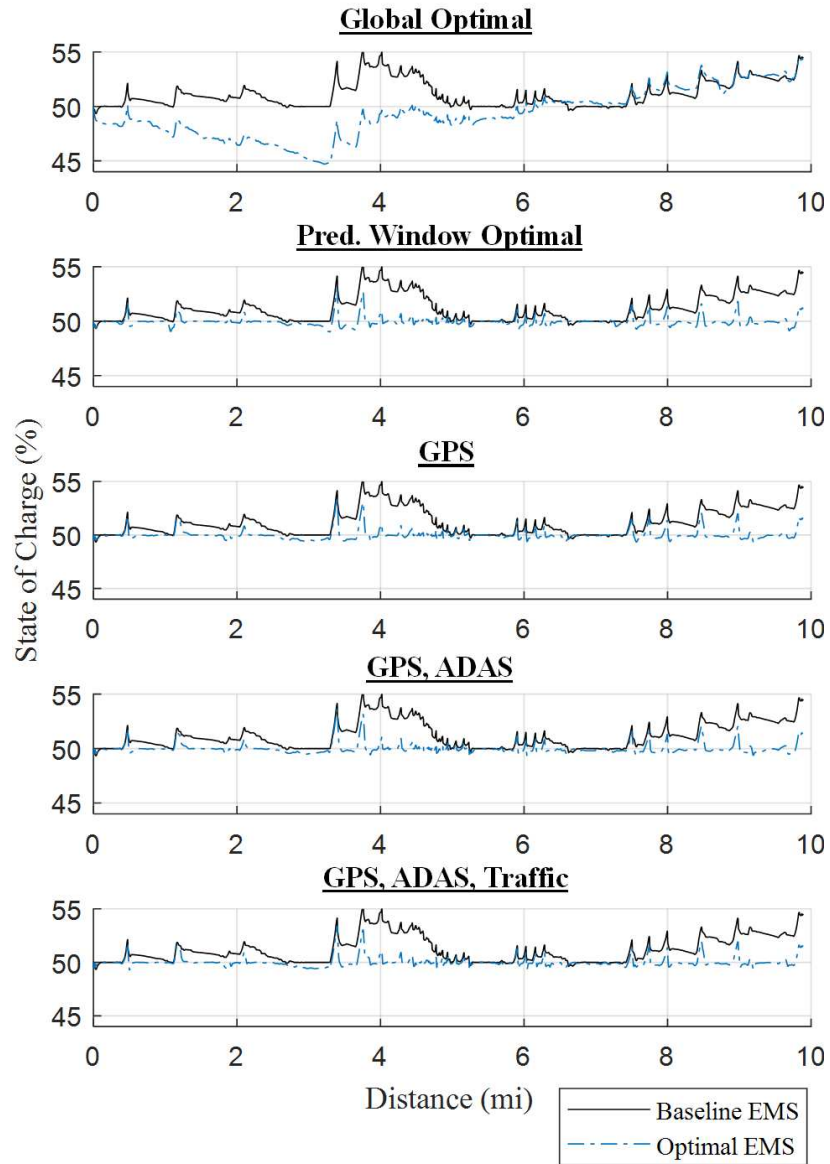
Figure 6.14: Battery state of charge comparison for a Denver downtown drive cycle.

6.3.2 Highway-Focused Drive Cycle

For the highway-focused drive cycle, the FE results are shown in Figure 17, the engine operation is shown in Figure 18, and the battery state of charge results are shown in Figure 19.
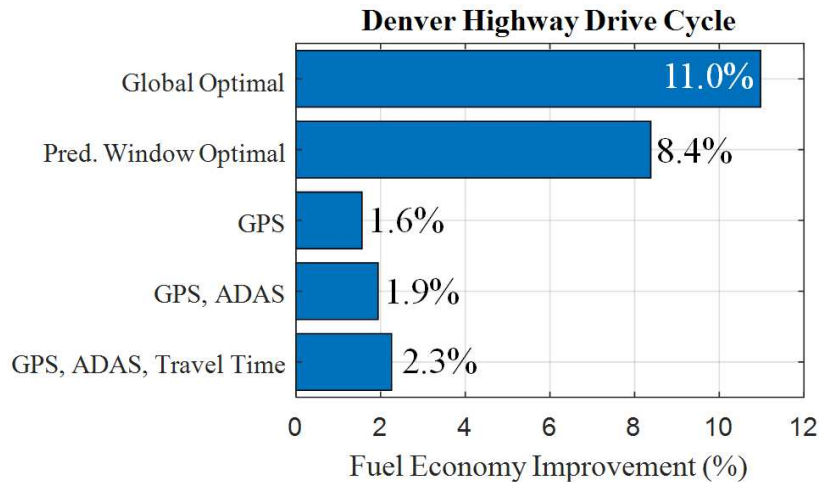
Figure 6.15: Average FE improvement results for the Denver highway drive cycles.

The Baseline EMS for the highway-focused Denver drive cycle was able to achieve 64.0 mpg, which was improved by the globally Optimal EMS to 71.1 mpg; a total percent improvement of 11.0% as shown in Figure 17. Figure 17 also shows a 8.4% improvement for 15 second perfect prediction and reduced FE improvements for all sensor configurations. There is a 1.6% FE increase for prediction using only GPS and current velocity. There is a 1.9% FE increase when using GPS, current velocity, and ADAS. Lastly, there is a 2.3% FE increase when using GPS, current velocity, ADAS, and travel time information, which is the largest non-perfect prediction result. These results suggest that for highway-focused driving, travel time information provides a significant prediction advantage and FE improvement. For highway driving, there is limited environmental information to aid in prediction therefore the current resolution of travel time data (shown in Figure 8) is useful. Due to the unpredictability of traffic induced slowdown regions on the highway, prediction using GPS and current vehicle velocity provide the lowest FE improvements. The evidence for the results in Figure 17 can be seen in Figure 18, which shows that prediction using GPS, current velocity, ADAS, and travel time (traffic) information provides the most similar engine response to the 15 second perfect prediction (prediction window optimal) engine response. Additionally, prediction using GPS and current velocity produces its own engine response.

141
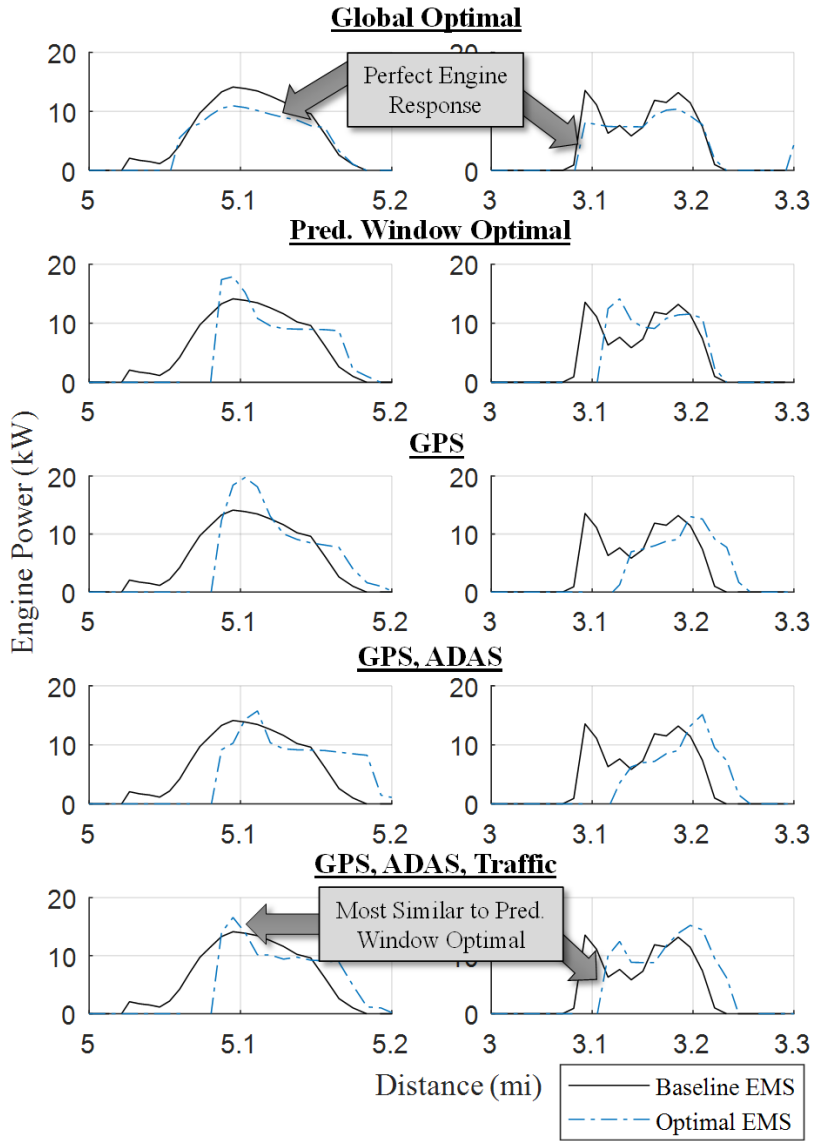
Figure 6.16: Engine power comparison for a Denver highway drive cycle.

As with the city-focused drive cycle, the globally Optimal EMS for the highway-focused drive cycle produces a battery state of charge that varies significantly over the drive cycle as shown in Figure 19. Also, similar to the city-focused drive cycle, all other cases that use a 15 second prediction windows achieve rigid charge sustaining behavior since each 15 second prediction window is constrained to end at 50% state of charge. This rigid charge sustaining operation may improve battery longevity. The final FE numbers are computed using charge corrections [104].
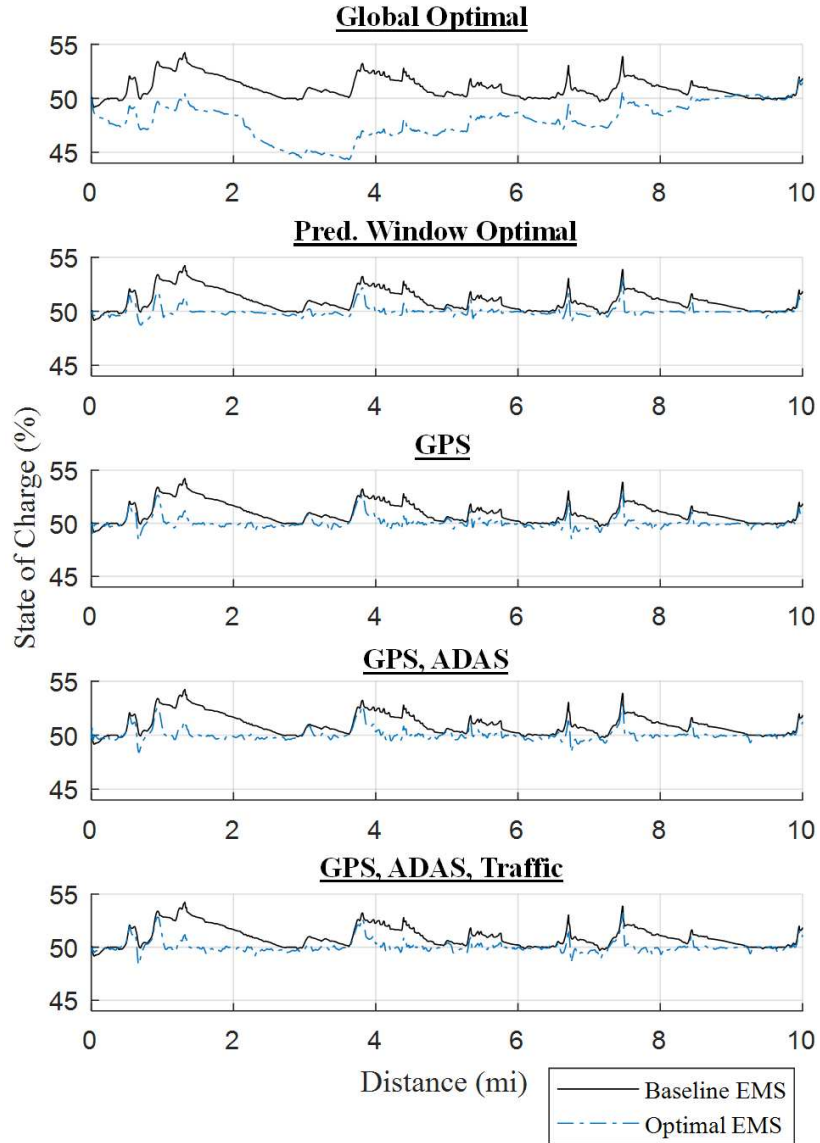
Figure 6.17: Battery state of charge comparison for a Denver highway drive cycle.

6.4 Conclusions

In this study, a unique set of sensors and signals was composed to investigate optimal vehicle control over ten mile long, busy drive cycles in a major capital city. City-focused and highway-focused drive cycles were driven during which GPS, current vehicle velocity, ADAS detection, and travel time data was recorded. These sensor and signal outputs were then input into a neural network perception model to determine future vehicle operation. The future vehicle operation was

then used to derive the Optimal EMS using DP for 15 second prediction windows. The Optimal EMS was then implemented in a validated model of a 2010 Toyota Prius in the Autonomie software. The results show that for the city-focused drive cycle, large portion of the globally optimal Improvement can be achieved using GPS, current velocity and ADAS detection data in a prediction model coupled with optimal control. The results also show that for the highway-focused drive cycle, a large portion of the globally Optimal FE improvement can be achieved using GPS, current velocity, ADAS detection, and travel time data in a prediction model coupled with optimal control.

Adding future vehicle operation prediction to the existing safety objectives of ADAS is a viable method to enable and improve prediction for an Optimal EMS. In addition, travel time information significantly improves prediction for an Optimal EMS when driving on the highway. Exact and full prediction of the entire drive cycle is not required to obtain a significant FE improvement through implementation of an Optimal EMS which agrees with previous research [72]. Additionally, these sensors and signals are already in widespread commercial use, which suggests that it may be possible to implement an Optimal EMS in current vehicles. This could be achieved by either implementing the proposed methods in vehicles as they are manufactured, or via a retrofit kit for vehicles currently on the road. The retrofit kit would likely involve a software/firmware update and an external processor. The main costs associated with this FE improvement method are from development and testing. Once thoroughly developed, FE savings would quickly payback the retrofit cost. Exact payback would depend on vehicle use and architecture.

6.5   Chapter Conclusions

This section of the research effort has allowed us to partially address Research Question 3, which is restated here:

Research Question 3: *What prediction and computational effort is required to realize a fuel economy improvement when using current technology integrated with predictive energy management?*

Research Question 3 is associated with Hypothesis 3:

144

Hypothesis 3: *FE improvements can be realized using only current vehicle technology.*

This research effort has provided additional support for this hypothesis. By recording real data outputs from current vehicle technology and integrating the results using an artificial neural network, FE improvements from a predictive energy management strategy were realized. This demonstrates that predictive energy management implementation does not require future technologies to realize a prediction fidelity level necessary to achieve FE improvements. This shows that the predictions required for predictive energy management can be achieved in modern vehicles and further demonstrates the potential of predictive energy management implementation today.

Chapter 7

Conclusions

7.1 Conclusions

This dissertation has defined and completed a series of tasks to address the primary research challenges associated with implementing predictive energy management. Research to date has shown that with full drive cycle prediction, FE improvements of up to 30% are possible. This research has advanced this concept by exploring the tradeoffs between information sensing, computation power requirements for prediction, and prediction effort. It was found that there are numerous types of mispredictions for which FE improvements from predictive energy management are maintained. It was found that predicting short sections of drive cycles can result in a FE improvement with predictive energy management. In fact, those short sections of the drive cycle do not have to be predicted exactly to result in a significant and robust FE improvement. This also potentially eliminates the need for real-time computations. Lastly, it was found that using only currently available technology, prediction fidelity for FE improvements through predictive energy management are possible. It is anticipated that these research findings can inform new research that can further allow predictive energy management to be implemented in vehicles.

7.2 Research Contributions of this Dissertation

The primary contributions of this dissertation are presented below:

1. A more holistic and systems-level understanding of the subsystems and integrations needed to implement an Optimal EMS in vehicles

2. A definition of the research gaps existing between the current state-of-the-art and the end state of predictive Optimal EMS usage in vehicles

3. A proposal for a set of research directives that will enable progress towards predictive Optimal EMS implementation in vehicles

4. Dynamic programming is used to evaluate mispredictions

5. Driving-derived mispredictions are analyzed

6. Vehicle parameter mispredictions are analyzed

7. The dynamic programming solution matrix time state variable is converted to a distance state variable for improved misprediction robustness

8. Comprehensive analysis of thousands of AEs using an Optimal EMS

9. Feasibility investigation of applying precomputed AE Optimal EMS

10. Performance categorization of an Optimal EMS applied to AEs

11. Use of optimal control solutions that are a function of velocity which only works for monotonic drive segments

12. ADAS and travel time technology is then used to generate predictions for use in an Optimal EMS.

7.3   Future Work

This dissertation involves improving an understanding of implementability of predictive energy management. As such, the models and methods developed for this research effort are widely applicable to future studies. The research gaps presented in Chapter 1 are addressed by subsequent chapters but there is still much more work to be done. Future work in each of the presented studies is required which could include an examination of robust optimal control vs globally optimal control with real-world mispredictions, exploration of predicting different sections of drive cycles including deceleration and steady state sections used with an Optimal EMS, and a rigorous comparison of current and near future vehicle technologies to derive predictions are just a few of

the planned future research efforts. Additionally, research gap 3 in Chapter 1 also needs to be addressed which involves implementation in a real vehicle. All of these studies could also investigate additional vehicle architectures and incorporation of other vehicle control strategies such as driver-less control.

Bibliography

[1] Vipin K Kukkala, Jordan Tunnell, Sudeep Pasricha, and Thomas Bradley. A survey of advanced driver assistance systems and current challenges. In Review.

[2] Jeremiah Singer, A Emanuel Robinson, Jessica Krueger, Jennifer E Atkinson, and Matthew C Myers. Travel time on arterials and rural highways: State-of-the-Practice synthesis on rural data collection technology. Technical report, 2013.

[3] Z D Asher, V Wifvat, A Navarro, S Samuelsen, and T H Bradley. The importance of HEV fuel economy and two research gaps preventing real world implementation of optimal energy management. In *SAE Technical Paper Series*, SAE Technical Paper 2017-26-0106, 2017.

[4] Zachary D Asher, Van T Wifvat, Scott Samuelsen, Andrew A Frank, and Thomas H Bradley. Review of research gaps to optimal fuel economy vehicle control.

[5] D J Fagnant and K Kockelman. Preparing a nation for autonomous vehicles: opportunities, barriers and policy recommendations. *Transp. Res. Part A: Policy Pract.*, 77:167–181, 1 July 2015.

[6] International Energy Agency. *Key World Energy Statistics 2016*. International Energy Agency, 2015.

[7] Mike van Moerkerk and Wina Crijns-Graus. A comparison of oil supply risks in EU, US, japan, china and india under different climate scenarios. *Energy Policy*, 88:148–158, 2016.

[8] Petroleum and other liquids: Europe brent spot price FOB. https://www.eia.gov/dnav/pet/hist/LeafHandler.ashx?n=PET&s=RBRTE&f=M, 28 April 2017. Accessed: 2017-5-8.

[9] Petroleum and other liquids: U.S. imports of crude oil and petroleum products. https://www.eia.gov/dnav/pet/hist/LeafHandler.ashx?n=PET&s=MTTIMUS1&f=M, 28 April 2017. Accessed: 2016-5-8.

[10] David L Greene and Sanjana Ahmad. *Costs of US oil dependence: 2005 update*. United States. Department of Energy, 2005.

[11] International Energy Agency. CO2 emissions from fuel combustion. Technical report, 2016.

[12] *Advancing the Science of Climate Change*. 2010.

[13] Joeri Rogelj, Michel den Elzen, Niklas Höhne, Taryn Fransen, Hanna Fekete, Harald Winkler, Roberto Schaeffer, Fu Sha, Keywan Riahi, and Malte Meinshausen. Paris agreement climate proposals need a boost to keep warming well below 2 Âřc. *Nature*, 534(7609):631–639, 30 June 2016.

[14] International Energy Agency. Energy and climate change - world energy outlook special report. Technical report, 2015.

[15] World energy outlook special report: Energy and air pollution. Technical report, International Energy Agency, 2016.

[16] World Health Organization. *World Health Statistics 2016: Monitoring Health for the Sustainable Development Goals (SDGs)*. World Health Organization, 2016.

[17] A E Atabani, Irfan Anjum Badruddin, S Mekhilef, and A S Silitonga. A review on global fuel economy standards, labels and technologies in the transportation sector. *Renewable Sustainable Energy Rev.*, 15(9):4586–4610, December 2011.

[18] Annual energy outlook 2017. Technical report, Energy Information Administration, 5 January 2017.

[19] S M Lukic and A Emadi. Effects of drivetrain hybridization on fuel economy and dynamic performance of parallel hybrid electric vehicles. *IEEE Trans. Veh. Technol.*, 53(2):385–389, March 2004.

[20] Rajesh Rajamani. *Vehicle Dynamics and Control*. Springer Science & Business Media, 21 December 2011.

[21] K Bengler, K Dietmayer, B Farber, M Maurer, C Stiller, and H Winner. Three decades of driver assistance systems: Review and future perspectives. *IEEE Intell. Transp. Syst. Mag.*, 6(4):6–22, 2014.

[22] S Thrun. Toward robotic cars. *Commun. ACM*, 53(4):99–106, 2010.

[23] Richard Bishop. *Intelligent vehicle technology and trends*. trid.trb.org, 2005.

[24] Oleg Gusikhin, Dimitar Filev, and Nestor Rychtyckyj. Intelligent vehicle systems: Applications and new trends. In *Informatics in Control Automation and Robotics*, pages 3–14. Springer Berlin Heidelberg, 2008.

[25] Dan Gray. 10 cars with adaptive cruise control. http://www.autobytel.com/car-buying-guides/features/10-cars-ith-adaptive-cruise-control-131148/, 2016. Accessed: 2017-5-8.

[26] P Enge and P Misra. Special issue on global positioning system. *Proc. IEEE*, 87(1):3–15, January 1999.

[27] Contributing Writer Staff. 7 cars with 360-degree cameras. http://www.web2carz.com/autos/car-tech/5630/7-cars-with-360-degree-cameras, 14 April 2016. Accessed: 2017-5-5.

[28] Kyoungho Ahn and Hesham A Rakha. Network-wide impacts of eco-routing strategies: A large-scale case study. *Transp. Res. Part D: Trans. Environ.*, 25:119–130, December 2013.

[29] Victor Pillac, Michel Gendreau, Christelle Guéret, and Andrés L Medaglia. A review of dynamic vehicle routing problems. *Eur. J. Oper. Res.*, 225(1):1–11, 16 February 2013.

[30] P Michel, D Karbowski, and A Rousseau. Impact of connectivity and automation on vehicle energy use. Technical report, SAE Technical Paper, 2016.

[31] S Mandava, K Boriboonsomsin, and M Barth. Arterial velocity planning based on traffic signal information under light traffic conditions. In *2009 12th International IEEE Conference on Intelligent Transportation Systems*, pages 1–6. ieeexplore.ieee.org, October 2009.

[32] Chan-Chiao Lin, Jun-Mo Kang, J W Grizzle, and Huei Peng. Energy management strategy for a parallel hybrid electric truck. In *Proceedings of the 2001 American Control Conference. (Cat. No.01CH37148)*, volume 4, pages 2878–2883 vol.4. ieeexplore.ieee.org, 2001.

[33] D G Evans, M E Polom, S G Poulos, K D Van Maanen, and others. Powertrain architecture and controls integration for GM's hybrid full-size pickup truck. 2003.

[34] Börje Grandin and Hans-Erik Ångström. Replacing fuel enrichment in a turbo charged SI engine: lean burn or cooled EGR. Technical report, SAE Technical Paper, 1999.

[35] T H Ma. Effect of variable engine valve timing on fuel economy. Technical report, SAE Technical Paper, 1988.

[36] Thomas G Leone and M Pozar. Fuel economy benefit of cylinder deactivation-sensitivity to vehicle application and operating constraints. Technical report, SAE Technical Paper, 2001.

[37] Andrew A Frank. Control method and apparatus for internal combustion engine electric hybrid vehicles, 25 April 2000.

[38] Koichiro Muta, Makoto Yamazaki, and Junji Tokieda. Development of new-generation hybrid system THS II-Drastic improvement of power performance and fuel economy. *SAE Trans. J. Mater. Manuf.*, 113(3):182–192, 2004.

[39] Q Wang and A A Frank. Plug-in HEV with CVT: configuration, control, and its concurrent multi-objective optimization by evolutionary algorithm. *Int.J Automot. Technol.*, 15(1):103–115, 1 February 2014.

[40] Thomas H Bradley and Casey W Quinn. Analysis of plug-in hybrid electric vehicle utility factors. *J. Power Sources*, 195(16):5399–5408, 15 August 2010.

[41] Yifan Tang. Control system for an all-wheel drive electric vehicle, 15 June 2010.

[42] Andrew David Baglino, Heath Fred Hofmann, and Greg Grant Solberg. Varying flux versus torque for maximum efficiency, 7 December 2010.

[43] Jianning Zhao and Antonio Sciarretta. Design and control Co-Optimization for hybrid powertrains: Development of dedicated optimal energy management strategy. *IFAC-PapersOnLine*, 49(11):277–284, 1 January 2016.

[44] A Sciarretta, M Back, and L Guzzella. Optimal control of parallel hybrid electric vehicles. *IEEE Trans. Control Syst. Technol.*, 12(3):352–363, May 2004.

[45] P Zhang, F Yan, and C Du. A comprehensive analysis of energy management strategies for hybrid electric vehicles based on bibliometrics. *Renewable Sustainable Energy Rev.*, 48:88–104, 2015.

[46] N Kim, S Cha, and H Peng. Optimal control of hybrid electric vehicles based on pontryagin's minimum principle. *IEEE Trans. Control Syst. Technol.*, 19(5):1279–1287, 2011.

[47] Chan-Chiao Lin, Huei Peng, and J W Grizzle. A stochastic control strategy for hybrid electric vehicles. In *Proceedings of the 2004 American Control Conference*, volume 5, pages 4710–4715 vol.5. ieeexplore.ieee.org, June 2004.

[48] Simona Onori, Lorenzo Serrao, and Giorgio Rizzoni. Adaptive equivalent consumption minimization strategy for hybrid electric vehicles. In *ASME 2010 Dynamic Systems and Control Conference*, pages 499–505. American Society of Mechanical Engineers, 1 January 2010.

[49] Domenico Bianchi, Luciano Rolando, Lorenzo Serrao, Simona Onori, Giorgio Rizzoni, Nazar Al-Khayat, Tung-Ming Hsieh, and Pengju Kang. A Rule-Based strategy for a Series/Parallel hybrid electric vehicle: An approach based on dynamic programming. In *ASME 2010 Dynamic Systems and Control Conference*, pages 507–514. American Society of Mechanical Engineers, 1 January 2010.

[50] G Paganelli, S Delprat, T M Guerra, J Rimaux, and J J Santin. Equivalent consumption minimization strategy for parallel hybrid powertrains. In *Vehicular Technology Conference.*

IEEE 55th Vehicular Technology Conference. VTC Spring 2002 (Cat. No.02CH37367), volume 4, pages 2076–2081 vol.4. ieeexplore.ieee.org, 2002.

[51] H A Borhan, A Vahidi, A M Phillips, M L Kuang, and I V Kolmanovsky. Predictive energy management of a power-split hybrid electric vehicle. In *2009 American Control Conference*, pages 3970–3976. ieeexplore.ieee.org, June 2009.

[52] M Campbell, M Egerstedt, J P How, and R M Murray. Autonomous driving in urban environments: approaches, lessons and challenges. *Philos. Trans. A Math. Phys. Eng. Sci.*, 368(1928):4649–4672, 13 October 2010.

[53] John C Mankins. Technology readiness levels. *White Paper*, 6(6):1995, 1995.

[54] John C Mankins. Technology readiness assessments: A retrospective. *Acta Astronaut.*, 65(9–10):1216–1223, November 2009.

[55] B Sauser, D Verma, and others. From TRL to SRL: The concept of systems readiness levels. *UCLA Law Rev.*, 2006.

[56] Q Gong, Y Li, and Z R Peng. Trip-Based optimal power management of plug-in hybrid electric vehicles. *IEEE Trans. Veh. Technol.*, 57(6):3393–3401, November 2008.

[57] Q Gong, Y Li, and Z Peng. Power management of plug-in hybrid electric vehicles using neural network based trip modeling. In *2009 American Control Conference*, pages 4601–4606. ieeexplore.ieee.org, June 2009.

[58] F A Bender, M Kaszynski, and O Sawodny. Drive cycle prediction and energy management optimization for hybrid hydraulic vehicles. *IEEE Trans. Veh. Technol.*, 62(8):3581–3592, October 2013.

[59] Mohd Azrin Mohd Zulkefli, Jianfeng Zheng, Zongxuan Sun, and Henry X Liu. Hybrid powertrain optimization with trajectory prediction based on inter-vehicle-communication

and vehicle-infrastructure-integration. *Transp. Res. Part C: Emerg. Technol.*, 45:41–63, 2014.

[60] C Sun, X Hu, S J Moura, and F Sun. Velocity predictors for predictive energy management in hybrid electric vehicles. *IEEE Trans. Control Syst. Technol.*, 23(3):1197–1204, May 2015.

[61] C Sun, S J Moura, X Hu, J K Hedrick, and F Sun. Dynamic traffic feedback data enabled energy management in plug-in hybrid electric vehicles. *IEEE Trans. Control Syst. Technol.*, 23(3):1075–1086, May 2015.

[62] David Baker, Zachary Asher, and Thomas Bradley. Investigation of vehicle speed prediction from neural network fit of real world driving data for improved engine On/Off control of the EcoCAR3 hybrid camaro. Technical report, SAE Technical Paper, 2017.

[63] Chao Sun, Fengchun Sun, and Hongwen He. Investigating adaptive-ECMS with velocity forecast ability for hybrid electric vehicles. *Appl. Energy*, 185, Part 2:1644–1653, 1 January 2017.

[64] Anderw A Frank, Bruce R Thomas, and Catherine J DeMauro. PHEVLERs are the zero CO2 clean green machines of the future. *Green Car Congress*, 22 April 2016.

[65] Michael Patrick O'Keefe and Tony Markel. Dynamic programming applied to investigate energy management strategies for a plug-in HEV. Technical report, National Renewable Energy Laboratory Golden, Colorado, USA, 2006.

[66] L Fu, Ü Ö zgüner, P Tulpule, and V Marano. Real-time energy management and sensitivity study for hybrid electric vehicles. In *Proceedings of the 2011 American Control Conference*, pages 2113–2118. ieeexplore.ieee.org, June 2011.

[67] Yiming He, Mashrur Chowdhury, Pierluigi Pisu, and Yongchang Ma. An energy optimization strategy for power-split drivetrain plug-in hybrid electric vehicles. *Transp. Res. Part C: Emerg. Technol.*, 22:29–41, 2012.

[68] Daniel F Opila, Xiaoyong Wang, Ryan McGee, R Brent Gillespie, Jeffrey A Cook, and J W Grizzle. Real-World robustness for hybrid vehicle optimal energy management strategies incorporating drivability metrics. *J. Dyn. Syst. Meas. Control*, 136(6):061011, 1 November 2014.

[69] Mohd Azrin Mohd Zulkefli and Zongxuan Sun. Real-Time powertrain optimization strategy for connected hybrid electrical vehicle. In *ASME 2016 Dynamic Systems and Control Conference*, pages V002T20A006–V002T20A006. âĂę .asmedigitalcollection.asme.org, 2016.

[70] Zachary D Asher, Thomas Cummings, and Thomas H Bradley. The effect of hill planning and route type identification prediction signal quality on hybrid vehicle fuel economy. Technical report, SAE Technical Paper, 2016.

[71] Thomas Cummings, Thomas H Bradley, and Zachary D Asher. The effect of trip preview prediction signal quality on hybrid vehicle fuel economy. *IFAC-PapersOnLine*, 48(15):271–276, 1 January 2015.

[72] Z D Asher, D A Baker, and T H Bradley. Prediction error applied to hybrid electric vehicle optimal fuel economy. *IEEE Trans. Control Syst. Technol.*, PP(99):1–14, 2017.

[73] Mohammad Alzorgan, Joshua Carroll, Essam Al-Masalmeh, and Abdel Raouf Turki Mayyas. Look-Ahead information based optimization strategy for hybrid electric vehicles. Technical report, SAE Technical Paper, 2016.

[74] Chan-Chiao Lin, Huei Peng, Jessy W Grizzle, Jason Liu, and Matt Busdiecker. Control system development for an advanced-technology medium-duty hybrid electric truck. Technical report, SAE Technical Paper, 2003.

[75] Mohd Azrin Mohd Zulkefli, Pratik Mukherjee, Zongxuan Sun, Jianfeng Zheng, Henry X Liu, and Peter Huang. Hardware-in-the-loop testbed for evaluating connected vehicle applications. *Transp. Res. Part C: Emerg. Technol.*, 78:50–62, 2017.

[76] Jiankun Peng, Hongwen He, and Rui Xiong. Rule based energy management strategy for a series–parallel plug-in hybrid electric bus optimized by dynamic programming. *Appl. Energy*, 185, Part 2:1633–1643, 1 January 2017.

[77] G Paganelli, M Tateno, A Brahma, G Rizzoni, and Y Guezennec. Control development for a hybrid-electric sport-utility vehicle: strategy, implementation and field test results. In *Proceedings of the 2001 American Control Conference. (Cat. No.01CH37148)*, volume 6, pages 5064–5069 vol.6. ieeexplore.ieee.org, 2001.

[78] Giorgio Rizzoni and Simona Onori. Energy management of hybrid electric vehicles: 15 years of development at the ohio state university. *Oil & Gas Science and Technology – Revue dâĂŹIFP Energies nouvelles*, 70(1):41–54, 2015.

[79] Thijs van Keulen, Dominique van Mullem, Bram de Jager, John T B A Kessels, and Maarten Steinbuch. Design, implementation, and experimental validation of optimal power split control for hybrid electric trucks. *Control Eng. Pract.*, 20(5):547–558, 2012.

[80] Lei Wang, Yong Zhang, Chengliang Yin, Hu Zhang, and Cunlei Wang. Hardware-in-the-loop simulation for the design and verification of the control system of a series–parallel hybrid electric city-bus. *Simulation Modelling Practice and Theory*, 25:148–162, 2012.

[81] Alexandre Chasse, Philippe Pognant-Gros, and Antonio Sciarretta. Online implementation of an optimal supervisory control for a parallel hybrid powertrain. *SAE International Journal of Engines*, 2(2009-01-1868):1630–1638, 2009.

[82] A Chasse and A Sciarretta. Supervisory control of hybrid powertrains: An experimental benchmark of offline optimization and online energy management. *Control Eng. Pract.*, 19(11):1253–1265, November 2011.

[83] O Grondin, L Thibault, P Moulin, A Chasse, and A Sciarretta. Energy management strategy for diesel hybrid electric vehicle. In *2011 IEEE Vehicle Power and Propulsion Conference*, pages 1–8. ieeexplore.ieee.org, 2011.

[84] Jinming Liu, Jonathan Hagena, Huei Peng, and Zoran S Filipi. Engine-in-the-loop study of the stochastic dynamic programming optimal control design for a hybrid electric HMMWV. *Int. J. Heavy Veh. Syst.*, 15(2-4):309–326, 1 January 2008.

[85] Daniel F Opila, Xiaoyong Wang, Ryan McGee, and J W Grizzle. Real-Time implementation and hardware testing of a hybrid vehicle energy management controller based on stochastic dynamic programming. *J. Dyn. Syst. Meas. Control*, 135(2):021002, 1 March 2013.

[86] E Pagliara, G Parlangeli, T Donateo, and F Adamo. Real time implementation of an optimal power management strategy for a plug-in hybrid electric vehicle. In *52nd IEEE Conference on Decision and Control*, pages 2214–2219. ieeexplore.ieee.org, December 2013.

[87] International Energy Agency. World energy outlook special report: Energy and air pollution. Technical report, 2016.

[88] C Zhang and A Vahidi. Route preview in energy management of plug-in hybrid vehicles. *IEEE Trans. Control Syst. Technol.*, 20(2):546–553, March 2012.

[89] C C Chan. The state of the art of electric, hybrid, and fuel cell vehicles. *Proc. IEEE*, 95(4):704–718, April 2007.

[90] U S Department of Energy. 2017 best and worst fuel economy vehicles. https://www.fueleconomy.gov/feg/best-worst.shtml. Accessed: 2017-2-21.

[91] Nobuki Kawamoto, Kiyoshi Naiki, Toshihiro Kawai, Takasuke Shikida, and Mamoru Tomatsuri. Development of new 1.8-liter engine for hybrid vehicles. Technical report, SAE Technical Paper, 2009.

[92] *Toyota 2010 Prius Owners Manual*.

[93] A S White. Twenty years of projects on vehicle aerodynamics. *Int. J. Mech. Eng. Educ.*, 27(1):71–87, 1999.

[94] William Blythe, Terry D Day, and Wesley D Grimes. 3-dimensional simulation of vehicle response to tire blow-outs. Technical report, SAE Technical Paper, 1998.

[95] Samuel K Clark. *Mechanics of Pneumatic Tires*. U.S. Government Printing Office, 1981.

[96] T van Keulen, B de Jager, A Serrarens, and M Steinbuch. Optimal energy management in hybrid electric trucks using route information. *Oil & Gas Science and Technology – Revue de lâĂŹInstitut Français du Pétrole*, 65(1):103–113, 1 January 2010.

[97] Namwook Kim, Aymeric Rousseau, and Eric Rask. Autonomie model validation with test data for 2010 toyota prius. Technical report, SAE Technical Paper, 2012.

[98] Argonne National Lab. Downloadable dynamometer database, 16 April 2015. Title of the publication associated with this dataset: Test Summary Sheet.

[99] Dimitri P Bertsekas, Dimitri P Bertsekas, Dimitri P Bertsekas, and Dimitri P Bertsekas. *Dynamic programming and optimal control*, volume 1. Athena Scientific Belmont, MA, 1995.

[100] R Bellman. Dynamic programming and lagrange multipliers. *Proc. Natl. Acad. Sci. U. S. A.*, 42(10):767–769, October 1956.

[101] John Paul Arata, III. *Simulation and control strategy development of power-split hybrid-electric vehicles*. PhD thesis, Georgia Institute of Technology, 2011.

[102] Energy Efficiency and Renewable Energy. Evaluation of the 2010 toyota prius hybrid synergy drive system. 2011.

[103] Richard F Gunst. Response surface methodology: Process and product optimization using designed experiments. *Technometrics*, 38(3):284–286, 1996.

[104] SAE International. Recommended practice for measuring the exhaust emissions and fuel economy of Hybrid-Electric vehicles. Technical Report J1711, 2002.

[105] David Baker, Zachary Asher, and Thomas Bradley. Investigation of vehicle speed prediction from neural network fit of real world driving data for improved engine On/Off control of the EcoCAR3 hybrid camaro. Technical report, SAE Technical Paper, 2017.

[106] David A Trinko, Zachary D Asher, and Thomas H Bradley. Application of Pre-Computed acceleration event control to improve fuel economy in hybrid electric vehicles.

[107] Zachary D Asher, David A Trinko, Joshua D Payne, Bejamin M Geller, and Thomas H Bradley. Improved fuel economy through acceleration event prediction part 1: Optimal control. *IEEE Transactions on Control System Technology*.

[108] Key world energy statistics 2017. Technical report, International Energy Agency, September 2017.

[109] Charles Issawi. The 1973 oil crisis and after. *J. Post Keynes. Econ.*, 1(2):3–26, 1978.

[110] CO2 emissions from fuel combustion 2017. Technical report, International Energy Agency, October 2017.

[111] National Research Council, Division on Earth and Life Studies, Board on Atmospheric Sciences and Climate, and America's Climate Choices: Panel on Advancing the Science of Climate Change. *Advancing the Science of Climate Change*. National Academies Press, January 2011.

[112] Global Fuel Economy Initiative. 50by50 global fuel economy initiative. Technical report, 2009.

[113] Global Fuel Economy Initiative. Global fuel economy: An update for COP22. Technical report, 2017.

[114] Jack Ewing. France plans to end sales of gas and diesel cars by 2040. *The New York Times*, July 2017.

[115] Somini Sengupta. Both climate leader and oil giant? a norwegian paradox. *The New York Times*, June 2017.

[116] Stephen Castle. Britain to ban new diesel and gas cars by 2040. *The New York Times*, July 2017.

[117] Keith Bradsher. China hastens the world toward an Electric-Car future. *The New York Times*, October 2017.

[118] Geeta Anand. India, once a coal goliath, is fast turning green. *The New York Times*, June 2017.

[119] U.S. Environmental Protection Agency. What is the clean air act? https://www.epa.gov/clean-air-act-overview/clean-air-act-text, May 2015. Accessed: 2018-2-22.

[120] California Air Resources Board. Air quality and climate legislation – 2017 annual summary. Technical report, State of California, November 2017.

[121] Ching-Shin Norman Shiau, Jeremy J Michalek, and Chris T Hendrickson. A structural analysis of vehicle design responses to corporate average fuel economy policy. *Transp. Res. Part A: Policy Pract.*, 43(9):814–828, November 2009.

[122] Light-Duty vehicle greenhouse gas emission standards and corporate average fuel economy standards; final rule. Technical Report EPA–HQ–OAR–2009–0472; FRL-9134-6; NHTSA-2009-0059, Environmental Protection Agency (EPA) and National Highway Traffic Safety Administration (NHTSA), April 2010.

[123] Corporate average fuel economy for MY 2012-MY 2016 passenger cars and light trucks. Technical Report Final Regulatory Impact Analysis, National Highway Traffic Safety Administration, U.S. Department Of Transportation, March 2010.

[124] NHTSA and EPA set standards to improve fuel economy and reduce greenhouse gases for passenger cars and light trucks for model years 2017 and beyond: Fact sheet. Technical

report, The National Highway Traffic Safety Administration (NHTSA) and the U.S. Environmental Protection Agency (EPA), 2011.

[125] Corporate average fuel economy for MY 2017-MY 2025 passenger cars and light trucks. Technical Report Final Regulatory Impact Analysis, National Highway Traffic Safety Administration, U.S. Department Of Transportation, August 2012.

[126] Draft technical assessment report: Midterm evaluation of Light-Duty vehicle greenhouse gas emission standards and corporate average fuel economy standards for model years 2022-2025 (EPA-420-D-16-900, july 2016). Technical Report EPA-420-D-16-900, Office of Transportation, Air Quality U.S. Environmental Protection Agency National Highway Traffic Safety Administration U.S. Department of Transportation, and the California Air Resources Board, July 2016.

[127] Final determination on the appropriateness of the model year 2022-2025 Light-Duty vehicle greenhouse gas emissions standards under the midterm evaluation. Technical Report EPA-420-R-17-001, Environmental Protection Agency, January 2017.

[128] Jack Danielson. Civil penalties. Technical Report NHTSA-2016-0136, National Highway Traffic Safety Administration (NHTSA), Department of Transportation (DOT), July 2017.

[129] Jack Danielson. Civil penalties. Technical Report NHTSA-2017-0059, National Highway Traffic Safety Administration (NHTSA), Department of Transportation (DOT), July 2017.

[130] Zachary D Asher, David A Trinko, and Thomas H Bradley. Increasing the fuel economy of connected and autonomous Lithium-Ion electrified vehicles. In *Behaviour of Lithium-Ion Batteries in Electric Vehicles*, Green Energy and Technology, pages 129–151. Springer, Cham, 2018.

[131] A E Bryson. Optimal control-1950 to 1985. *IEEE Control Syst.*, 16(3):26–33, June 1996.

[132] Vladimir Grigor'evich Boltyanskii, Revaz Valer'yanovich Gamkrelidze, and Lev Semen-ovich Pontryagin. The theory of optimal processes. i. the maximum principle. Technical report, TRW SPACE TECHNOLOGY LABS LOS ANGELES CALIF, 1960.

[133] C Vagg, S Akehurst, C J Brace, and L Ash. Stochastic dynamic programming in the Real-World control of hybrid electric vehicles. *IEEE Trans. Control Syst. Technol.*, 24(3):853–866, May 2016.

[134] Chao Yang, Siyu Du, Liang Li, Sixong You, Yiyong Yang, and Yue Zhao. Adaptive real-time optimal energy management strategy based on equivalent factors optimization for plug-in hybrid electric vehicle. *Appl. Energy*, 203(Supplement C):883–896, October 2017.

[135] B HomChaudhuri, A Vahidi, and P Pisu. Fast model predictive Control-Based fuel efficient control strategy for a group of connected vehicles in urban road conditions. *IEEE Trans. Control Syst. Technol.*, 25(2):760–767, March 2017.

[136] Simona Onori, Lorenzo Serrao, and Giorgio Rizzoni. Equivalent consumption minimization strategy. In *Hybrid Electric Vehicles*, SpringerBriefs in Electrical and Computer Engineering, pages 65–77. Springer London, 2016.

[137] David J LeBlanc, Michael Sivak, and Scott Bogard. Using naturalistic driving data to assess variations in fuel efficiency among individual drivers. 2010.

[138] R Akcelik and D C Biggs. Acceleration profile models for vehicles in road traffic. *Transportation Science*, 21(1):36–54, February 1987.

[139] Rahmi Akçelik and Mark Besley. Acceleration and deceleration models. In *23rd Conference of Australian Institutes of Transport Research (CAITR 2001), Monash University, Melbourne, Australia*, volume 10, page 12. sidrasolutions.com, 2001.

[140] Jun Wang, Karen Dixon, Hainan Li, and Jennifer Ogle. Normal acceleration behavior of passenger vehicles starting from rest at All-Way Stop-Controlled intersections. *Transportation*

Research Record: Journal of the Transportation Research Board, 1883:158–166, January 2004.

[141] Gary Long. Acceleration characteristics of starting vehicles. *Transportation Research Record: Journal of the Transportation Research Board*, 1737:58–70, January 2000.

[142] David A. Trinko, Zachary D. Asher, Thomas H. Bradley. Application of Pre-Computed acceleration event control to improve fuel economy in hybrid electric vehicles. October 2017.

[143] 2018 best and worst fuel economy vehicles. https://www.fueleconomy.gov/feg/best-worst. shtml. Accessed: 2018-2-16.

[144] Zachary D Asher, David A Trinko, and Thomas H Bradley. Improved fuel economy through acceleration event prediction part 2: Drive cycle application. *IEEE Transactions on Transportation Electrification*.

[145] M Jacobs Juncture and 2016. High pressure for low emissions: How civil society created the paris climate agreement. *Wiley Online Library*, 2016.

[146] Peter Christoff. The promissory note: COP 21 and the paris climate agreement. *Env. Polit.*, 25(5):765–787, 2016.

[147] Raymond Clémençon. The two sides of the paris climate agreement: Dismal failure or historic breakthrough? *J. Environ. Dev.*, 25(1):3–24, February 2016.

[148] Hans Joachim Schellnhuber, Stefan Rahmstorf, and Ricarda Winkelmann. Why the right climate target was agreed in paris. *Nat. Clim. Chang.*, 6(7):nclimate3013, June 2016.

[149] Mike Hulme. 1.5 [deg] C and climate research after the paris agreement. *Nat. Clim. Chang.*, 6(3):222–224, 2016.

[150] Miranda A Schreurs. The paris climate agreement and the three largest emitters: China, the united states, and the european union. *Politics and Governance*, 4(3):219–223, 2016.

[151] Lisa Friedman. Syria joins paris climate accord, leaving only U.S. opposed. *The New York Times*, November 2017.

[152] Michael Giberson. Trump's policy may undermine pro-growth intentions. *Nature Energy*, 1:16156, 2016.

[153] Jason Bordoff. Withdrawing from the paris climate agreement hurts the US. *Nature Energy*, 2(9):nenergy2017145, 2017.

[154] R Meyer. AmericaâĂŹs pledgeâĂŹ: Can states and cities really address climate change. *Atlantic*, 2, 2017.

[155] United Nations Framework Convention on Climate Change. Paris declaration on Electro-Mobility and climate change and call to action, 2015.

[156] Global Fuel Economy Initiative. Global fuel economy: An update for COP22. Technical report, 2016.

[157] Global Fuel Economy Initiative. GFEI action for more fuel efficient vehicles: COP23 update. Technical Report Global Fuel Economy - An Update For Cop23, 2017.

[158] Global Fuel Economy Initiative. 50by50 prospects and progress. Technical report, 2011.

[159] M Montazeri-Gh and M Naghizadeh. Development of car drive cycle for simulation of emissions and fuel economy. In *Proceedings of 15th European simulation symposium*. Citeseer, 2003.

[160] M Gautam, N Clark, W Riddle, R Nine, W S Wayne, and others. Development and initial use of a heavy-duty diesel truck test schedule for emissions characterization. 2002.

[161] Jairo A Sandoval Leon. *Study of Transit Bus Duty Cycle and its Influence on Fuel Economy and Emissions of Diesel-Electric Hybrids*. PhD thesis, West Virginia University, Ann Arbor, United States, 2011.

[162] Richard E Fairley and Richard H Thayer. The concept of operations: The bridge from operational requirements to technical specifications. *Annals of Software Engineering*, 3(1):417–432, January 1997.

[163] U.S. Environmental Protection Agency. Final technical support document: Fuel economy labeling of motor vehicle revisions to improve calculation of fuel economy estimates. Technical Report EPA420-R-06-017, Office of Transportation and Air Quality, December 2006.

[164] Li Chen, Futang Zhu, Minmin Zhang, Yi Huo, Chengliang Yin, and Huei Peng. Design and analysis of an electrical variable transmission for a series–parallel hybrid electric vehicle. *IEEE Trans. Veh. Technol.*, 60(5):2354–2363, 2011.

[165] Behnam Ganji, Abbas Z Kouzani, and H M Trinh. Drive cycle analysis of the performance of hybrid electric vehicles. In *Life System Modeling and Intelligent Computing*, pages 434–444. Springer Berlin Heidelberg, 2010.

[166] R A Barnitt, A D Brooker, and L Ramroth. Model-Based analysis of electric drive options for Medium-Duty parcel delivery vehicles: Preprint. Technical Report NREL/CP-5400-49253, National Renewable Energy Lab. (NREL), Golden, CO (United States), December 2010.

[167] M Amrhein and P T Krein. Dynamic simulation for analysis of hybrid electric vehicle system and subsystem interactions, including power electronics. *IEEE Trans. Veh. Technol.*, 54(3):825–836, May 2005.

[168] S M Aceves and J R Smith. Hybrid and conventional hydrogen engine vehicles that meet EZEV emissions. Technical Report UCRL-JC-125891; CONF-970210-6, Lawrence Livermore National Lab., CA (United States), December 1996.

[169] Benjamin M Geller and Thomas H Bradley. Analyzing drive cycles for hybrid electric vehicle simulation and optimization. *J. Mech. Des.*, 137(4):041401, April 2015.

[170] Teresa Donateo, Damiano Pacella, and Domenico Laforgia. Development of an energy management strategy for plug-in series hybrid electric vehicle based on the prediction of the future driving cycles by ICT technologies and optimized maps. Technical report, SAE Technical Paper, 2011.

[171] Amir Rezaei and Jeffrey B Burl. Prediction of vehicle velocity for model predictive control. *IFAC-PapersOnLine*, 48(15):257–262, 1 January 2015.

[172] Jordan A Tunnell, Zachary D Asher, Sudeep Pasricha, and Thomas H Bradley. Towards improving vehicle fuel economy with ADAS. In *SAE World Congress*.

[173] Zachary D Asher, Jordan A Tunnell, David A Baker, Robert J Fitzgerald, Farnoush Banaei-Kashani, Sudeep Pasricha, and Thomas H Bradley. Enabling prediction for optimal fuel economy vehicle control. In *SAE World Congress*, April 2018.

[174] World Health Organization. *World Health Statistics 2016: Monitoring Health for the Sustainable Development Goals (SDGs)*. World Health Organization, 2016.

[175] S M Lukic and A Emadi. Effects of drivetrain hybridization on fuel economy and dynamic performance of parallel hybrid electric vehicles. *IEEE Trans. Veh. Technol.*, 53(2):385–389, March 2004.

[176] National Highway Traffic Safety Administration. National motor vehicle crash causation survey. Technical Report Report DOT HS 811 059, U.S. Department of Transportation, 2008.

[177] Haneet Singh Mahajan, Thomas Bradley, and Sudeep Pasricha. Application of systems theoretic process analysis to a lane keeping assist system. *Reliab. Eng. Syst. Saf.*, 167:177–183, November 2017.

[178] Niket Prakash, Gionata Cimini, Anna G Stefanopoulou, and Matthew J Brusstar. Assessing fuel economy from automated driving: Influence of preview and velocity con-

straints. In *ASME 2016 Dynamic Systems and Control Conference*, pages V002T19A001–V002T19A001. âĂę .asmedigitalcollection.asme.org, 2016.

[179] L Tang, G Rizzoni, and M Lukas. Comparison of dynamic programming-based energy management strategies including battery life optimization. In *2016 International Conference on Electrical Systems for Aircraft, Railway, Ship Propulsion and Road Vehicles International Transportation Electrification Conference (ESARS-ITEC)*, pages 1–6. ieeexplore.ieee.org, November 2016.

[180] Engin Ozatay, Umit Ozguner, and Dimitar Filev. Velocity profile optimization of on road vehicles: Pontryagin's maximum principle based approach. *Control Eng. Pract.*, 61(Supplement C):244–254, April 2017.

[181] Pouyan Ahmadizadeh, Behrooz Mashadi, and Dhaval Lodaya. Energy management of a Dual-Mode Power-Split powertrain based on the pontryagin minimum principle. *IET Intel. Transport Syst.*, 2017.

[182] Hua Zhou, Peng-Yu Zhao, Ying-Long Chen, and Hua-Yong Yang. Prediction-based stochastic dynamic programming control for excavator. *Autom. Constr.*, 83(Supplement C):68–77, November 2017.

[183] A Rezaei, J B Burl, A Solouk, B Zhou, M Rezaei, and M Shahbakhti. Catch energy saving opportunity (CESO), an instantaneous optimal energy management strategy for series hybrid electric vehicles. *Appl. Energy*, 2017.

[184] P Golchoubian and N L Azad. Real-Time nonlinear model predictive control of a Battery-Supercapacitor hybrid energy storage system in electric vehicles. *IEEE Trans. Veh. Technol.*, PP(99):1–1, 2017.

[185] Changle Xiang, Feng Ding, Weida Wang, and Wei He. Energy management of a dual-mode power-split hybrid electric vehicle based on velocity prediction and nonlinear model predictive control. *Appl. Energy*, 189(Supplement C):640–653, March 2017.

[186] A Rezaei, J B Burl, and B Zhou. Estimation of the ECMS equivalent factor bounds for hybrid electric vehicles. *IEEE Trans. Control Syst. Technol.*, PP(99):1–8, 2017.

[187] J Han, D Kum, and Y Park. Synthesis of predictive equivalent consumption minimization strategy for hybrid electric vehicles based on Closed-Form solution of optimal equivalence factor. *IEEE Trans. Veh. Technol.*, 66(7):5604–5616, July 2017.

[188] Youngho Jun, Byung Chun Jeon, and Woongro Youn. Equivalent consumption minimization strategy for mild hybrid electric vehicles with a belt driven motor. Technical report, SAE Technical Paper, 2017.

[189] Howard B Demuth, Mark H Beale, Orlando De Jess, and Martin T Hagan. *Neural Network Design*. Martin Hagan, USA, 2nd edition, 2014.

[190] K S Narendra and K Parthasarathy. Identification and control of dynamical systems using neural networks. *IEEE Trans. Neural Netw.*, 1(1):4–27, 1990.

[191] Argonne National Laboratory. Downloadable dynamometer database: 2010 toyota prius, August 2013.

Appendix A

Prediction Error Applied to Hybrid Electric Vehicle Optimal Fuel Economy: Supplementary Material

A.1 Study 1: Expected Drive Cycle
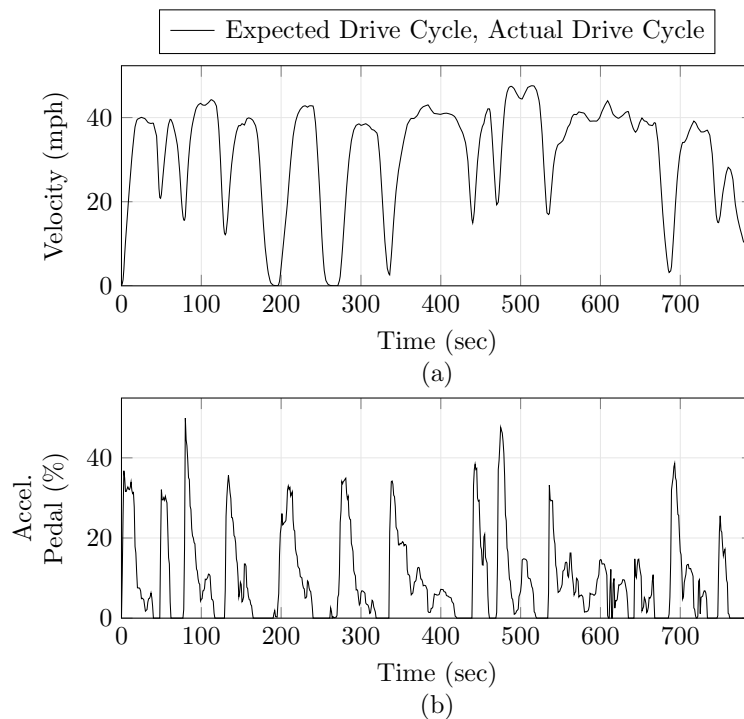
Figure A.1: Velocity and acceleration pedal request for the expected drive cycle.
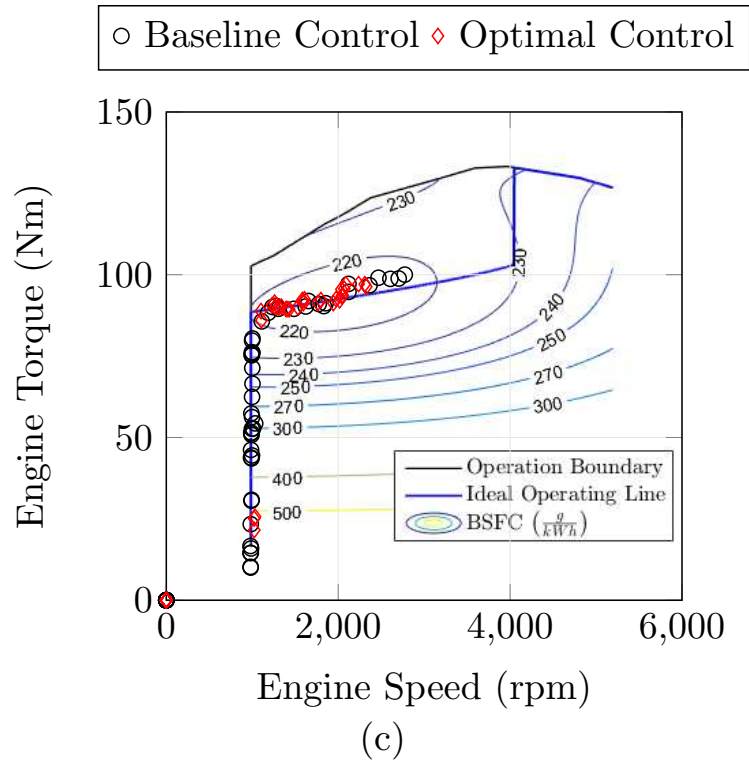
Figure A.2: Engine operation comparison of baseline energy management and optimal energy management for the expected drive cycle.
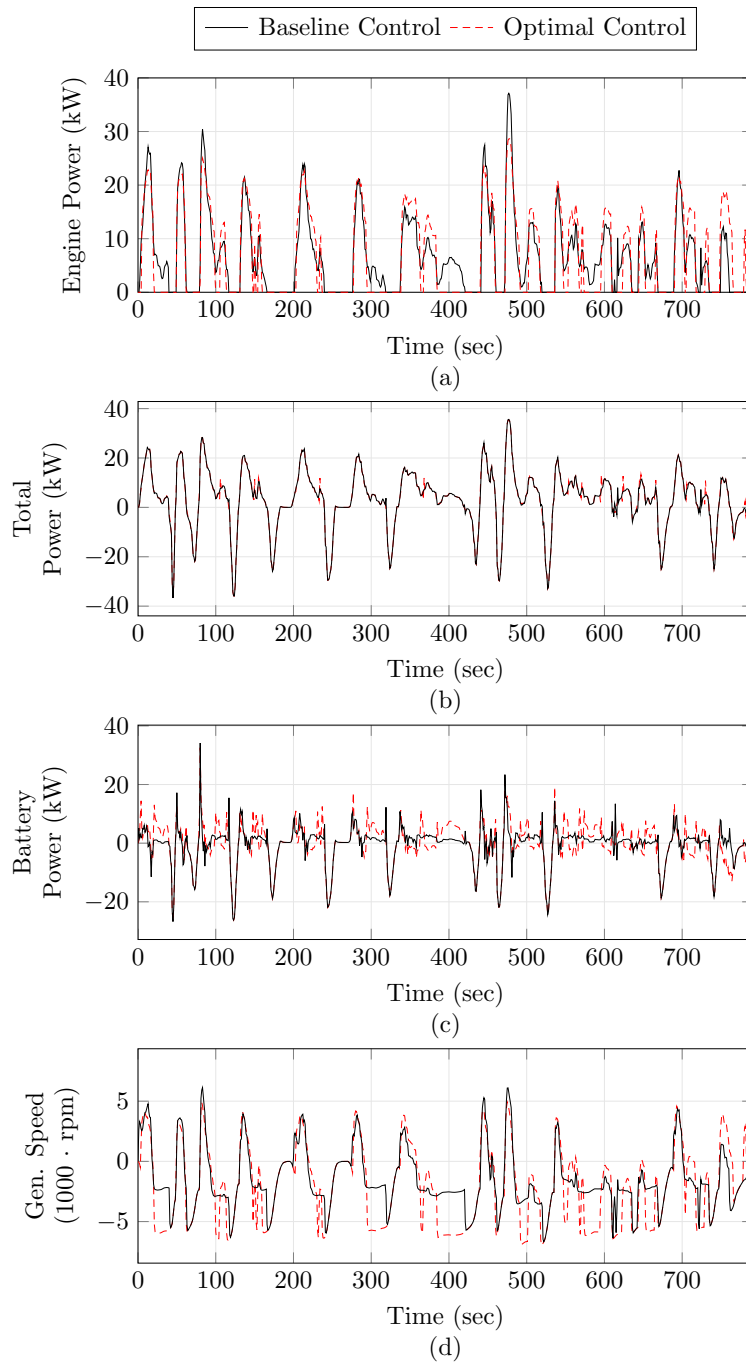
Figure A.3: Vehicle signal comparisons of baseline energy management and optimal energy management for the expected drive cycle.

A.2 Study 1: Stop Misprediction
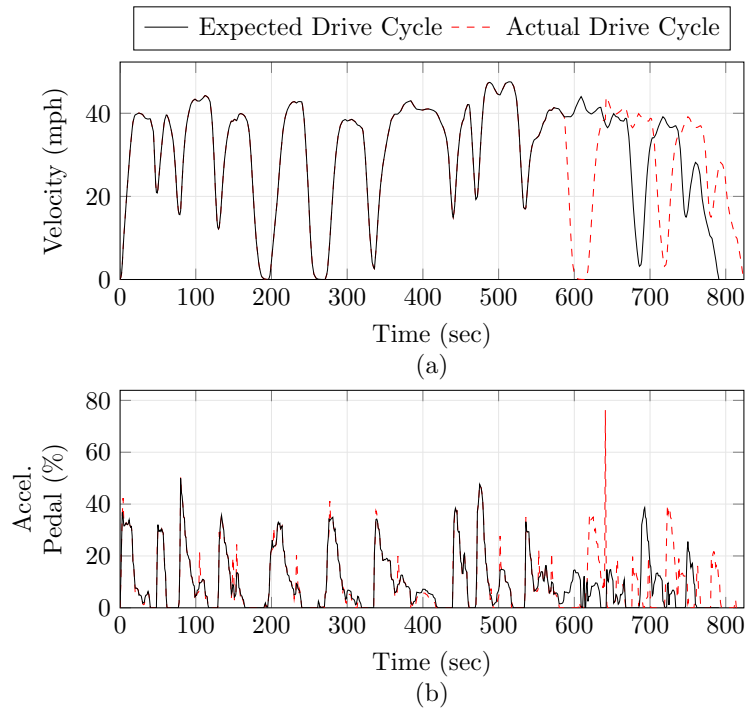
Figure A.4: Velocity and acceleration pedal request for the "1 Stop" misprediction drive cycle (Note that the actual drive cycle acceleration pedal request signal is calculated and not measured, thus it differs from the expected drive cycle).
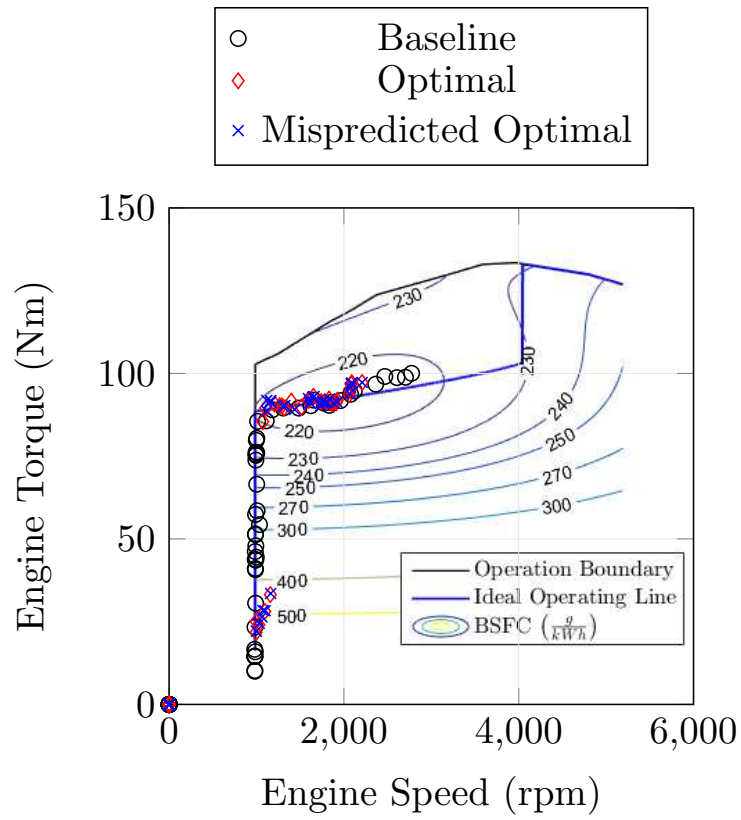
Figure A.5: Engine operation comparison of baseline energy management and optimal energy management for the "1 Stop" misprediction drive cycle.
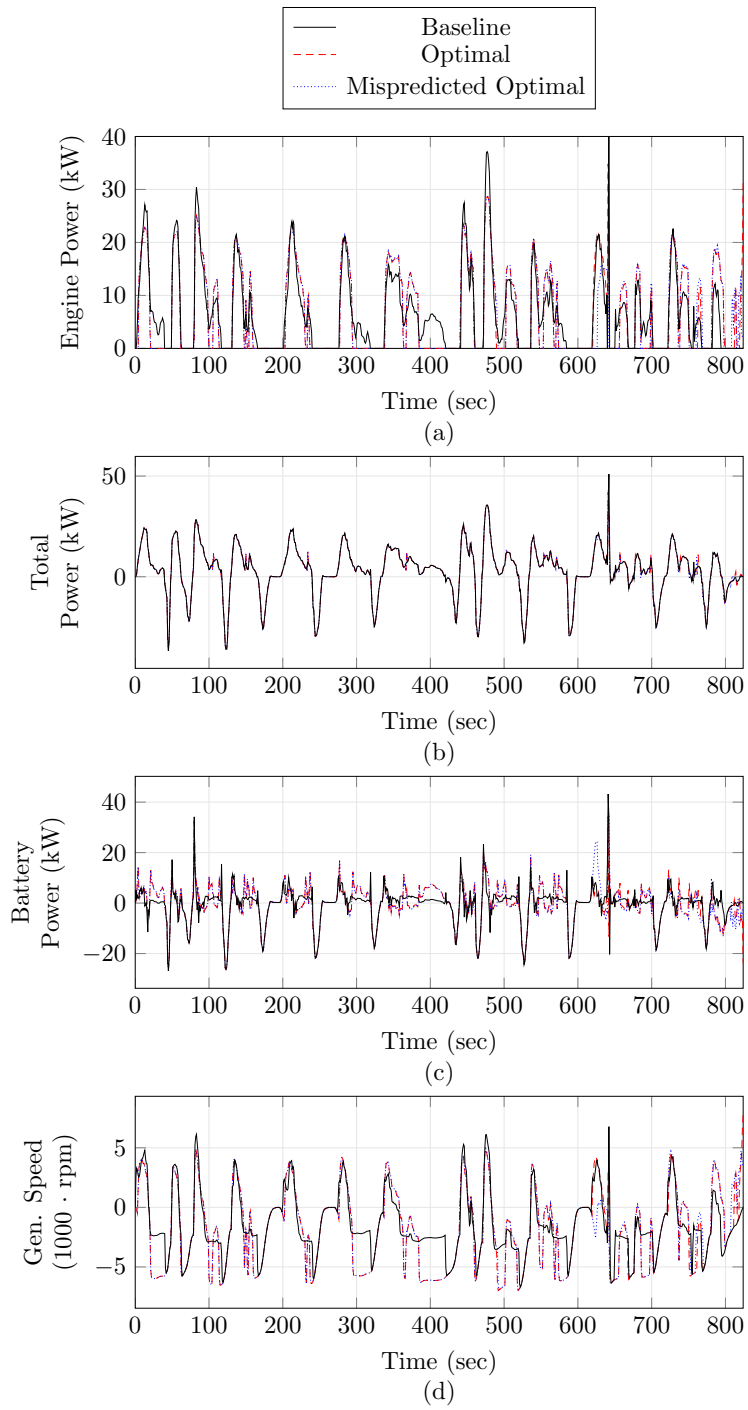
Figure A.6: Vehicle signal comparisons of baseline energy management and optimal energy management for the "1 Stop" misprediction drive cycle.

A.3 Study 1: Route Change Misprediction
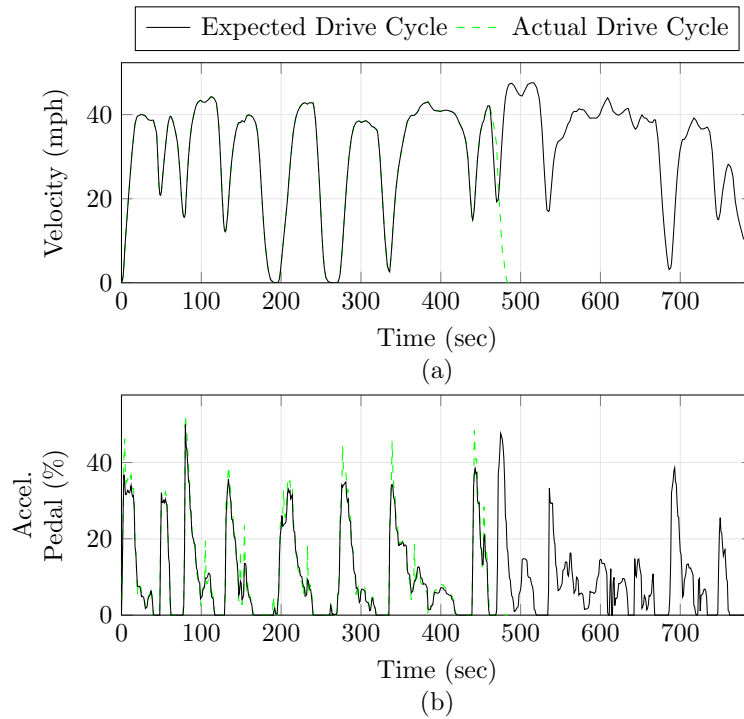
Figure A.7: Velocity and acceleration pedal request for the "Route Change 1" drive cycle (Note that the actual drive cycle acceleration pedal request signal is calculated and not measured, thus it differs from the expected drive cycle).
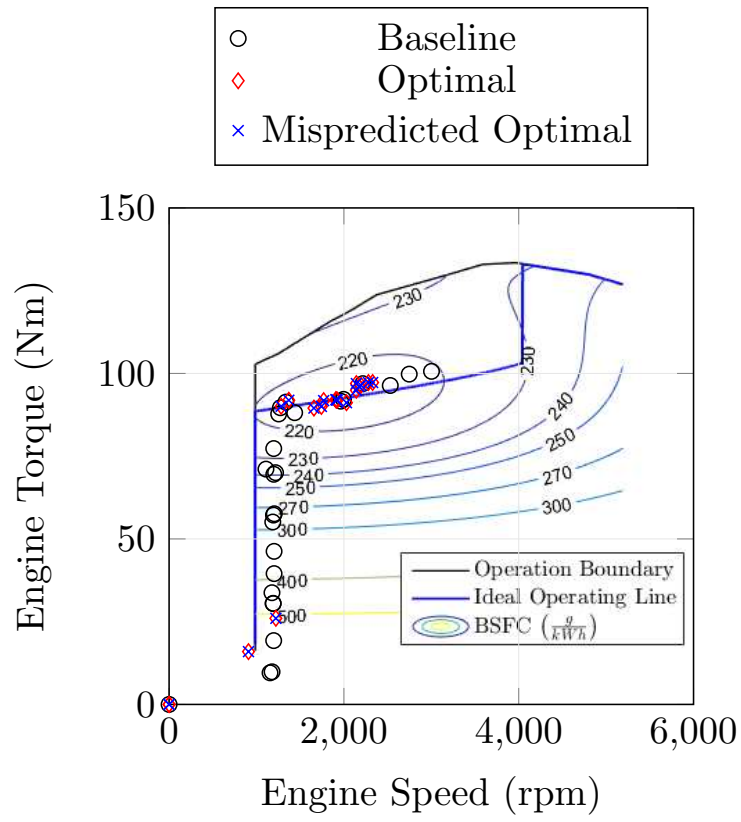
Figure A.8: Engine operation comparison of baseline energy management and optimal energy management for the "Route Change 1" drive cycle.
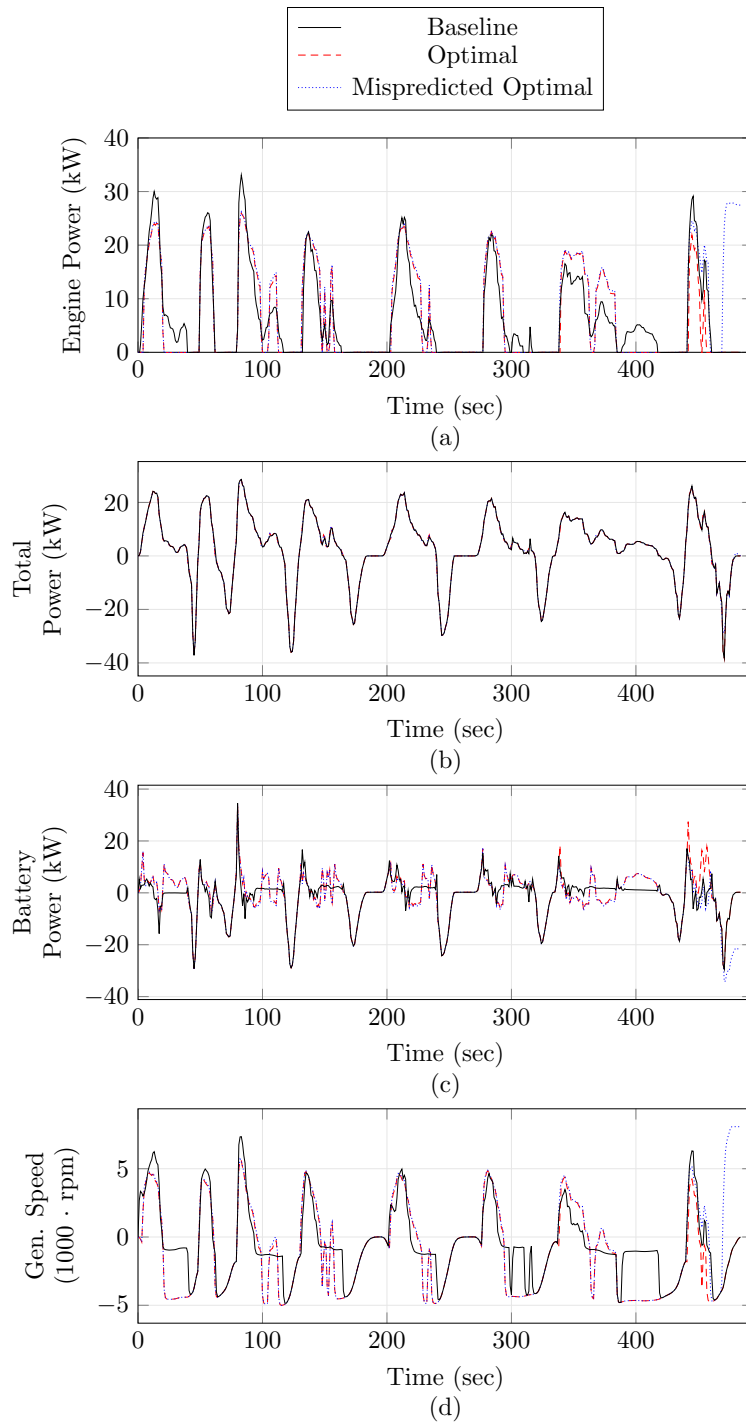
Figure A.9: Vehicle signal comparisons of baseline energy management and optimal energy management for the "Route Change 1" drive cycle.

A.4 Study 1: Traffic Misprediction
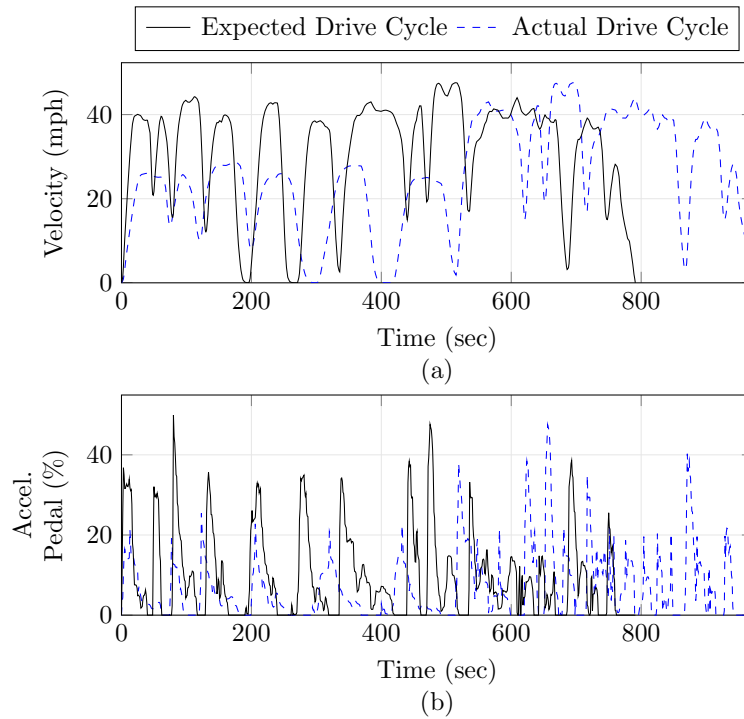
Figure A.10: Velocity and acceleration pedal request for the "Low Traffic" drive cycle (Note that the actual drive cycle acceleration pedal request signal is calculated and not measured, thus it differs from the expected drive cycle).
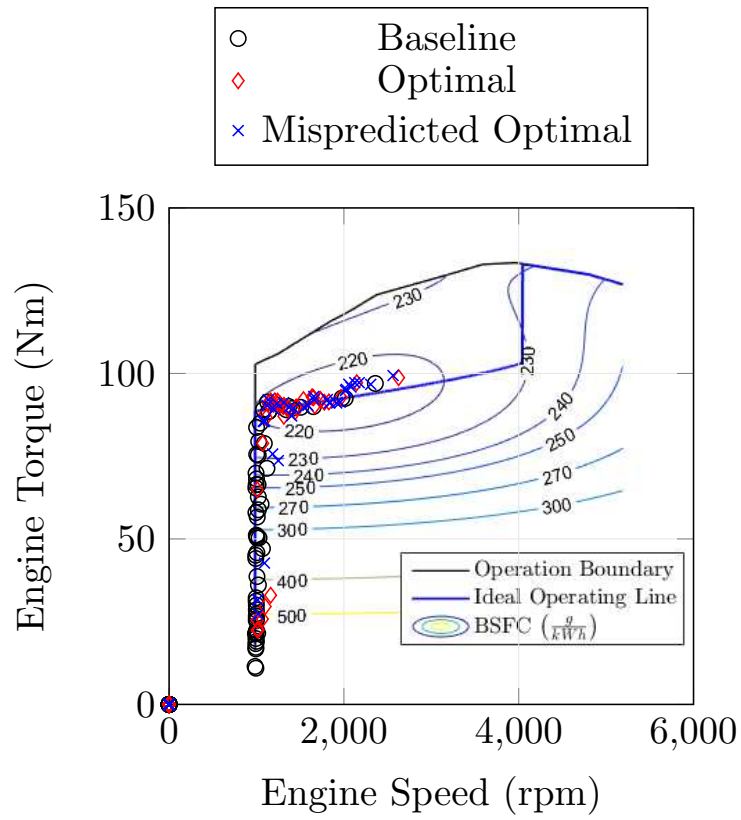
Figure A.11: Engine operation comparison of baseline energy management and optimal energy management for the "Low Traffic" drive cycle.
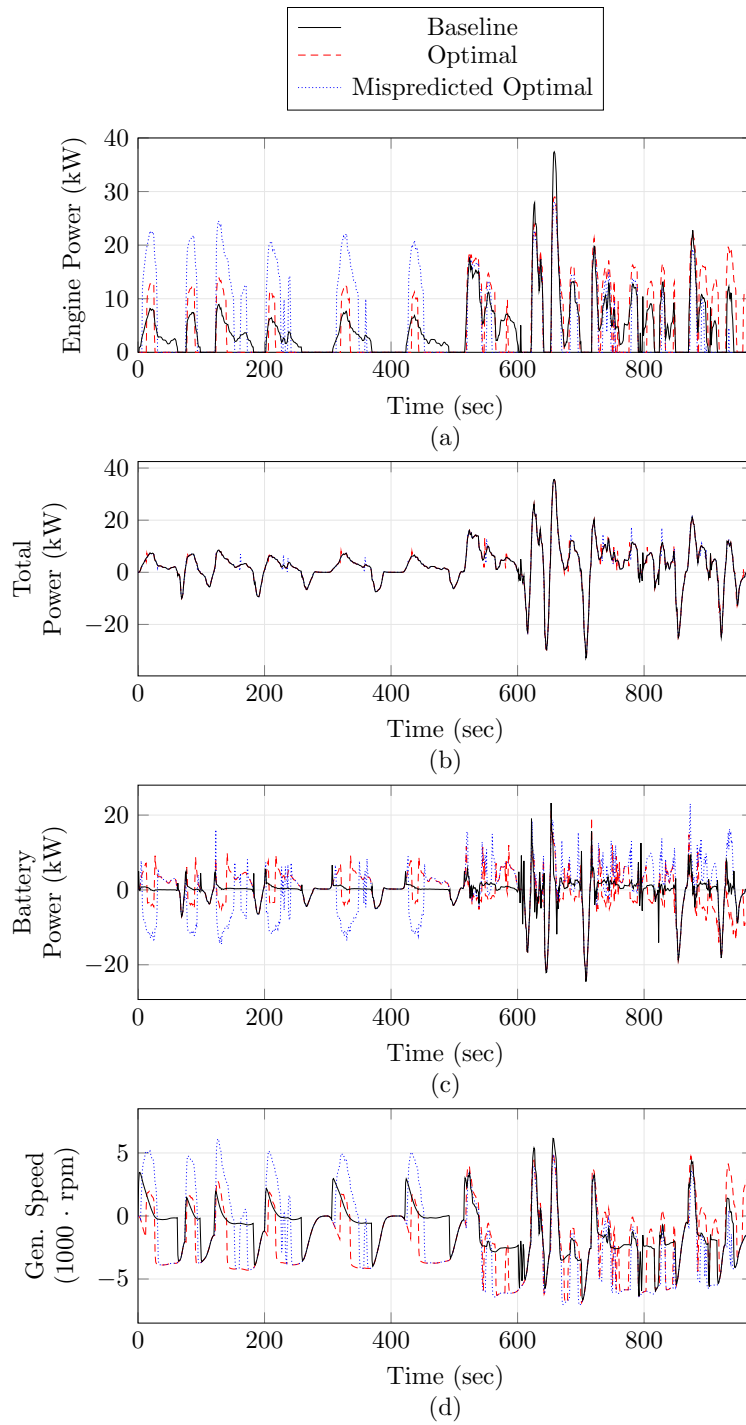
Figure A.12: Vehicle signal comparisons of baseline energy management and optimal energy management for the "Low Traffic" drive cycle.

A.5   Study 1: Compounded Misprediction
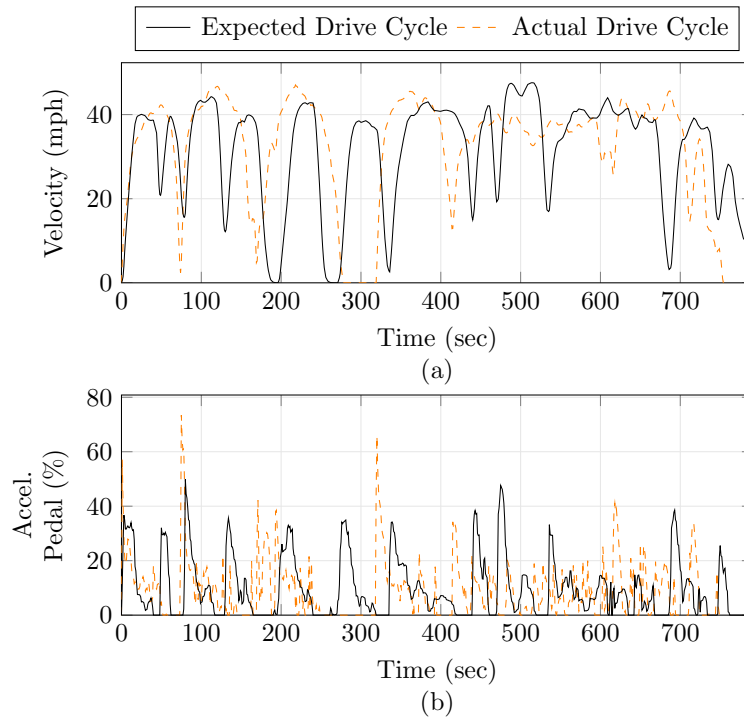
Figure A.13: Velocity and acceleration pedal request for the "Compounded 4" drive cycle (Note that the actual drive cycle acceleration pedal request signal is calculated and not measured, thus it differs from the expected drive cycle).
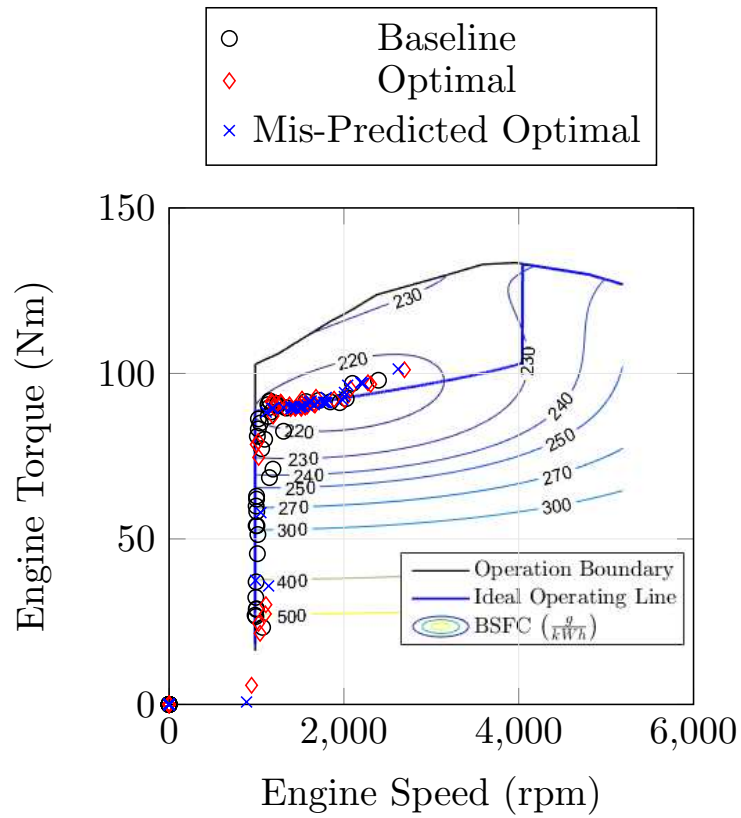
Figure A.14: Engine operation comparison of baseline energy management and optimal energy management for the "Compounded 4" drive cycle.
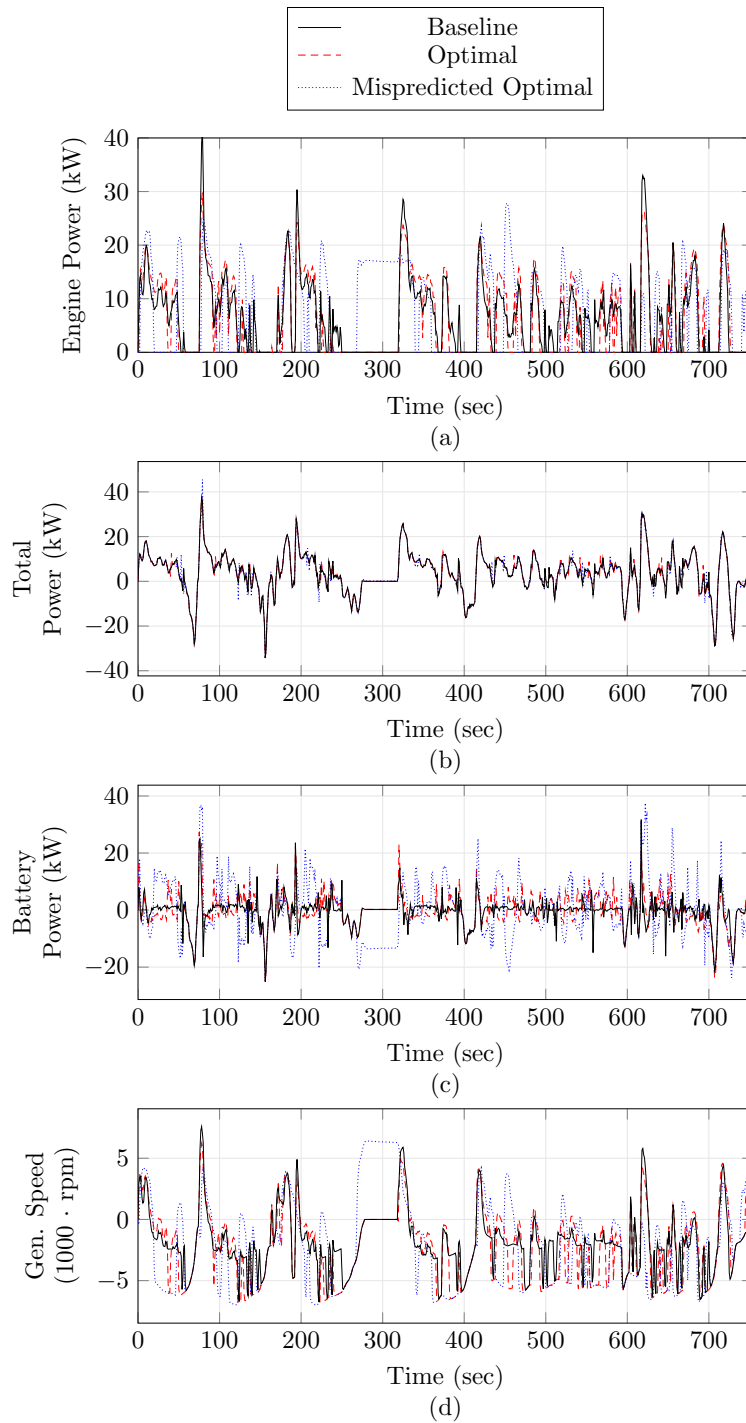
Figure A.15: Vehicle signal comparisons of baseline energy management and optimal energy management for the "Compounded 4" drive cycle.

A.6   Study 2: Higher Power than Expected Misprediction
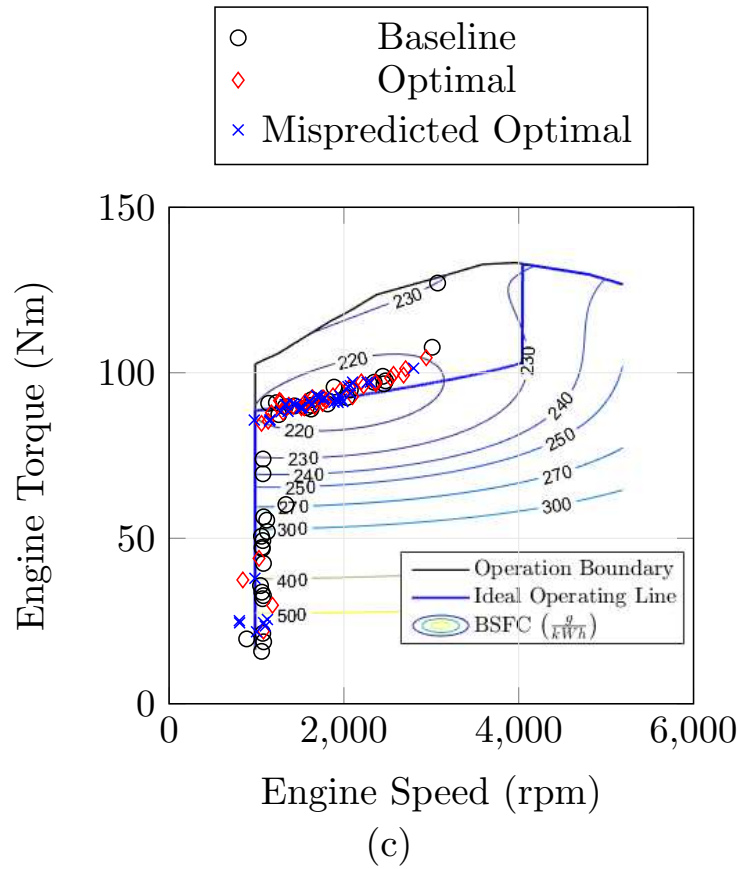
Figure A.16: Engine operation comparison of baseline energy management and optimal energy management for the "Higher Mass Misprediction".
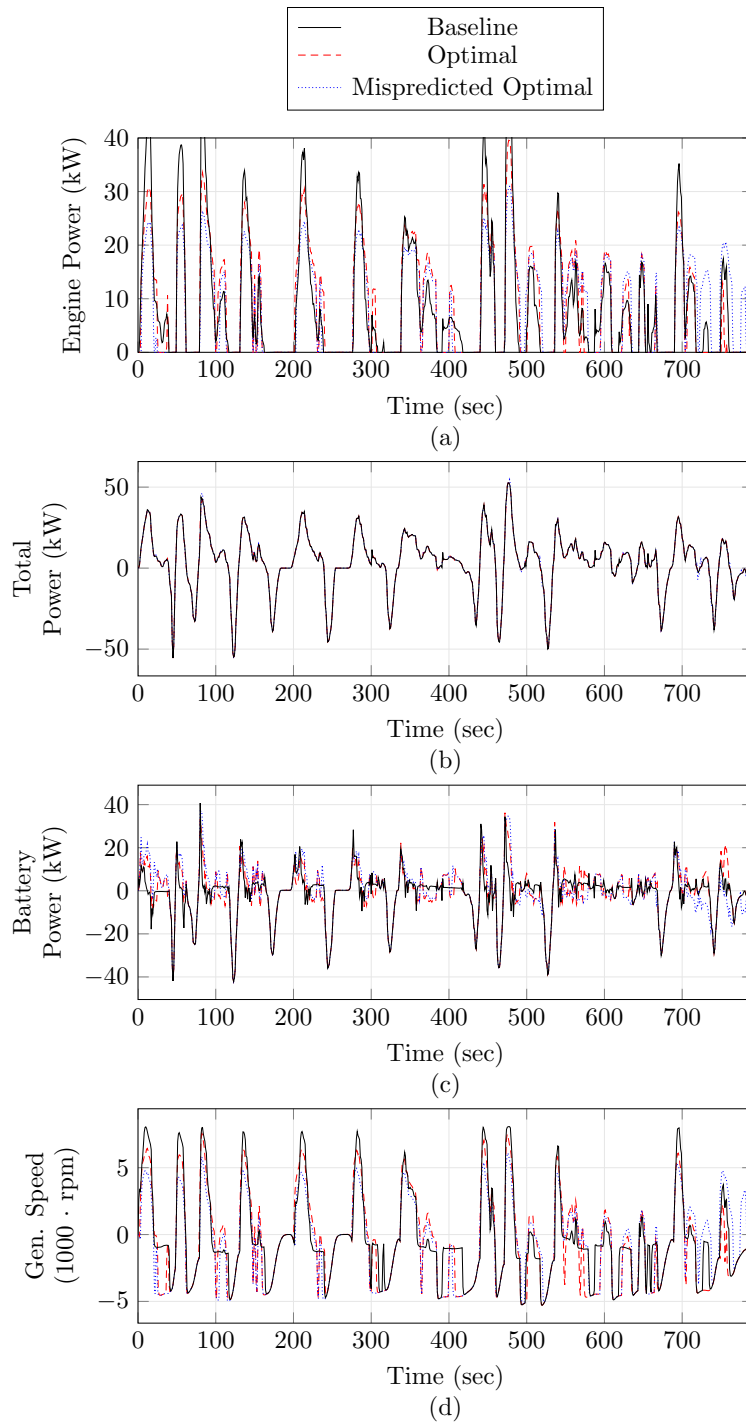
Figure A.17: Vehicle signal comparisons of baseline energy management and optimal energy management for the "Higher Mass Misprediction".

A.7 Study 2: Lower Power than Expected Misprediction
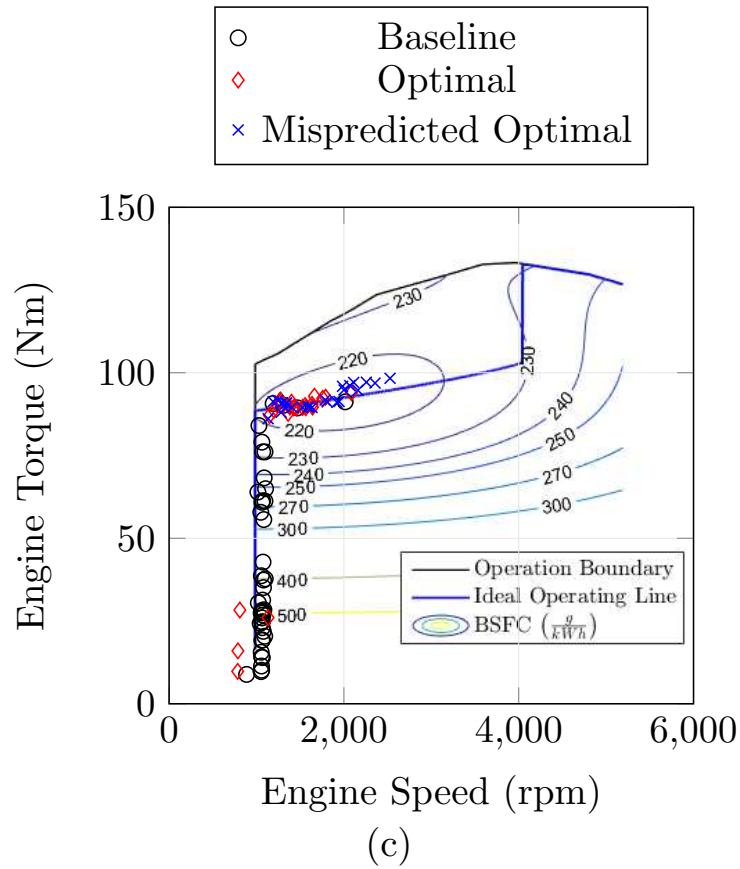
Figure A.18: Engine operation comparison of baseline energy management and optimal energy management for the "Lower Mass Misprediction".
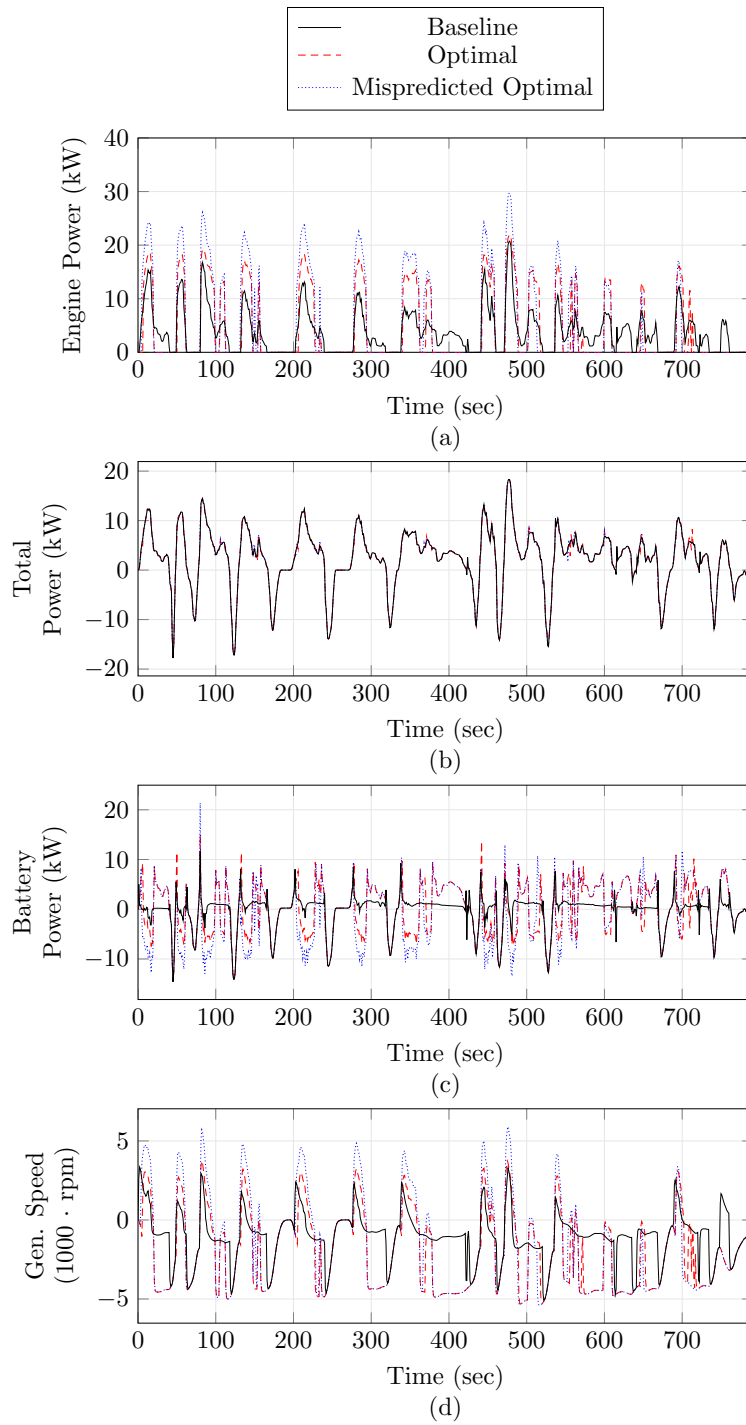
Figure A.19: Vehicle signal comparisons of baseline energy management and optimal energy management for the "Lower Mass Misprediction".

Appendix B

Additional Model Validation

Details of the Baseline EMS and a FE validation are shown in section 4.2.3. Additional validation can be accomplished by comparing the simulated and physically measured battery state of charge (SOC) and engine speeds. The physically measured data was taken from the Argonne National Laboratory Digital Dynamometer Database [191].

Simulated and measured battery SOC is shown in Figs. B.1, B.2, B.3. Each of these figures show that the simulated SOC trace for each cycle closely follows the experimental trace for the duration of the cycle. Simulated and measured engine speed are shown in figures B.4, B.5, B.6. Each of these figures show that the simulated engine speed for each cycle closely follows the experimental trace for the duration of the cycle. Overall when comparing traces of battery SOC and engine speed, the results are very similar. The model is considered to be sufficiently validated for implementation.
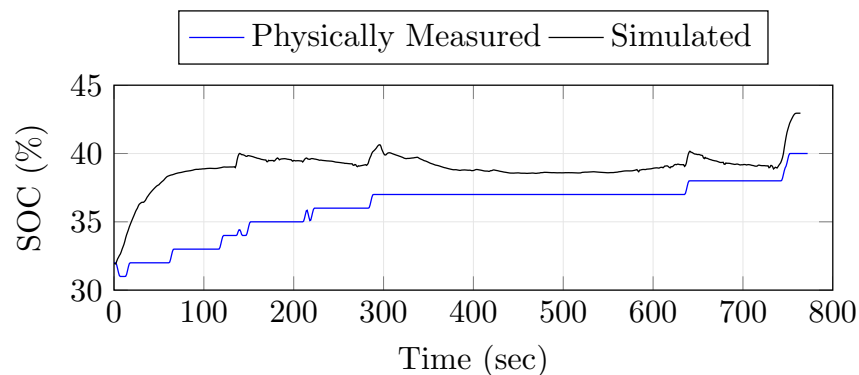
Figure B.1: Battery state of charge validation that compares the simulated model used in this study with a physical 2010 Toyota Prius over the HWFET cycle.
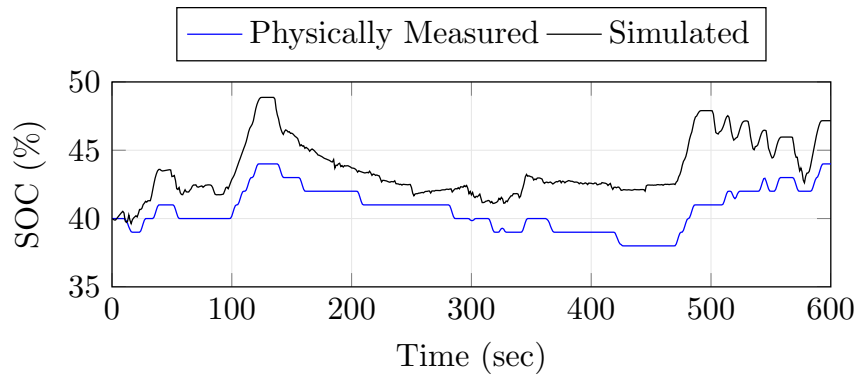
Figure B.2: Battery state of charge validation that compares the simulated model used in this study with a physical 2010 Toyota Prius over the US06 cycle.
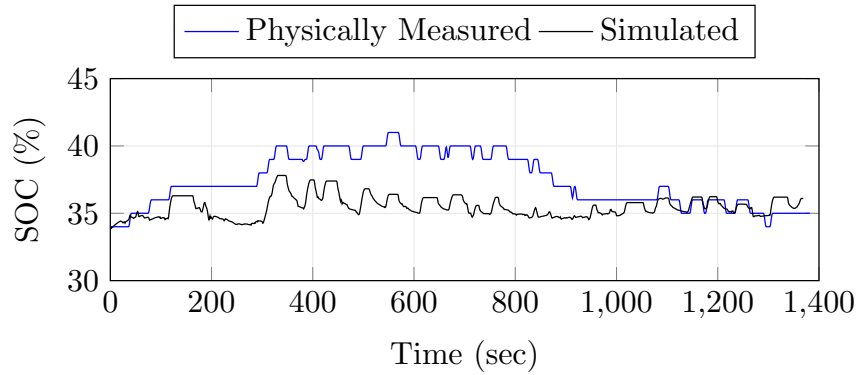
Figure B.3: Battery state of charge validation that compares the simulated model used in this study with a physical 2010 Toyota Prius over the UDDS cycle.
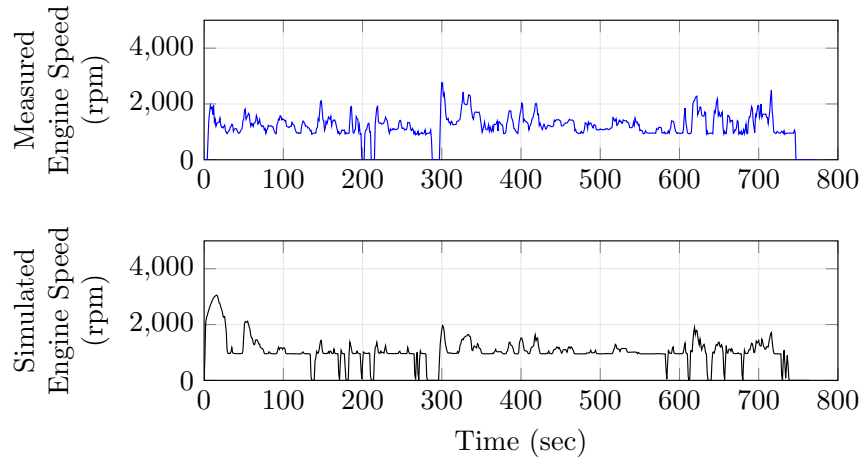
Figure B.4: Engine speed validation that compares the simulated model used in this study with a physical 2010 Toyota Prius over the HWFET cycle.
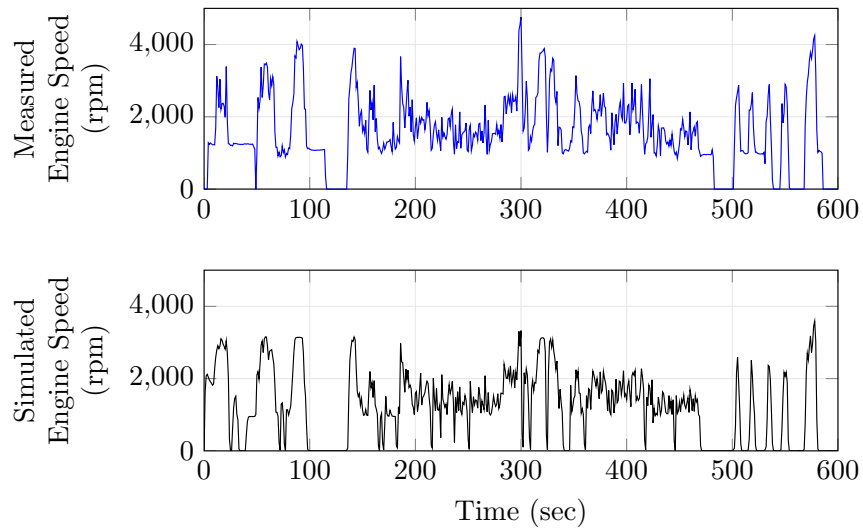
Figure B.5: Engine speed validation that compares the simulated model used in this study with a physical 2010 Toyota Prius over the US06 cycle.
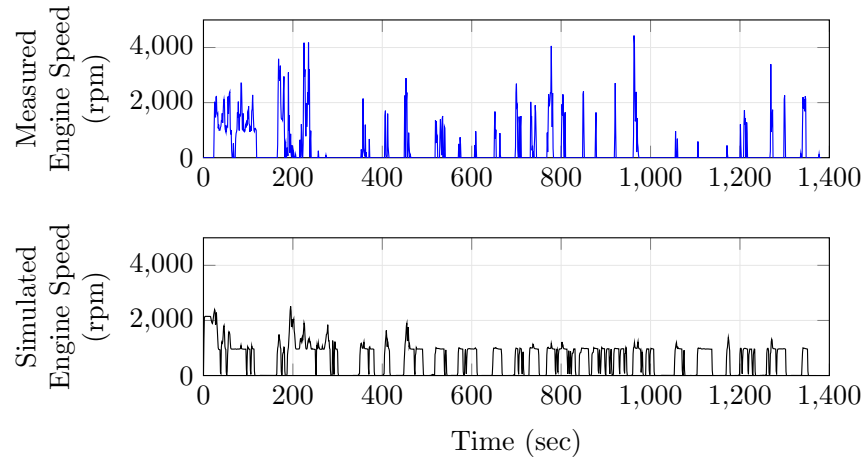
Figure B.6: Engine speed validation that compares the simulated model used in this study with a physical 2010 Toyota Prius over the UDDS cycle.

Appendix C

Additional Drive Cycle Analysis

Representative cases of (1) nearly the same FE improvement from AE category prediction and perfect AE prediction, (2) an overall FE improvement but a reduction when compared to perfect AE prediction, and (3) a FE loss when compared to the Baseline EMS are shown in section 5.3.2. This appendix presents the second-by-second velocity, FE improvement, and battery SOC of the remaining drive cycles which include the Denver City Cycle (Fig. C.5), the UDDS cycle (Fig. C.1), the Fort Collins City Cycle (Fig. C.2), the Fort Collins Highway Cycle Fig. (C.3), and the HWFET cycle (Fig. C.4). Details as to how FE is improved are presented and discussed in part one of this research.
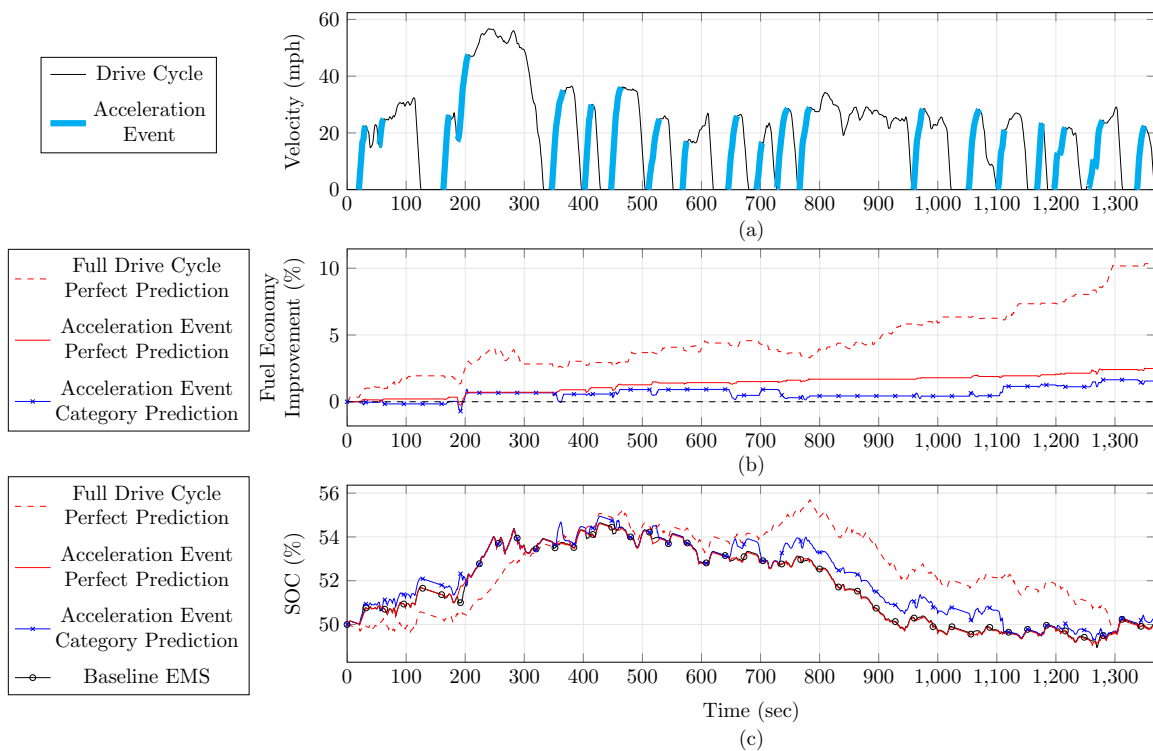
Figure C.1: The UDDS drive cycle which worse results between AE category prediction and perfect AE prediction.
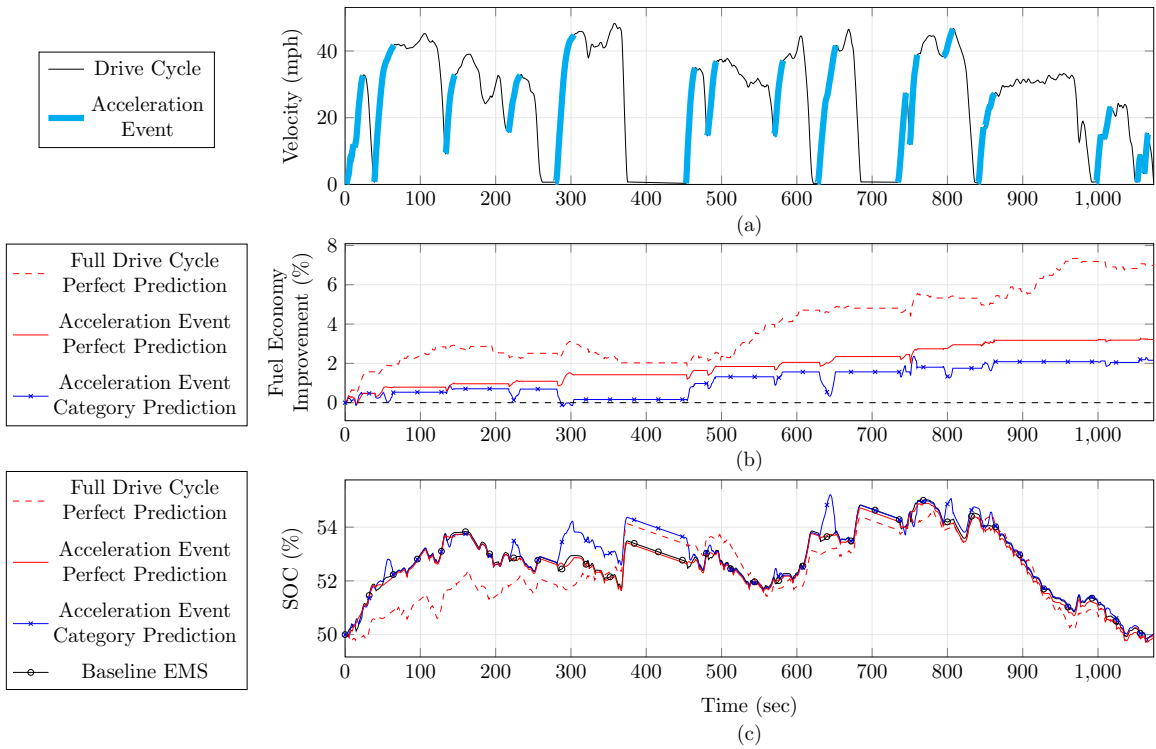
Figure C.2: The Fort Collins City drive cycle which shows a similar correlation between AE category prediction and perfect AE prediction.
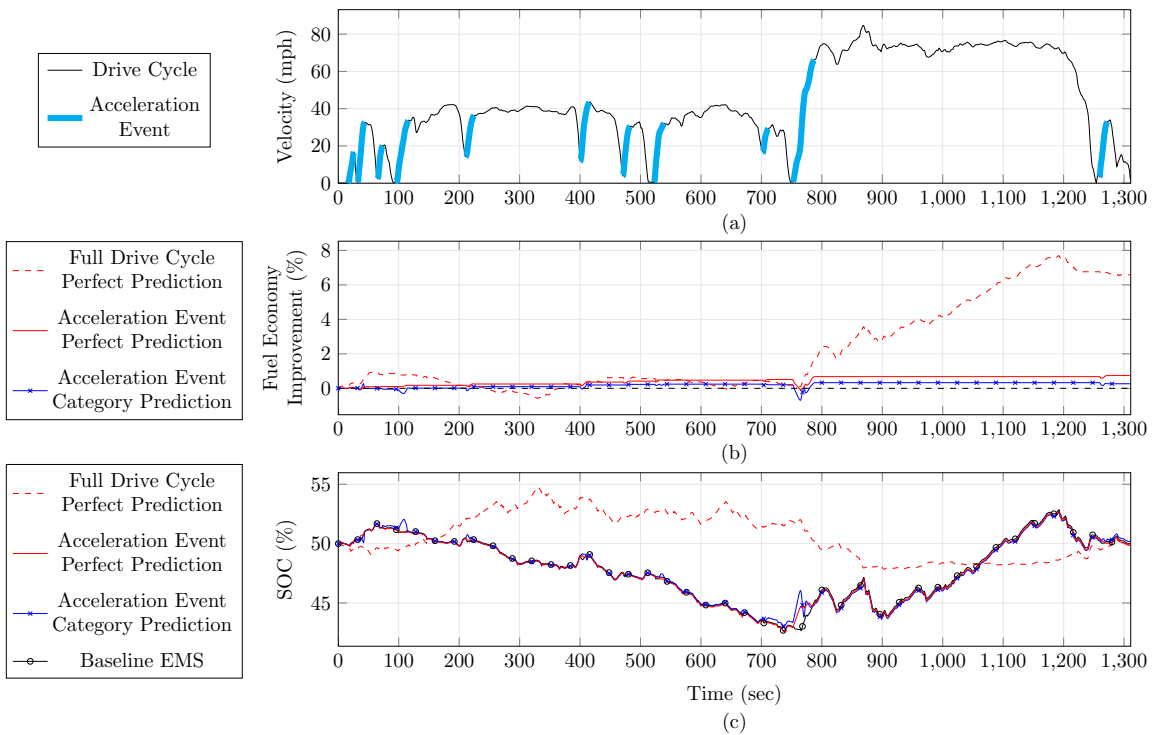
Figure C.3: The Fort Collins Highway drive cycle which worse results between AE category prediction and perfect AE prediction.
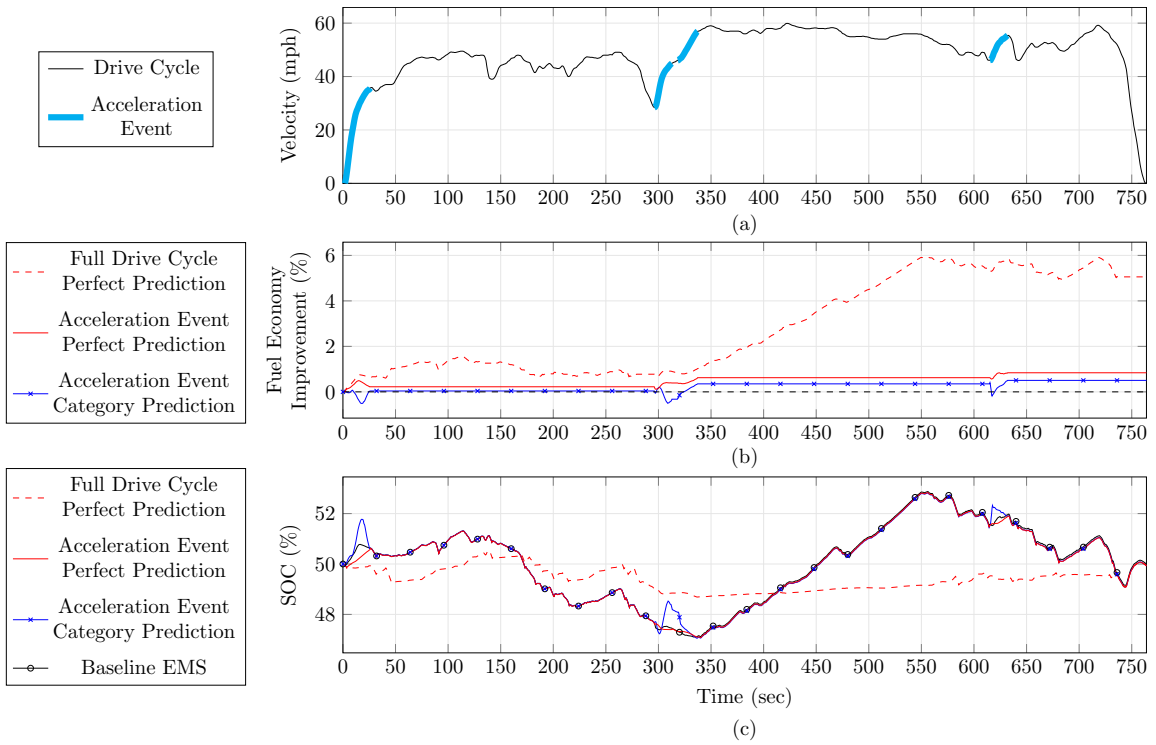
Figure C.4: The HWFET drive cycle which shows a similar correlation between AE category prediction and perfect AE prediction.
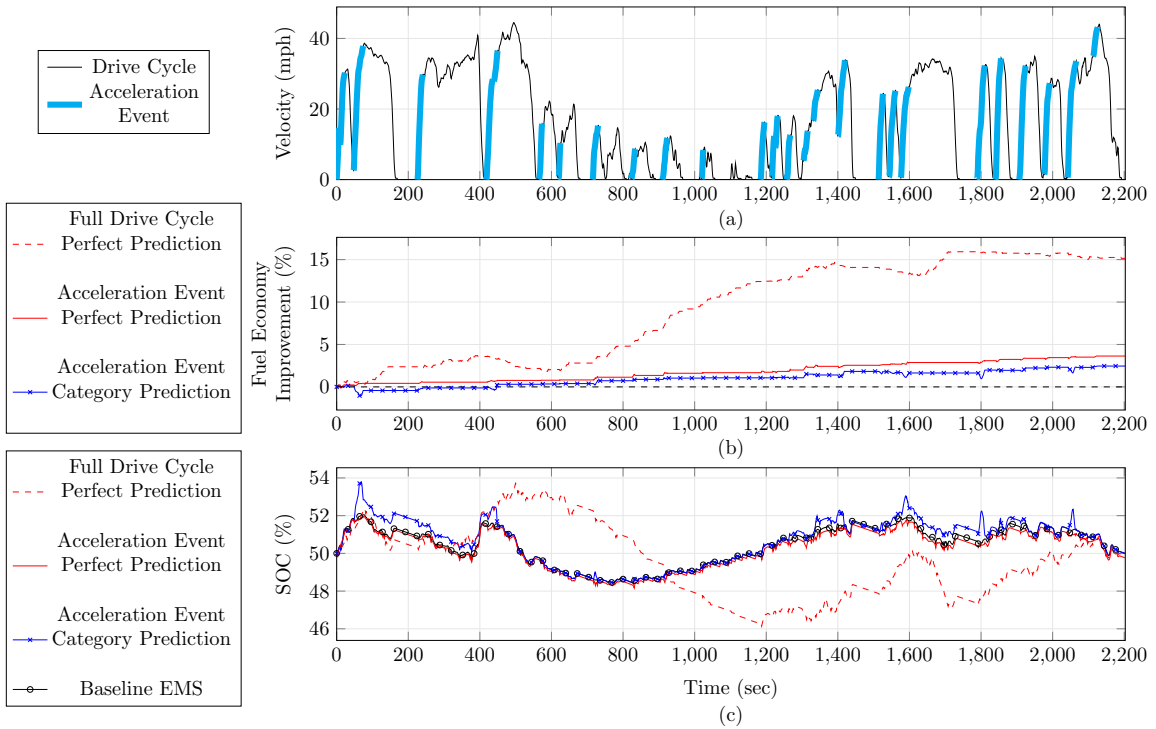
Figure C.5: The Denver City drive cycle which shows a similar correlation between AE category prediction and perfect AE prediction.